Journal of Parasitology 2025 111(4) 532–570

Published 7 August 2025

Contents and archives available through www.bioone.org or www.jstor.org

Journal of Parasitology

journal homepage: www.journalofparasitology.org

DOI: 10.1645/24-101

SISTERS PARASITIZING SISTERS: ON THE ONCHOBOTHRIIDEAN TAPEWORMS OF HAMMERHEAD AND REQUIEM SHARKS

Janine N. Caira[1], Veronica M. Bueno[1], and Kirsten Jensen[2]

[1] Department of Ecology & Evolutionary Biology, University of Connecticut, Storrs, Connecticut 06269-3043.
[2] Department of Ecology & Evolutionary Biology and the Biodiversity Institute, University of Kansas, Lawrence, Kansas 66045.
Correspondence should be sent to Janine N. Caira at: *janine.caira@uconn.edu*

KEY WORDS

Phoreiobothriidae
Sphyrnacestus
Phoreiobothrium
Carcharhinidae
Sphyrnidae
New species
New genus
Onchoproteocephalidea
Hammerhead sharks
Requiem sharks
Molecular phylogeny

ABSTRACT

The onchoproteocephalidean cestodes reported on herein were obtained from requiem (Carcharhinidae) and hammerhead (Sphyrnidae) sharks during fieldwork conducted over the past several decades off Australia, Japan, Malaysian and Indonesian Borneo, Mexico, Mozambique, Senegal, Taiwan, the United States, and Vietnam. Sequence data were generated for the D1–D3 region of the *28S* rDNA gene for 36 specimens of 23 species of onchoproteocephalideans. The phylogenetic tree resulting from a Maximum Likelihood analysis revealed 3 subclades consistent with major morphological and host differences among included taxa. One subclade consisted of species of *Triloculatum*, which have bothridia with 3 subloculi, basal prongs on their hooks that are at least half as long as the axial and abaxial prongs, and a uterus that extends essentially the length of the proglottid. These species parasitize requiem sharks. Another subclade consisted of a subset of species currently assigned to *Phoreiobothrium*, all of which came from hammerhead sharks. These species have bothridia with 5–11 subloculi, basal prongs on their hooks that are less than half as long as the axial and abaxial prongs or are entirely absent, and a uterus that extends only to the level of the terminal genitalia. The final subclade consisted of species of *Phoreiobothrium* that have bothridia with 8 or more subloculi, basal prongs on their hooks that are more than half as long as the axial and abaxial prongs, and a uterus that extends much of the length of the proglottid, all of which parasitize requiem sharks. *Sphyrnacestus* n. gen. is erected for species in the second subclade, and the diagnoses of *Phoreiobothrium* and *Triloculatum* are emended. Four new species of *Sphyrnacestus* n. gen. are described, and the 5 species from hammerhead sharks currently assigned to *Phoreiobothrium* that are consistent with the morphology of members of the second subclade are transferred to the new genus. Six new species of *Phoreiobothrium* are also described. Evidence of 16 undescribed species of *Phoreiobothrium* and 1 undescribed species of *Triloculatum* is presented. The family Phoreiobothriidae is resurrected for the 3 genera, which all possess bothridia with tri- or bi-pronged hooks and subloculi. Members of this family are predicted to be found in other species of Carcharhinidae and Sphyrnidae. Furthermore, we predict they will not be found to parasitize members of other families of carcharhiniform sharks because phoreiobothriids appear to be restricted to sharks that possess the scroll type rather than the conicospiral type of spiral intestine.

Questions surrounding the taxonomy and systematics of tapeworms of carcharhiniform sharks of the families Sphyrnidae Gill (i.e., hammerhead sharks) and Carcharhinidae Jordan and Evermann (i.e., requiem sharks) are becoming more and more challenging to investigate. This is largely because of difficulties associated with obtaining fresh material from these charismatic taxa, some of which are categorized on the IUCN Red List as Critically Endangered (Fowler et al., 2021). This study takes advantage of fieldwork aimed at opportunistically collecting tapeworms from commercial fisheries and fishers around the world over the past 4 decades. Examination of this material resulted in the discovery of 4 new species from hammerhead sharks and as many as 22 undescribed species from requiem sharks, which collectively prompted re-evaluation of the current concept of the genus *Phoreiobothrium* Linton, 1889.

Version of Record, first published online with fixed content and layout, in compliance with ICZN Arts. 8.1.3.2, 8.5, and 21.8.2 as amended, 2012. ZooBank publication registration: urn:lsid:zoobank.org:pub:48BB08E4-96EF-4E9D-A1CC-37D95A769EF5.

Phoreiobothrium is unique among the hooked tapeworms that parasitize sharks (i.e., the Onchoproteocephalidea II sensu Caira et al., 2017a) in that its members possess bothridia with a posterior row of subloculi. Unlike species of the related genus *Triloculatum* Caira and Jensen, 2009, species of *Phoreiobothrium* invariably possess 5 or more, rather than 3, subloculi (Caira and Jensen, 2009). However, among species of *Phoreiobothrium*, notable differences in scolex morphology exist between the species that parasitize hammerhead sharks and those that parasitize requiem sharks. For exvample, the basal prongs in each pair of hooks of species parasitizing requiem sharks are relatively elongate, being only slightly shorter than the axial and abaxial prongs, and the cephalic peduncle of these species bears large gladiate spinitriches. In contrast, in species parasitizing hammerhead sharks, the basal prongs of each pair of hooks are highly reduced or absent, and the cephalic peduncle bears extremely large spinitriches. The primary question of interest is whether these differences signal more fundamental differences between the taxa parasitizing these 2 host groups. The single exception to this pattern, *Phoreiobothrium tiburonis* Cheung, Nigrelli, and Ruggieri, 1982, is also of interest because it exhibits a scolex morphology like that of species parasitizing requiem sharks but parasitizes the bonnethead shark, *Sphyrna tiburo* (L.) (see Cheung et al., 1982).

A phylogenetic analysis that included newly generated sequence data for the D1–D3 region of the *28S* rDNA gene allowed us to explore the morphology and host associations of this group of worms in a phylogenetic context. The resulting tree helped inform the development of a taxonomic framework that reflects phylogenetic relationships. That framework retains the species that parasitize requiem sharks as members of *Phoreiobothrium*. A new genus is erected to accommodate the majority of the species that parasitize hammerhead sharks. The family Phoreiobothriidae Baer and Euzet, 1955, is resurrected to house *Triloculatum*, *Phoreiobothrium*, and the new genus.

MATERIALS AND METHODS

Collection of sharks and cestodes

Cestodes used in this study came from 34 specimens of 17 species of carcharhinid sharks representing 7 genera (*Carcharhinus* Blainville, *Lamiopsis* Gill, *Loxodon* Müller and Henle, *Negaprion* Whitley, *Rhizoprionodon* Whitley, *Scoliodon* Müller and Henle, and *Triaenodon* Müller and Henle) and 13 specimens of 4 species of sphyrnid sharks representing 2 genera (*Eusphyra* Gill and *Sphyrna* Rafinesque). These specimens were collected from the Atlantic, Indian, and Pacific Oceans between 1995 and 2013. Sharks were caught by hook and line, trawling, or gill netting, or obtained at local fish markets, and most were subsequently measured and photographed. Each shark was assigned a unique host specimen number consisting of a collection code and accession number (e.g., AU-70). Table I provides information on the size, sex, and basic collecting details for each host specimen. Additional information can be accessed by searching for the unique specimen number in the Global Cestode Database (Caira et al., 2024).

In the cases of all but 3 host specimens, the body cavity was opened with a mid-ventral incision, and the spiral intestine was removed. This organ was then opened longitudinally and rinsed with sea water. The rinse and the spiral intestine were then examined for tapeworms. A subset of the tapeworms encountered was fixed in 95% ethanol for molecular work. The spiral intestines and the remaining tapeworms were fixed in 10% seawater-buffered formalin and eventually transferred to 70% ethanol for storage. The exceptions were a specimen of *Triaenodon obesus* (Rüppell) (host specimen no. TJL-1) and 2 specimens of *Sphyrna lewini* 1 (host specimens nos. MOT-24 and MOT-25), which were provided to us by collaborators. In the first case, we received worms fixed in buffered formalin, and in the latter case, we received spiral intestines fixed in buffered formalin.

Morphological analysis

Specimens prepared for light microscopy were hydrated in a graded ethanol series, stained for 30–40 min with a diluted solution of Delafield's hematoxylin (1:9 mixture of hematoxylin stock: distilled water), differentiated in tap water, destained in 70% acid ethanol, alkalinized in 70% basic ethanol, dehydrated in a graded ethanol series, cleared in methyl salicylate, mounted on glass slides under coverslips in Canada balsam, and left to dry in an oven set to 55 C for ~1 wk. Measurements were taken using either a Lumenera Infinity 3 camera and the Infinity Analyze image analysis software (Teledyne Lumenera, Ottawa, Ontario, Canada) or a SPOT Diagnostic Instrument Digital Camera System and SPOT software (ver. 4.6, SPOT Imaging Solutions, Sterling Heights, Michigan) on a Zeiss Axioskop 2 Plus compound microscope (Zeiss, Thornwood, New York). All measurements are reported in micrometers (μm) unless otherwise stated and are given as the range followed by the mean, standard deviation, number of worms examined (N), and total number of measurements (n) if more than 1 measurement was taken per worm; only range is given in instances in which N is less than 5. Line drawings were prepared with the aid of a camera lucida attached to a Zeiss Axioskop 2 Plus compound microscope. Hook measurements taken follow Caira (1985) and are illustrated for hooks of different forms in Figure 1.

Prior to the preparation of specimens for scanning electron microscopy (SEM), the scolex was removed from the strobila and the latter was prepared as a whole mount to serve as a voucher following the protocol described above. Scoleces were then hydrated in a graded ethanol series, post-fixed in a 1% solution of osmium tetroxide overnight at 4 C, washed in distilled water, dehydrated in a graded ethanol series, transferred to hexamethyldisilazane (HMDS) for 20–30 min, and allowed to air dry. Specimens were mounted on aluminum stubs on double-sided PELCO adhesive carbon tape (Ted Pella Inc., Redding, California), sputter coated with c. 20–30 nm of gold-palladium or 35 nm of gold, and examined with a Hitachi S4700 field emission scanning electron microscope (Hitachi High-Tech, Schaumburg, Illinois) at the Microscopy and Analytical Imaging Research Resource Core Lab at the University of Kansas, Lawrence, Kansas, or with an FEI Nova NanoSEM 450 field emission SEM (FEI, Hillsboro, Oregon) at the Bioscience Electron Microscopy Laboratory at the University of Connecticut, Storrs, Connecticut. Hook terminology follows Caira (1985). Microthrix terminology follows Chervy (2009). Elasmobranch taxonomy follows Naylor et al. (2012b). Shape terminology follows Clopton (2004). In general, gladiate spinitriches that are between 10 and 15 μm in length were categorized as large, and those that are greater than 15 μm in length are categorized as extremely large; in some species, the latter can attain a length of 30 μm.

Table I. Host specimen data.

Host family / Host species	Unique host specimen number	Sex	Total length (in cm)	Collector	Collection date	Locality
Carcharhinidae						
Carcharhinus acronotus	KC-5	male	100	K. Jensen	18 Aug 1996	Florida (28°37′9.0″N, 84°12′48.6″W), Gulf of Mexico, Atlantic Ocean
Carhcarhinus altimus	KC-18	female	162	C. Healy	8 Sep 1996	Maryland (38°13′49.2″N, 74°15′37.2″W), Atlantic Ocean
Carcharhinus amblyrhynchoides	AU-100	female	138	J. N. Caira, K. Jensen	12 Aug 1997	Dundee Beach (12°45′33″S, 130°21′7″E), Northern Territory, Australia, Fog Bay, Timor Sea, Indian Ocean
Carcharhinus amboinensis 1	AU-72	female	79	J. N. Caira	10 Aug 1997	Dundee Beach (12°45′33″S, 130°21′7″E), Northern Territory, Australia, Fog Bay, Timor Sea, Indian Ocean
Carcharhinus amboinensis 1	NT-113	female	242	J. N. Caira, K. Jensen	21 Nov 1999	East of Wessel Islands (11°17′44″S, 136°59′48″E), Northern Territory, Australia, Arafura Sea, Pacific Ocean
Carcharhinus brevipinna	KA-4	male	107	J. N. Caira, K. Jensen	21 Nov 2006	Manggar (01°12′55.20″S, 116°58′27.50″E), East Kalimantan, Borneo, Indonesia, Makassar Strait, Pacific Ocean
Carcharhinus brevipinna	MS05-357	unkown	unkown	S. A. Bullard, J. Peterson	21 Jun 2006	Near oil rig MO-990 (29°58′58.20″N, 88°36′16.80″W), Louisiana, Gulf of Mexico, Atlantic Ocean
Carcharhinus brevipinna	MS05-456	male	174	S. A. Bullard	8 Oct 2006	Southwest end of Horn Island (30°14′9″N, 88°46′2″W), Mississippi, Gulf of Mexico, Atlantic Ocean
Carcharhinus brevipinna	MS05-5	female	103	S. A. Bullard, K. Jensen	15 Jun 2005	~3 miles south of the Shallow Fields (29°37′22.8″N, 88°30′11.0″W), Mississippi, Gulf of Mexico, Atlantic Ocean
Carcharhinus isodon	MS05-86	female	56	E. Hoffmayer	21 Jun 2005	Round Island (30°17′42.45″N, 88°35′11.55″W), Mississippi, Gulf of Mexico, Atlantic Ocean
Carcharhinus isodon	MS05-495	female	125	D. Bethea, L. Hollensead	22 May 2007	Florida (29°40′8″N, 85°13′30″W), Indian Pass, Gulf of Mexico, Atlantic Ocean
Carcharhinus cf. *leucas* 1	BJ-191	male	302	J. N. Caira	8 Aug 1993	Bahia de Los Angeles (28°59′9″N, 113°32′53″W), Baja California, Mexico, Gulf of California, Pacific Ocean
Carcharhinus pleurotaenia	AU-8	male	77.5	J. N. Caira	5 Aug 1997	Darwin (12°20′11″S, 130°54′39″E), Northern Territory, Australia, Buffalo Creek, Timor Sea, Indian Ocean
Carcharhinus limbatus	KC-7	male	134	K. Jensen	23 Aug 1996	Florida (25°19′3.0″N, 82°29′45.6″W), Gulf of Mexico, Atlantic Ocean
Carcharhinus limbatus	MS05-24	male	80	E. Hoffmayer	16 Jun 2005	North of east end of Horn Island (30°14′1.31″N, 88°36′0.83″W), Mississippi, Gulf of Mexico, Atlantic Ocean
Carcharhinus limbatus	MS05-435	female	135	S. A. Bullard, D. Bethea	6 Oct 2006	Panama City (30°8′4.69″N, 85°41′36.93″W), Florida, St. Andrew Bay, Gulf of Mexico, Atlantic Ocean
Carcharhinus limbatus	MS05-481	male	75	K. Jensen	22 May 2007	Florida (29°40′8.05″N, 85°13′30.17″W), Indian Pass, Gulf of Mexico, Atlantic Ocean
Carcharhinus tilsoni	NT-55	female	148	J. N. Caira, K. Jensen	11 Nov 1999	East of Wessel Islands (11°17′44″S, 136°59′48″E), Northern Territory, Australia, Arafura Sea, Pacific Ocean
Lamiopsis tephrodes	BO-259	male	71	J. N. Caira, K. Jensen	20 May 2002	Mukah (2°53′52.16″N, 112°5′44.12″E), Sarawak, Borneo, Malaysia, South China Sea, Pacific Ocean

Table I. Continued.

Host family / Host species	Unique host specimen number	Sex	Total length (in cm)	Collector	Collection date	Locality
Lamiopsis tephrodes	BO-488	male	105.1	J. N. Caira, K. Jensen	30 Apr 2004	Mukah (2°53′52.16″N, 112°5′44.12″E), Sarawak, Borneo, Malaysia, South China Sea, Pacific Ocean
Lamiopsis tephrodes	BO-74	male	106	J. N. Caira, K. Jensen	14 Jun 2002	Mukah (2°53′52.16″N, 112°5′44.12″E), Sarawak, Borneo, Malaysia, South China Sea, Pacific Ocean
Loxodon cf. *macrorhinus*	MZ-29	male	83	J. N. Caira, K. Jensen, F. Marques	29 Jun 2016	Ibo (2°17′3.44″S, 40°35′10.83″E), Cabo Delgado, Mozambique, Mozambique Channel, Indian Ocean
Loxodon cf. *macrorhinus*	MZ-30	male	87	J. N. Caira, K. Jensen, F. Marques	29 Jun 2016	Ibo (2°17′3.44″S, 40°35′10.83″E), Cabo Delgado, Mozambique, Mozambique Channel, Indian Ocean
Loxodon cf. *macrorhinus*	MZ-32	male	86	J. N. Caira, K. Jensen, F. Marques	29 Jun 2016	Ibo (2°17′3.44″S, 40°35′10.83″E), Cabo Delgado, Mozambique, Mozambique Channel, Indian Ocean
Negaprion acutidens	AU-30	female	235	J. N. Caira	6 Aug 1997	Darwin (12°20′11″S, 130°54′39″E), Northern Territory, Australia, Buffalo Creek, Timor Sea, Indian Ocean
Negaprion acutidens	CM03-7	male	80	J. N. Caira, K. Jensen	6 Jun 2003	Weipa (12°35′11″S, 141°42′34″E), Queensland, Australia, Gulf of Carpentaria, Indian Ocean
Rhizoprionodon oligolinx	KA-87	male	52.5	J. N. Caira, K. Jensen	30 Nov 2006	Muara Kintap (3°54′15.40″S, 115°15′31.80″E), South Kalimantan, Borneo, Indonesia, Java Sea, Pacific Ocean
Rhizoprionodon terraenovae	MS05-499	male	86	L. Hollensead, M. Winton	23 May 2007	Florida (29°46′3″N, 85°21′4″W), St. Joseph Bay, Gulf of Mexico, Atlantic Ocean
Rhizoprionodon terraenovae	PE-18	female	unkown	V. McKenzie	17 May 1996	North Carolina, Atlantic Ocean
Scoliodon macrorhynchos	BO-244	female	32	J. N. Caira, K. Jensen	18 May 2003	Mukah (2°53′52.16″N, 112°05′44.12″E), Sarawak, Borneo, Malaysia, South China Sea, Pacific Ocean
Scoliodon macrorhynchos	BO-262	male	33	J. N. Caira, K. Jensen	20 May 2003	Mukah (2°53′52.16″N, 112°05′44.12″E), Sarawak, Borneo, Malaysia, South China Sea, Pacific Ocean
Scoliodon macrorhynchos	BO-266	male	30.5	J. N. Caira, K. Jensen	20 May 2003	Mukah (2°53′52.16″N, 112°05′44.12″E), Sarawak, Borneo, Malaysia, South China Sea, Pacific Ocean
Scoliodon macrorhynchos	VN-11	male	57.5	J. N. Caira, K. Jensen	10 Mar 2010	Cat Ba Island (20°43′31.1″N, 107°02′54.9″E), Haiphong Province, Vietnam, Gulf of Tonkin, Pacific Ocean
Triaenodon obesus	TJL-1	male	104.8	T. J. Lisney	1999	Heron Island, Queensland, Australia, Pacific Ocean
Sphyrnidae						
Eusphyra blochii	AU-70	female	141	J. N. Caira, K. Jensen	10 Aug 1997	Dundee Beach (12°45′33″S, 130°21′7″E), Northern Territory, Australia, Fog Bay, Timor Sea, Indian Ocean
Eusphyra blochii	AU-71	female	112	J. N. Caira, K. Jensen	10 Aug 1997	Dundee Beach (12°45′33″S, 130°21′7″E), Northern Territory, Australia, Fog Bay, Timor Sea, Indian Ocean
Sphyrna lewini 1	DEL-2	male	274.3	K. Jensen	17 Apr 2001	South of Florida Keys (24°34′15″N, 81°13′33″W), Florida, Atlantic Ocean
Sphyrna lewini 1	MOT-24	male	247	C. Manire	8 Aug 1995	Florida (27°33′8.4″N, 82°39′9.0″W), Tampa Bay, Gulf of Mexico, Atlantic Ocean
Sphyrna lewini 1	MOT-25	unkown	101	C. Manire	8 Aug 1995	Florida (27°33′8.4″N, 82°39′9.0″W), Tampa Bay, Gulf of Mexico, Atlantic Ocean

Table I. Continued.

Host family Host species	Unique host specimen number	Sex	Total length (in cm)	Collector	Collection date	Locality
Sphyrna lewini 1	MS05-433	male	58.5	S. A. Bullard, D. Bethea	5 Oct 2006	Florida (29°40′8″N, 85°13′30″W), Indian Pass, Gulf of Mexico, Atlantic Ocean
Sphyrna mokarran	CG-8	male	280.7	G. Tyler	10 Aug 1995	Georgia (31°20′5.4″N, 80°45′45.6″W), Atlantic Ocean
Sphyrna mokarran	KC-9	female	195	K. Jensen	23 Aug 1996	Florida (25°2′55.8″N, 82°23′3.0″W), Atlantic Ocean
Sphyrna zygaena	BJ-666	female	197	J. N. Caira	8 Jun 1996	El Barril (28°18′28″N, 112°52′31″W), Baja California, Mexico, Gulf of California, Pacific Ocean
Sphyrna zygaena	BJ-668	unkown	unkown	J. N. Caira	8 Jun 1996	El Barril (28°18′28″N, 112°52′31″W), Baja California, Mexico, Gulf of California, Pacific Ocean
Sphyrna zygaena	JN-14	female	113.2	J. N. Caira	14 Oct 1999	Shimizu (35°04′N, 138°33′E), Japan, Pacific Ocean
Sphyrna zygaena	SE-313	female	100	J. N. Caira, K. Jensen	17 Jan 2005	Mbour (14°24′22″N, 16°58′6″W), Senegal, Atlantic Ocean
Sphyrna zygaena	TW-103	female	189	H.-W. Chen, J. N. Caira, K. Jensen	10 Nov 2013	Fugang (22°47′29.8″N, 121°11′36.7″E), Taitung, Taiwan, Pacific Ocean

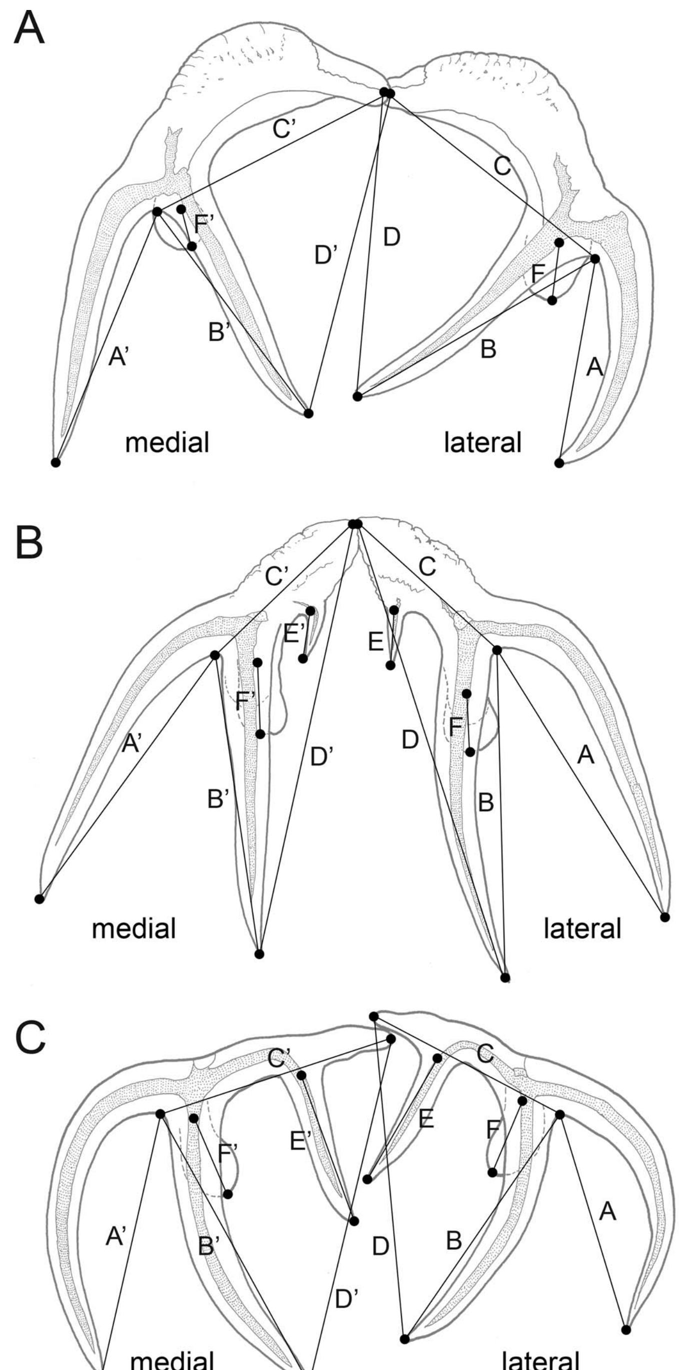

Figure 1. Hook measurements taken from bi-pronged hooks (**A**) and tri-pronged hooks (**B, C**).

Museum abbreviations used are as follows: LRP, Lawrence R. Penner Parasitology Collection, Department of Ecology and Evolutionary Biology, University of Connecticut, Storrs, Connecticut; MZUM(P), Muzium Zoologi, Universiti Malaya, Kuala Lumpur, Malaysia; MAGNT, Museum and Art Gallery Northern Territory, Darwin, Northern Territory, Australia; NMB-P, National Museum, Bloemfontein, South Africa, Parasite Collection; USNM, National Museum of Natural History, Smithsonian Institution, Washington, DC.

DNA extraction, gene amplification, and sequencing

Sequence data were generated *de novo* for 36 tapeworm specimens representing 23 species. These consisted of 2 specimens of 1 species of *Triloculatum*, 14 specimens of 6 species of the new genus, and 20 specimens of 16 species of *Phoreiobothrium*. Detailed data on each specimen are provided in Table II. The scolex and terminal portion of the strobila of 35 of the specimens were prepared as whole mounts as described above to serve as hologenophores (sensu Pleijel et al., 2008); in 1 case a photo serves as the voucher. All hologenophores have been deposited in LRP. Further information about each can be obtained from the LRP database (see https://lrpennerdb.uconn.edu/) by searching by accession number.

Sequence data for the D1–D3 region of the *28S* rDNA gene were generated in 2 ways. For a subset of specimens (i.e., those indicated with an asterisk in Table II) they were obtained using Sanger sequencing by Andrea Waeschenbach (Natural History Museum, London, U.K.) with the following extraction and amplification protocols. Total genomic DNA was extracted using the DNeasy Blood and Tissue kit or Genomictip 20/G (Qiagen, Venlo, the Netherlands) following the manufacturer's instructions. The D1–D3 region of the *28S* rDNA was amplified in 1 fragment using primer pairs LSU5 5′-TAGGTCGACCCGCTGAAYTTAAGCA-3′ (Littlewood et al., 2000) or ZX-1 5′-ACCCGCTGAATTTAAG-CATAT-3′ (modified from Van der Auwera et al., 1994) and 1500R 5′-GCTATCCTGAGGGAAACTTCG-3′ (Tkach et al., 2003). In cases of suboptimal amplification, semi-nested PCRs on primary amplicons using the same forward primer and reverse primer 1200R 5′-GCATAGTTCACCATCTTTCGG-3′ (Lockyer et al., 2003) were carried out. The total reaction volume for PCRs was 25 μl using Illustra PuRe Taq Ready-to-go PCR beads (GE Healthcare, Little Chalfont, Buckinghamshire, U.K.) and 1 μl of 10 μM of each primer. Cycling conditions were as follows: initial denaturation for 5 min at 95 C, followed by 40 cycles of 30 sec at 95 C, 30 sec at 55 C, 2 min at 72 C, and completed by 10 min at 72 C. PCR products were purified using QIAquick Gel Extraction Kit or QIAquick PCR Purification Kit (Qiagen). Sequencing of both strands was carried out on an Applied Biosystems 3730 DNA Analyser, using Big Dye version 1.1. Sequence identity was checked using the Basic Local Alignment Search Tool (BLAST) (www.ncbi.nih.gov/BLAST/). Contigs were assembled using Sequencher 4.8 (GeneCodes Corporation, Ann Arbor, Michigan). For the other subset of specimens (i.e., those indicated with a dagger in Table II), data were extracted from complete ribosomal assemblies obtained by Hannah Ralicki and Elizabeth Jockusch (University of Connecticut) using MITObim (ver. 1.9.1; Hahn et al., 2013) from Next Generation Sequencing Illumina short reads generated for a related project. GenBank and hologenophore accession numbers for all sequences generated *de novo* are provided in Table II as well as in the phylogenetic tree (Fig. 2).

Although partial sequence data for the *28S* rDNA gene are available in GenBank for 51 specimens identified as members of *Phoreiobothrium*, we chose to include only the sequence data for *Phoreiobothrium lewinense* (KF685896) from Caira et al. (2014) in our phylogenetic analysis because this is the only specimen that has been identified to species. Sequence data for outgroups were also obtained from GenBank; outgroup species selected were *Platybothrium auriculatum* Yamaguti, 1952 (KF685898) and *Symcallio violae* (Nasin, Caira, and Euzet, 1997) Bernot, Caira, and Pickering, 2015 (KF685881) from Caira et al. (2014), and *Calliobothrium euzeti* Bernot, Caira, and Pickering, 2015 (KP128029) from Bernot et al. (2015).

Phylogenetic analysis

Sequences were aligned and trimmed using the MAFFT Multiple Alignment (ver. 1.5.0; Katoh and Standley 2013; Katoh et al., 2019) plugin in Geneious Prime 2022 (ver. 2022.0.1; Geneious, Boston, Massachusetts) using default parameter settings. The final alignment consisted of 40 sequences and 1,276 nucleotide sites, with the ingroup representing 6 valid species, 8 of the 10 species described here, 9 putative new species that have been assigned unique numbers, and 3 outgroup species. Maximum Likelihood (ML) phylogenetic analysis was performed on the cluster in the Bioinformatics facility of the Institute of Systems Genomics at the University of Connecticut using IQ-TREE (ver. 1.6.10; Nguyen et al., 2015). GTR + F + R2 was selected as the best-ranked model of molecular evolution according to the corrected Akaike Information Criterion (AICc) as implemented in ModelFinder (Kalyaanamoorthy et al., 2017) in IQ-TREE. This was followed by ML tree reconstruction and the generation of 200 non-parametric bootstrap replicates. The full IQ-TREE command used was iqtree -s datamatrix.fasta -m MFP -merit AICc -b 200. Nodes with bootstrap values of ≥70% were considered to be strongly supported (Hillis and Bull, 1993).

RESULTS

Phylogenetic analysis

The tree resulting from our ML phylogenetic analysis is provided in Figure 2. This topology provides evidence of 3 subclades. The first subclade consists of species that parasitize requiem sharks and have bothridia with at least 8 subloculi. In all members of this subclade, the basal prongs of hooks in a pair are roughly equal in length relative to one another and are at least half as long as the axial and abaxial prongs. In addition, the cephalic peduncle of these species bears large gladiate spinitriches, and the uterus extends throughout much of the length of the proglottid. The second subclade consists of species that parasitize hammerhead sharks. All species of this subclade bear bothridia with at least 5 subloculi. In these species, the basal prongs of hooks in a pair are either conspicuously unequal in length (i.e., the basal prong of the medial hook is much shorter than that of the lateral hook; e.g., *Phoreiobothrium pectinatum* Linton, 1924), equal in length but both are much shorter than the axial and abaxial prongs (e.g., *Phoreiobothrium exceptum* Linton, 1924), or they are absent entirely (e.g., *Phoreiobothrium manirei* Caira, Healy, and Swanson, 1996). The cephalic peduncle of species in this second subclade bears gladiate spinitriches that are much larger than those seen in members of the other 2 subclades. Furthermore, the uterus extends only to the cirrus sac (i.e., approximately to the midlevel of the proglottid). Represented by only 2 individuals of the same species in our analysis, the third subclade is *Triloculatum*. Members of this genus parasitize requiem sharks but have bothridia with only 3 subloculi. The basal prongs of hooks in a pair resemble those seen in a subset of species parasitizing hammerhead sharks in that the basal prong of the medial hook is conspicuously shorter than that of the

Table II. Species of phoreiobothriids included in the phylogenetic analysis.

Cestode species	Unique worm specimen number	Host species	Unique host specimen number	General locality	Source	LRP accession no.	GenBank no.
Sphyrnacestus exceptus n. comb.	JW501†	*Sphyrna zygaena*	BJ-668	Gulf of California	This study	11258	PQ760886
Sphyrnacestus exceptus n. comb.	ON31*	*Sphyrna zygaena*	BJ-668	Gulf of California	This study	11257	PQ760868
Sphyrnacestus latocapitus n. sp.	JW511†	*Sphyrna lewini* 1	MS05-433	Florida, Gulf of Mexico	This study	11247	PQ760896
Sphyrnacestus latocapitus n. sp.	ON24*	*Sphyrna lewini* 1	MS05-433	Florida, Gulf of Mexico	This study	11248	PQ760879
Sphyrnacestus lewinensis n. comb.	JW507†	*Sphyrna lewini* 1	DEL-2	Florida Keys, Atlantic Ocean	This study	11259	PQ760884
Sphyrnacestus lewinensis n. comb.	JW508†	*Sphyrna lewini* 1	DEL-2	Florida Keys, Atlantic Ocean	This study	11260	PQ760885
Sphyrnacestus lewinensis n. comb.	ON22*	*Sphyrna lewini* 1	DEL-2	Florida Keys, Atlantic Ocean	This study	11261	PQ760866
Sphyrnacestus lewinensis n. comb.	TE53*	*Sphyrna lewini* 1	DEL-1	Florida Keys, Atlantic Ocean	Caira et al. (2014)	8295	KF685896
Sphyrnacestus manirei n. comb.	JW15†	*Sphyrna mokarran*	KC-9	Florida, Atlantic Ocean	This study	11263	PQ760881
Sphyrnacestus manirei n. comb.	ON28*	*Sphyrna mokarran*	KC-9	Florida, Atlantic Ocean	This study	11262	PQ760863
Sphyrnacestus paralewinensis n. sp.	ON29*	*Sphyrna mokarran*	KC-9	Florida, Atlantic Ocean	This study	11256	PQ760867
Sphyrnacestus pectinatus n. comb.	JW23†	*Sphyrna zygaena*	JN-14	Japan, Pacific Ocean	This study	11265	PQ760882
Sphyrnacestus pectinatus n. comb.	ON33*	*Sphyrna zygaena*	JN-14	Japan, Pacific Ocean	This study	11264	PQ760864
Sphyrnacestus pectinatus n. comb.	JW503†	*Sphyrna zygaena*	TW-103	Taiwan, Pacific Ocean	This study	11267	PQ760883
Sphyrnacestus pectinatus n. comb.	ON34*	*Sphyrna zygaena*	SE-313	Senegal, Atlantic Ocean	This study	11266	PQ760865
Phoreiobothrium angustivastum n. sp.	KW8†	*Carcharhinus isodon*	MS05-86	Mississippi, Gulf of Mexico	This study	11189	PQ760890
Phoreiobothrium angustivastum n. sp.	ON1*	*Carcharhinus isodon*	MS05-86	Mississippi, Gulf of Mexico	This study	11190	PQ760871
Phoreiobothrium danae n. sp.	KW6†	*Carcharhinus limbatus*	MS05-24	Mississippi, Gulf of Mexico	This study	11197	PQ760889
Phoreiobothrium magnaloculum n. sp.	JW469†	*Loxodon* cf. *macrorhinus*	MZ-30	Mozambique Channel	This study	11205	PQ760897
Phoreiobothrium perilocrocodilus	JW9†	*Negaprion acutidens*	CM03-7	Gulf of Carpentaria, Indian Ocean	This study	11224	PQ760880
Phoreiobothrium posteroporum n. sp.	ON15*	*Lamiopsis tephrodes*	BO-74	South China Sea, Pacific Ocean	This study	11212	PQ760878
Phoreiobothrium tesserascolex n. sp.	KW2*	*Carcharhinus brevipinna*	MS05-5	Mississippi, Gulf of Mexico	This study	11219	PQ760870
Phoreiobothrium waeschenbachae n. sp.	JW310†	*Scoliodon macrorhynchos*	VN-11	Gulf of Tonkin, Pacific Ocean	This study	11222	PQ760894
Phoreiobothrium waeschenbachae n. sp.	ON19*	*Scoliodon macrorhynchos*	BO-266	South China Sea, Pacific Ocean	This study	11223	PQ760875
Phoreiobothrium n. sp. 1	JW293†	*Carcharhinus brevipinna*	KA-4	Makassar Strait, Pacific Ocean	This study	11225	PQ760892
Phoreiobothrium n. sp. 2	KW299†	*Carcharhinus tilstoni*	NT-55	Arafura Sea, Pacific Ocean	This study	11226	PQ760893
Phoreiobothrium n. sp. 3	JW473†	*Rhizoprionodon oligolinx*	KA-87	Java Sea, Pacific Ocean	This study	11227	PQ760895
Phoreiobothrium n. sp. 4	ON17*	*Negaprion acutidens*	AU-30	Timor Sea, Indian Ocean	This study	11228	PQ760877
Phoreiobothrium n. sp. 5	KW291†	*Carcharhinus amboinensis* 1	NT-113	Arafura Sea, Pacific Ocean	This study	11229	PQ760898
Phoreiobothrium n. sp. 5	ON5*	*Carcharhinus amboinensis* 1	NT-113	Arafura Sea, Pacific Ocean	This study	11230	PQ760876
Phoreiobothrium n. sp. 6	KW5†	*Rhizoprionodon terraenovae*	MS05-499	Florida, Gulf of Mexico	This study	11231	PQ760888
Phoreiobothrium n. sp. 7	KW9†	*Carcharhinus isodon*	MS05-495	Florida, Gulf of Mexico	This study	11232	PQ760891
Phoreiobothrium n. sp. 8	ON4*	*Carcharhinus acronotus*	KC-5	Florida, Gulf of Mexico	This study	11233	PQ760872
Phoreiobothrium n. sp. 9	ON9*	*Carcharhinus limbatus*	KC-7	Florida, Gulf of Mexico	This study	11234	PQ760873
Phoreiobothrium n. sp. 9	ON12*	*Carcharhinus limbatus*	MS05-435	Florida, Gulf of Mexico	This study	11235	PQ760874
Triloculatum bullardi	KW4†	*Carcharhinus brevipinna*	MS05-5	Mississippi, Gulf of Mexico	This study	11269	PQ760887
Triloculatum bullardi	ON7*	*Carcharhinus brevipinna*	MS05-456	Mississippi, Gulf of Mexico	This study	11268	PQ760869

* Sequence data for the D1–D3 region of the *28S* rDNA gene generated using Sanger sequencing.
† Sequence data for the D1–D3 region of the *28S* rDNA gene extracted from complete ribosomal assemblies generated using MTObim (ver. 1.9.1, Hahn et al., 2013) with Illumina short reads.

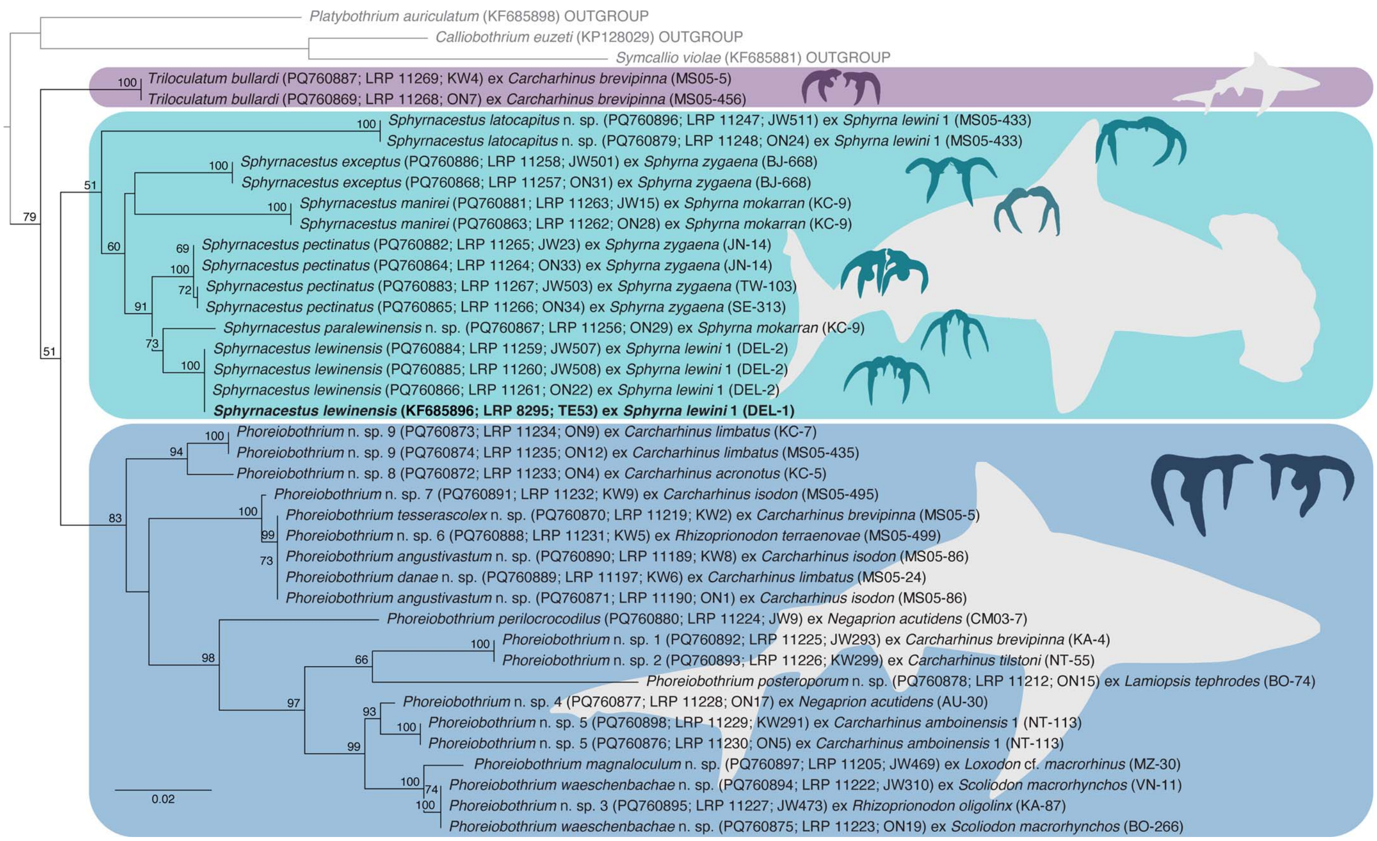

Figure 2. Phylogenetic relationships of 37 specimens of *Sphyrnacestus* n. gen., *Phoreiobothrium*, and *Triloculatum* resulting from a Maximum Likelihood analysis of 1,276 bp of the D1–D3 region of the *28S* rDNA gene. Taxon labels include cestode species with GenBank accession number, LRP hologenophore accession number, unique worm specimen number in parentheses, and host species followed by unique host specimen number in parentheses. Specimen for which sequence data were obtained from GenBank is indicated in boldface type. Nodal support values calculated with 200 non-parametric bootstrap replicates. Scale bar indicates number of substitutions per site. Color version available online.

lateral hook, and the basal prongs of both hooks are much shorter than the axial and abaxial prongs of both hooks. The cephalic peduncle of species of *Triloculatum* are covered with large gladiate spinitriches. The uterus of members of this genus also extends much of the length of the proglottid. This latter subclade is sister to the group consisting of the first 2 subclades.

To align the classification of these cestodes with their phylogenetic relationships we propose that each subclade be recognized as a distinct genus. Given that *Phoreiobothrium lasium* Linton, 1889, the type species of *Phoreiobothrium*, parasitizes a species of requiem shark and is morphologically consistent with members of the first subclade, this genus name is retained for members of this group. *Sphyrnacestus* n. gen. is erected to house species in the second subclade, all of which parasitize hammerhead sharks. Species in the second subclade that were originally described in *Phoreiobothrium* are transferred to this new genus; the diagnosis of *Phoreiobothrium* is revised below to reflect the transfer of these species. *Triloculatum* is retained as the valid genus name for members of the third subclade.

Given that both morphological and molecular data support the fact that *Phoreiobothrium*, *Triloculatum*, and *Sphyrnacestus* n. gen. appear to represent a cohesive group, we are hereby resurrecting the family Phoreiobothriidae Baer and Euzet, 1955, to house these 3 genera.

DESCRIPTIONS

Phoreiobothriidae Baer and Euzet, 1955

Diagnosis: Onchoproteocephalidea II. Worms euapolytic or essentially hyperapolytic. Scolex with 4 bothridia and cephalic peduncle. Bothridia with anterior muscular pad, 1 pair of hooks, and 1 anterior and 1 posterior loculus. Muscular pad with apical sucker or in form of loculus, with or without apical papillae or papillae on latero-anterior margins. Anterior loculus longer than posterior loculus, with or without small papillae on posterior margin. Posterior loculus with single row of 3 or more subloculi; boundary between anterior loculus and sublocular region with single or double septum. Hooks tri-pronged or occasionally bi-pronged, hollow, with talon. Cephalic peduncle covered with large or extremely large gladiate spinitriches. Strobila with sparsely arranged gladiate spinitriches throughout length. Proglottids acraspedote or occasionally craspedote. Testes numerous, arranged in 2 or more columns, 1 layer deep; post-poral field of testes present. Vas deferens minimal. Cirrus sac small. Genital pores lateral, irregularly alternating. Vagina opening anterior to cirrus sac. Ovary symmetrical, H-shaped or inverted A-shaped in frontal view, bi-lobed in cross section. Vitelline follicles in 2 lateral bands; each band consisting of at least 2 columns of follicles, extending much of length of proglottid, interrupted by terminal genitalia. Uterus saccate, medioventral, extending to level of terminal genitalia or to near anterior margin of testicular field. Excretory ducts in 2 lateral pairs. Parasites of Sphyrnidae and Carcharhinidae. Cosmopolitan.

Type genus: Phoreiobothrium Linton, 1889.

Additional genera: Sphyrnacestus n. gen., *Triloculatum* Caira and Jensen, 2009.

Remarks

Baer and Euzet (1955) established the family Phoreiobothriidae with *Phoreiobothrium* as its type genus. However, in the most recent comprehensive treatment of the family Onchobothriidae Braun, 1900, Euzet (1994) followed the convention at the time and considered all acetabulate genera with hooks that parasitize elasmobranchs, including *Phoreiobothrium*, as onchobothriids. Over the past 3 decades, work on many of these hooked genera has considerably altered our understanding of their interrelationships, revealing them to consist of multiple independent lineages (e.g., Olson and Caira, 1999; Caira et al., 2014). In fact, in their treatments of these taxa, Caira and colleagues considered a subset of these genera, including *Phoreiobothrium* and *Triloculatum*, to belong to the order Onchoproteocephalidea II (see Caira et al., 2017a) and assigned the remaining hooked genera to the nonmonophyletic assemblage of taxa which they referred to as the "Tetraphyllidea relics" (see Caira et al., 2017b). In the absence of a more taxon-dense phylogenetic analysis, in neither treatment did the authors attempt to revise the family-level classification.

By resurrecting the Phoreiobothriidae, we have begun the process of establishing a family-level framework that represents monophyletic groups for at least some of the Onchoproteocephalidea II. The diagnosis presented above includes information from the most recent diagnosis of the family, which is that of Euzet (1959), modified to accommodate species of *Phoreiobothrium* described over the past 65 yr as well as species of *Triloculatum* and *Sphyrnacestus* n. gen.

Sphyrnacestus n. gen.

Diagnosis: Onchoproteocephalidea II; Phoreiobothriidae. Worms euapolytic or essentially hyperapolytic. Scolex with 4 bothridia and cephalic peduncle. Bothridia with anterior muscular pad, 1 pair of hooks, and 1 anterior and 1 posterior loculus. Muscular pad with apical sucker and 3 to 6 small apical papillae, occasionally with multiple papillae on latero-anterior and medio-anterior margins. Anterior loculus conspicuously longer than posterior loculus, posterior margin occasionally with numerous small papillae; boundary between anterior loculus and sublocular region with double septum. Posterior loculus with single row of 5 to 11 subloculi. Hooks tri-pronged or occasionally bi-pronged, hollow, with talon; in tri-pronged hooks, basal prongs of medial and lateral hooks less than half as long as axial and abaxial prongs, or basal prong of lateral hook less than half as long as axial and abaxial prongs and basal prong of medial hook nearly as long as axial and abaxial prongs. Cephalic peduncle with extremely large gladiate spinitriches. Strobila with sparsely arranged gladiate spinitriches throughout length. Proglottids acraspedote. Testes numerous, arranged in multiple columns, 1 layer deep; post-poral field of testes present. Vas deferens minimal. Cirrus sac small. Genital pores lateral, irregularly alternating. Vagina opening anterior to cirrus sac. Ovary posterior, symmetrical, inverted A-shaped in frontal view, bi-lobed in cross section. Vitelline follicles in 2 lateral bands; each band consisting of at least 2 columns of follicles, extending length of proglottid, interrupted by terminal genitalia. Uterus saccate, medioventral, extending to level of terminal genitalia. Excretory ducts in 2 lateral pairs. Parasites of Sphyrnidae. Cosmopolitan.

Type species: Sphyrnacestus ananas n. sp.

Additional species: Sphyrnacestus eusphyrensis n. sp., *Sphyrnacestus exceptus* (Linton, 1924) n. comb., *Sphyrnacestus latocapitus* n. sp., *Sphyrnacestus lewinensis* (Caira, Richmond, and Swanson, 2005) n. comb., *Sphyrnacestus manirei* (Caira, Healy, and Swanson, 1996) n. comb., *Sphyrnacestus paralewinensis* n. sp., *Sphyrnacestus pectinatus* (Linton, 1924) n. comb., *Sphyrnacestus puriensis* (Srivastav and Capoor, 1982) n. comb.

ZooBank registration: urn:lsid:zoobank.org:act:29A01FF5-EDDF-4A07-9BBB-5072308EB7F5.

Etymology: The name of this cestode genus reflects the fact that its members parasitize hammerhead sharks (i.e., family Sphyrnidae).

Remarks

Sphyrnacestus n. gen., *Phoreiobothrium*, and *Triloculatum* are unique among the hooked genera that parasitize elasmobranchs in possessing bothridia with a posterior loculus divided into a row of subloculi. *Sphyrnacestus* n. gen. differs from *Phoreiobothrium* in bearing hooks in a pair in which the basal prongs are conspicuously unequal in length, highly reduced, or absent, rather than being relatively similar in length and more than half as long as the axial and abaxial prongs. The new genus is easily distinguished from *Triloculatum* in that its bothridia bear 5 to 11, rather than 3, subloculi. In addition, the new genus possesses a double, rather than a single, septum at the boundary between the anterior loculus and the sublocular region. *Sphyrnacestus* n. gen. further differs from both genera in that its uterus extends only to about the midlevel, rather than to near the anterior margin, of the proglottid, and also in that the gladiate spinitriches on the cephalic peduncle are typically much larger than those on the cephalic peduncle of members of both other genera.

Phoreiobothrium Linton, 1889 emend.

Diagnosis: Onchoproteocephalidea II; Phoreiobothriidae. Worms euapolytic or essentially hyperapolytic. Scolex with 4 bothridia and cephalic peduncle. Bothridia with anterior muscular pad, 1 pair of hooks, and 1 anterior and 1 posterior loculus, with or without constriction immediately posterior to hooks. Muscular pad in form of loculus, occasionally with 4–5 small apical papillae, lacking papillae on latero-anterior margins. Anterior loculus longer than posterior loculus, posterior margin occasionally with numerous small papillae; boundary between anterior loculus and sublocular region with double septum. Posterior loculus with single row of 8 or more subloculi. Hooks tri-pronged, hollow, with talon; basal prongs of medial and lateral hooks more than half as long as axial and abaxial prongs. Cephalic peduncle with large gladiate spinitriches. Strobila with sparsely arranged gladiate spinitriches throughout length. Proglottids acraspedote. Testes numerous, arranged in 2 or more columns, 1 layer deep; post-poral field of testes present. Vas deferens minimal. Cirrus sac small. Genital pores lateral, irregularly alternating. Vagina opening anterior to cirrus sac. Ovary posterior, symmetrical, H-shaped or inverted

A-shaped in frontal view, bi-lobed in cross section. Vitelline follicles in 2 lateral bands; each band consisting of 2 or more columns of follicles, extending length of proglottid, interrupted by terminal genitalia. Uterus saccate, medioventral, extending from ootype, stopping short of anterior margin of testicular field. Excretory ducts in 2 lateral pairs. Parasites of Carcharhinidae and rarely (i.e., *P. tiburonis*) Sphyrnidae. Cosmopolitan.

Type species: Phoreiobothrium lasium Linton, 1889.

Additional species: Phoreiobothrium angustivastum n. sp., *Phoreiobothrium anticaporum* Caira, Richmond, and Swanson, 2005, *Phoreiobothrium blissorum* Caira, Richmond, and Swanson, 2005, *Phoreiobothrium danae* n. sp., *Phoreiobothrium golchini* Darvishi and Haseli, 2019, *Phoreiobothrium iraniense* Javadi and Haseli, 2002, *Phoreiobothrium jahki* Caira and Jensen, 2015; *Phoreiobothrium magnaloculum* n. sp., *Phoreiobothrium martini* Van Der Spuy, Smit, Naidoo, and Schaeffner, 2023, *Phoreiobothrium nadiae* Caira and Jensen, 2015, *Phoreiobothrium perilocrocodilus* Caira, Richmond, and Swanson, 2005, *Phoreiobothrium posteroporum* n. sp.; *Phoreiobothrium robertsoni* Caira, Richmond, and Swanson, 2005, *Phoreiobothrium rozatii* Darvishi and Haseli, 2019, *Phoreiobothrium sarahae* Javadi and Haseli, 2022, *Phoreiobothrium sorrahcola* Ganjgah and Haseli, 2020, *Phoreiobothrium swaki* Caira and Jensen, 2015, *Phoreiobothrium tesserascolex* n. sp., *Phoreiobothrium tiburonis* Cheung, Nigrelli, and Ruggieri, 1982, *Phoreiobothrium waeschenbachae* n. sp.

Remarks

The most recent diagnosis of *Phoreiobothrium* is that of Caira and Jensen (2009). That diagnosis has been revised above to accommodate the removal of the 5 species transferred here to *Sphyrnacestus* and the addition of the 6 new species described below. Additional revisions were made to help align the diagnosis of this genus with those of *Sphyrnacestus* and *Triloculatum*. These modifications expand and standardize information on apolysis, cephalic peduncle, features of the muscular pad, microtriches, arrangement of the testes, vas deferens, cirrus sac, vitelline follicles, uterus, and excretory ducts. The most notable change is the recognition that some species possess an inverted A-shaped, rather than H-shaped, ovary. Our work here leads us to suspect that at least some of the members of this genus that are currently described as possessing an H-shaped ovary may ultimately be found to possess an ovary that is inverted A-shaped in frontal view.

***Triloculatum* Caira and Jensen, 2009 emend.**

Diagnosis: Onchoproteocephalidea II; Phoreiobothriidae. Worms euapolytic. Scolex with 4 bothridia and cephalic peduncle. Bothridia with anterior muscular pad, 1 pair of hooks, and 1 anterior and 1 posterior loculus. Muscular pad in form of loculus, lacking apical sucker, apical papillae, and papillae on latero-anterior margins. Anterior loculus longer than posterior loculus; boundary between anterior loculus and sublocular region with single septum. Posterior loculus with single row of 3 subloculi. Hooks tri-pronged, hollow, with talon; basal prongs of medial and lateral hooks less than half as long as axial and abaxial prongs. Cephalic peduncle with large gladiate spinitriches. Strobila with sparsely arranged gladiate spinitriches throughout length. Proglottids acraspedote or craspedote. Testes numerous, arranged in multiple columns, 1 layer deep; post-poral field of testes present. Vas deferens minimal. Cirrus sac small. Genital pores lateral, irregularly alternating. Vagina opening anterior to cirrus sac. Ovary posterior, symmetrical, H-shaped in frontal view, bi-lobed in cross section. Vitelline follicles in 2 lateral bands; each band consisting of 2 to many columns of follicles, extending length of proglottid, interrupted by terminal genitalia. Uterus saccate, medioventral, extending to near anterior margin of proglottid. Excretory ducts in 2 lateral pairs. Parasites of Carcharhinidae. Cosmopolitan.

Type species: Triloculatum triloculatum (Linton, 1901) Caira and Jensen, 2009.

Additional species: Triloculatum andersonorum Caira and Jensen, 2009, *Triloculatum bullardi* Caira and Jensen, 2009, *Triloculatum geeceearelensis* Caira and Jensen, 2009, *Triloculatum jodyi* Caira and Jensen, 2009, *Triloculatum oregontwoae* Caira and Jensen, 2009.

Remarks

Triloculatum was erected by Caira and Jensen (2009). Essentially no work has been done on this genus since that time. The diagnosis of *Triloculatum* is revised above solely to help align it with those of *Phoreiobothrium* and *Sphyrnacestus*. These modifications expand and standardize information on the cephalic peduncle, features of the muscular pad, microtriches, arrangement of the testes, vas deferens, cirrus sac, vitelline follicles, uterus, and excretory ducts.

DESCRIPTIONS

In the sections that follow, we present descriptions of 4 new species of *Sphyrnacestus* and 6 new species of *Phoreiobothrium*. These are followed by a section that provides information on the hosts and localities of the 16 additional putative new species of *Phoreiobothrium* and 1 new species of *Triloculatum* that we are not formally describing here, but that were included in our molecular phylogenetic analysis and/or for which a scolex was available for SEM.

***Sphyrnacestus ananas* n. sp.**

(Figs. 3, 4A–D)

Description (based on whole mounts of 9 complete immature worms and 3 scoleces prepared for SEM): Worms 2.2–3.3 mm (2.6 ± 0.4; 8) long, essentially hyperapolytic, greatest width generally at level of terminal proglottid (Fig. 3C); 7–13 (10 ± 2; 9) proglottids per worm. Scolex (Fig. 3A) consisting of scolex proper bearing 4 bothridia and cephalic peduncle, 180–211 (193 ± 11; 9) wide at level of subloculi. Bothridia 145–169 (151 ± 6; 9; 17) long by 76–97 (90 ± 5; 9; 18) wide; each with anterior muscular pad, 1 pair of hooks, and post-hook region divided into 1 anterior and 1 posterior loculus (Fig. 3A). Muscular pad 30–43 (35 ± 4; 9; 18) long by 79–92 (84 ± 4; 9; 18) wide, with apical sucker and 3–4 apical papillae, lacking papillae on latero-anterior and medio-anterior margins. Apical sucker 17–26 (20 ± 3; 9; 17) long by 19–31 (24 ± 4; 9; 17) wide. Anterior loculus considerably longer than posterior loculus, 83–101 (92 ± 5; 9; 18) long, posterior margin without small papillae; boundary between anterior loculus and sublocular region with double septum (Fig. 4A). Posterior loculus 14–25 (20 ± 3; 9; 18) long, subdivided into 5 (N = 9) subloculi; subloculi 14–23 (18 ± 3; 9; 28) wide. Hooks bi-pronged, hollow, with axial and abaxial prongs (Fig. 3B); basal prongs lacking; each hook with blunt talon embedded in musculature of scolex, covered with thin layer of tissue (Fig. 4A); bases elongate,

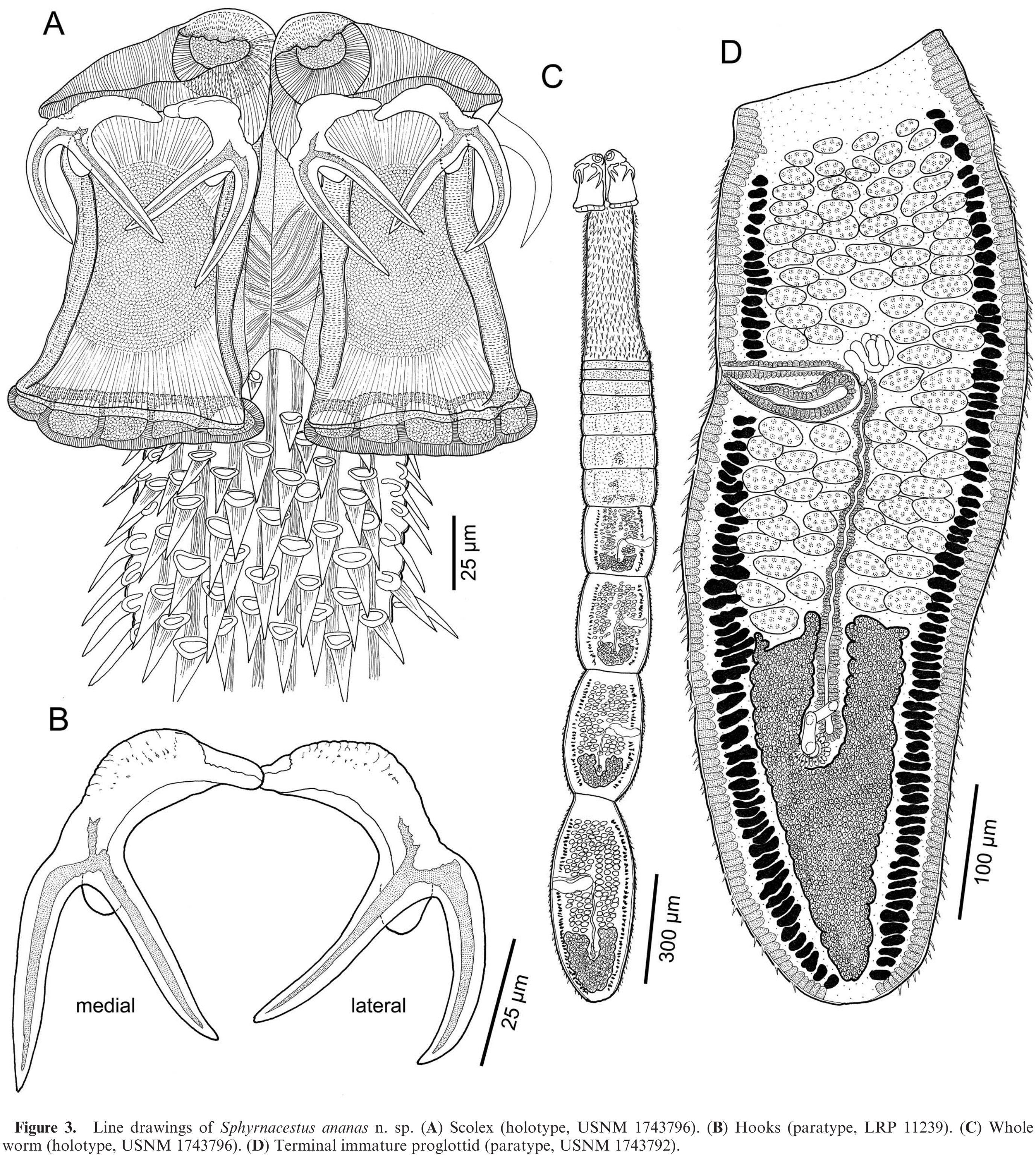

Figure 3. Line drawings of *Sphyrnacestus ananas* n. sp. (**A**) Scolex (holotype, USNM 1743796). (**B**) Hooks (paratype, LRP 11239). (**C**) Whole worm (holotype, USNM 1743796). (**D**) Terminal immature proglottid (paratype, USNM 1743792).

tapering towards medial region of bothridium. Lateral hook measurements: A 26–41 (36 ± 4; 9; 15), B 29–49 (42 ± 5; 9; 16), C 35–44 (40 ± 3; 9; 16), D 38–63 (51 ± 7; 9; 16), F 11–19 (14 ± 2; 9; 16); medial hook measurements: A′ 27–51 (42 ± 6; 9; 16), B′ 27–51 (43 ± 6; 9; 16), C′ 24–42 (36 ± 5; 9; 16), D′ 32–61 (50 ± 8; 9; 16), F′ 10–18 (14 ± 2; 9; 16). Cephalic peduncle 326–507 (436 ± 52; 9) long.

Apex of scolex proper, muscular pad, and proximal (Fig. 4D) and distal (Fig. 4C) bothridial surfaces covered with papilliform filitriches only. Cephalic peduncle covered with acicular filitriches

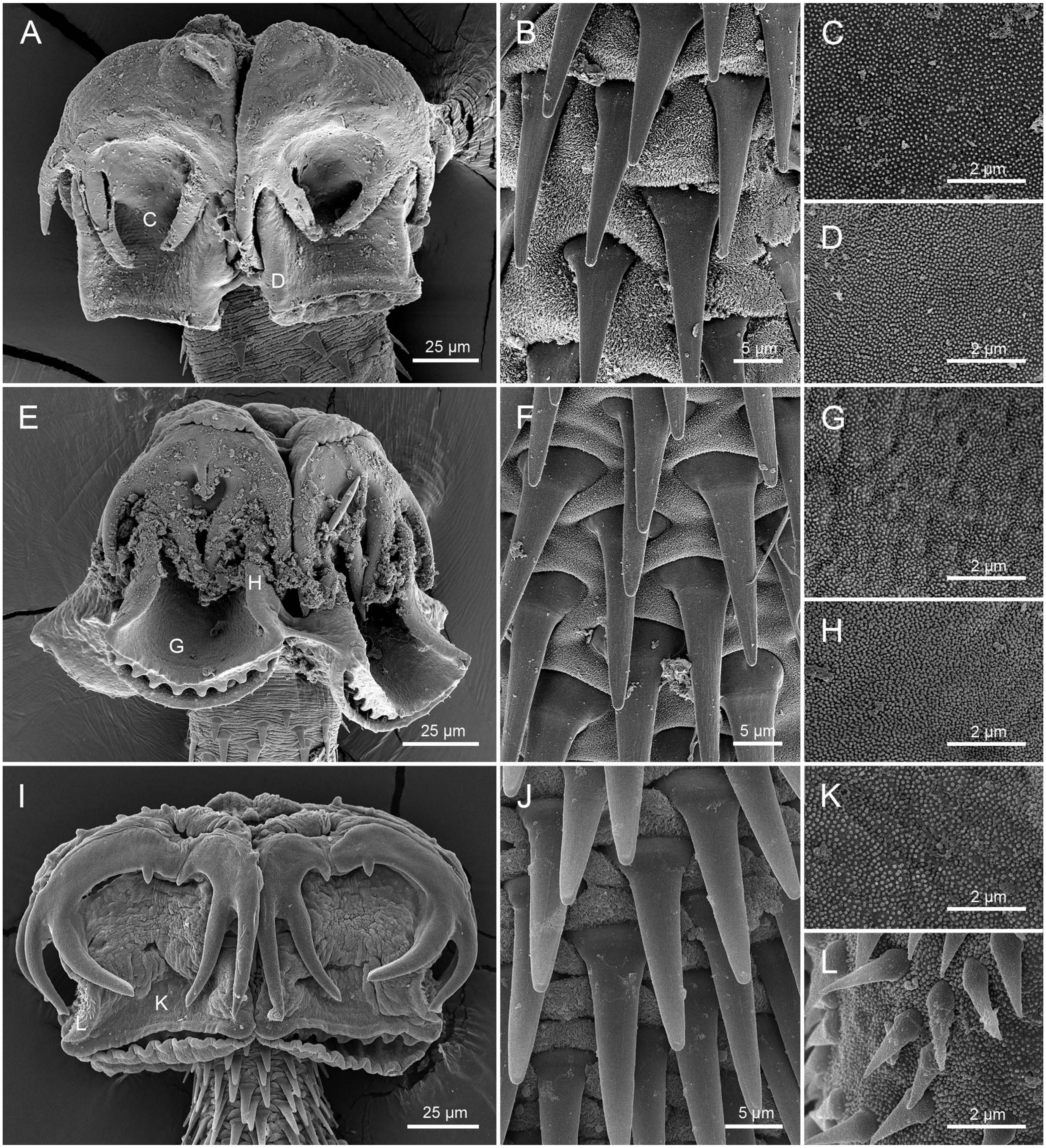

Figure 4. Scanning electron micrographs of *Sphyrnacestus ananas* n. sp. (**A–D**), *Sphyrnacestus eusphyrensis* n. sp. (**E–H**), and *Sphyrnacestus latocapitus* n. sp. (**I–L**). (**A**) Scolex of *S. ananas* n. sp., small letters indicate locations of C, D. (**B**) Extremely large gladiate spinitriches and small acicular filitriches on cephalic peduncle of *S. ananas* n. sp. (**C**) Papilliform filitriches on distal surface of bothridium of *S. ananas* n. sp. (**D**) Papilliform filitriches of proximal surface of bothridium of *S. ananas* n. sp. (**E**) Scolex of *S. eusphyrensis* n. sp., small letters indicate locations of G, H. (**F**) Extremely large gladiate spinitriches and papilliform filitriches on cephalic peduncle of *S. eusphyrensis* n. sp. (**G**) Papilliform filitriches on distal surface of bothridium *S. eusphyrensis* n. sp. (**H**) Papilliform filitriches on proximal surface of bothridium of *S. eusphyrensis* n. sp. (**I**) Scolex of *S. latocapitus* n. sp., small letters indicate locations of K, L. (**J**) Extremely large gladiate spinitriches and acicular filitriches on cephalic peduncle of *S. latocapitus* n. sp. (**K**) Papilliform filitriches on distal surface of bothridium of *S. latocapitus* n. sp. (**L**) Small gladiate spinitriches and papilliform filitriches on proximal surface of bothridium of *S. latocapitus* n. sp.

and extremely large gladiate spinitriches (Fig. 4B). Strobila covered with capilliform filitriches and sparsely arranged smaller gladiate spinitriches decreasing in density posteriorly.

Proglottids acraspedote. Immature proglottids 7–13 (10 ± 2; 9) in number, initially wider than long, becoming longer than wide with maturity (Fig. 3D). Posterior-most immature proglottid (Fig. 3D) 547–892 (725 ± 114; 9) long by 172–301 (225 ± 42; 9) wide. Fully mature proglottids not observed. Testes 87–112 (100 ± 12; 9) in total number, 15–22 (18 ± 3; 9) in post-poral field, elongate oval to round, 13–25 (18 ± 3; 9; 45) long by 16–40 wide (27 ± 6; 9; 45), 1 layer deep in cross section, extending from anterior margin of ovary to near anterior margin of proglottid, in 4–5 irregular columns anterior to cirrus sac. Vas deferens minimal, coiling at antero-medial margin of cirrus sac, entering cirrus sac at its antero-medial margin. Cirrus sac dolioform, slightly bent anteriorly, 94–116 (102 ± 7; 9) long by 25–39 (33 ± 5; 9) wide, containing coiled cirrus; cirrus spinitriches not observed. Genital pores lateral, irregularly alternating, 51–67% (58 ± 5; 9) of proglottid length from posterior end. Vagina weakly sinuous, extending along midline of proglottid from ootype region to anterior margin of cirrus sac, then laterally along anterior margin of cirrus sac, opening into common genital atrium anterior to cirrus sac. Ovary at posterior margin of proglottid, symmetrical, inverted-A shaped in frontal view, bi-lobed in cross section, very weakly lobulated, 137–317 (215 ± 55; 9) long by 119–189 (147 ± 20; 9) wide. Mehlis' gland posterior to ovarian isthmus. Vitelline follicles slightly oval, in 2 lateral bands; each band consisting of 1 dorsal and 1 ventral column of follicles, extending from posterior margin of proglottid to anterior margin of testicular field, interrupted dorsally and ventrally by terminal genitalia, uninterrupted by ovary. Uterus saccate, medioventral, extending from ootype to level of terminal genitalia. Excretory ducts in 2 lateral pairs. Gravid proglottids and eggs not observed.

Taxonomic summary

Type and only known host: *Sphyrna lewini* 1 (Sphyrnidae: Carcharhiniformes).

Type locality: Tampa Bay (27°33′8.4″N, 82°39′9.0″W), Florida, Gulf of Mexico, Atlantic Ocean (unique host specimen no. MOT-25). Additional host specimen from the type locality: MOT-24.

Additional localities: None.

Site of infection: Spiral intestine.

Specimens deposited: Holotype (USNM 1743796) and 4 paratypes (USNM 1743792–1743795); 4 paratypes (LRP 11238–11241). Scoleces prepared for SEM retained with JNC at the University of Connecticut.

ZooBank registration: urn:lsid:zoobank.org:act:290F6E7E-C3F7-4F63-8772-C4A4EBE618E1.

Etymology: The name is derived from *Ananas*, the generic name for the pineapple and its relatives, in reference to the extremely large spinitriches on the cephalic peduncle of this species.

Remarks

Sphyrnacestus ananas n. sp. conspicuously differs from *S. exceptus*, *S. lewinensis*, *S. pectinatus*, and *S. puriensis* in that both its medial and lateral hooks lack, rather than possess, basal prongs. With respect to *S. manirei*, the only other member of the genus that lacks basal prongs, this new species possesses fewer proglottids (7–13 vs. 20–33) and a shorter sublocular region (14–25 vs. 26–46).

Sphyrnacestus eusphyrensis n. sp.

(Figs. 4E–H, 5)

Description (based on whole mounts of 5 complete immature worms, 1 incomplete immature worm, 1 incomplete mature worm, and 1 scolex prepared for SEM): Worms 6.0–9.1 mm (7.4 ± 1.2; 5) long, euapolytic, greatest width generally at level of terminal proglottid (Fig. 5D); 17–23 (20 ± 2; 6) proglottids per worm. Scolex (Fig. 5A) consisting of scolex proper bearing 4 bothridia and cephalic peduncle, 175–193 (187 ± 7; 5) wide at level of subloculi. Bothridia 117–145 (130 ± 10; 5; 7) long by 77–94 (87 ± 6; 5; 7) wide; each with anterior muscular pad, 1 pair of hooks, and post-hook region divided into 1 anterior and 1 posterior loculus (Fig. 5A). Muscular pad 25–34 (29 ± 4; 3; 4) long by 52–64 (57 ± 5; 4; 5) wide, with apical sucker and 4–5 apical papillae, lacking papillae on latero-anterior and medio-anterior margins. Apical sucker 11–13 (12 ± 1; 4; 5) long by 19–30 (23 ± 4; 4; 5) wide. Anterior loculus considerably longer than posterior loculus, 71–104 (86 ± 12; 5; 7) long; posterior margin without small papillae; boundary between anterior loculus and sublocular region with double septum (Fig. 4E). Posterior loculus 11–20 (17 ± 3; 5; 7) long, subdivided into 7–10 (8 ± 1; 5; 7) subloculi; subloculi 8–12 (10 ± 1; 5; 18) wide. Hooks tri-pronged, hollow, with basal, axial, and abaxial prongs (Fig. 5B); basal prongs less than half as long as axial and abaxial prongs; each hook with blunt talon embedded in musculature of scolex, covered with thin layer of tissue (Fig. 4E); bases short; lateral hook base more robust than medial hook base. Lateral hook measurements: A 24–38 (31 ± 5; 5; 6), B 28–48 (39 ± 7; 5; 6), C 18–29 (24 ± 4; 5; 6), D 35–63 (48 ± 10; 5; 6), E 9–18 (13 ± 3; 5; 6), F 10–16 (13 ± 3; 5; 6); medial hook measurements: A′ 34–41 (37 ± 3; 6; 8), B′ 32–47 (41 ± 5; 6; 8), C′ 20–31 (24 ± 3; 6; 8), D′ 38–64 (53 ± 9; 6; 8), E′ 10–12 (11 ± 1; 6; 8), F′ 9–19 (14 ± 4; 6; 8). Cephalic peduncle 910–2,135 (1,635 ± 464; 6) long.

Apex of scolex proper, muscular pad, and proximal (Fig. 4H) and distal (Fig. 4G) bothridial surfaces covered with papilliform filitriches only. Cephalic peduncle covered with papilliform filitriches and extremely large gladiate spinitriches (Fig. 4F). Strobila covered with capilliform filitriches and sparsely arranged smaller gladiate spinitriches decreasing in density posteriorly.

Proglottids acraspedote. Immature proglottids 16–23 (20 ± 3; 6) in number, initially wider than long, becoming longer than wide with maturity (Fig. 5D). Posterior-most immature proglottid 860–1,169 (1,021 ± 118; 6) long by 238–464 (350 ± 80; 6) wide. Mature proglottids 1 (N = 1) in number. Terminal mature proglottid (Fig. 5E) 1,132 (N = 1) long by 477 (N = 1) wide. Testes 111–120 (116 ± 3; 5) in total number, 13–20 (17 ± 3; 5) in post-poral field, elongate oval to round, 25–47 (32 ± 5; 5; 25) long by 31–79 (54 ± 13; 5; 25) wide, 1 layer deep in cross section, extending from anterior margin of ovary to near anterior margin of proglottid, in 4–5 irregular columns anterior to cirrus sac. Vas deferens minimal, coiling at antero-medial margin of cirrus sac, entering cirrus sac at its antero-medial margin. Cirrus sac dolioform (Fig. 5C), 99–179 (135 ± 39; 5) long by 39–70 (51 ± 13; 5) wide, containing coiled cirrus; cirrus armed with small spinitriches. Genital pores lateral, irregularly alternating, 46–57% (52 ± 5; 6) of proglottid length from posterior end. Vagina weakly sinuous, extending along midline of proglottid from ootype region to anterior margin of cirrus sac, then laterally along

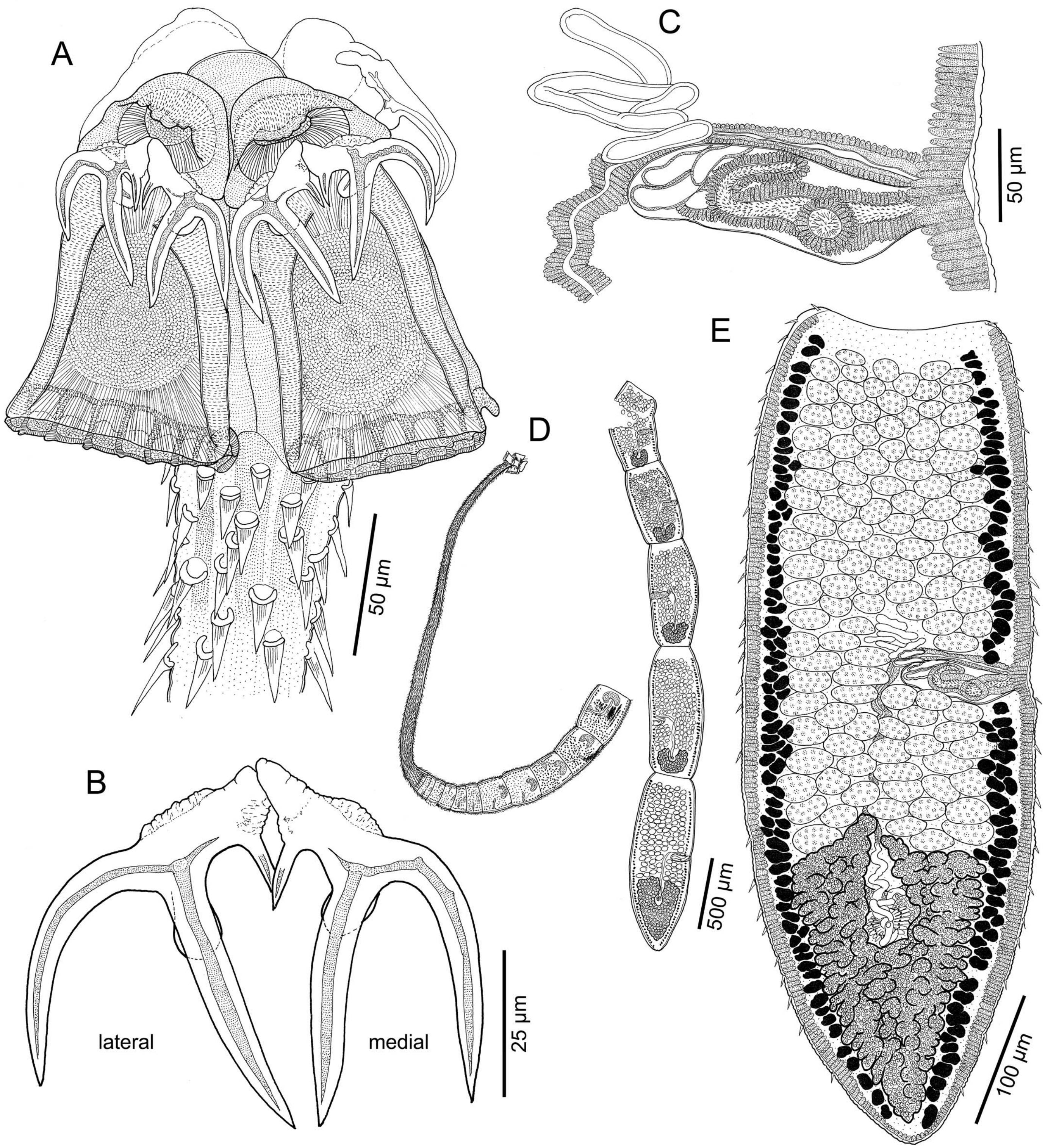

Figure 5. Line drawings of *Sphyrnacestus eusphyrensis* n. sp. (**A**) Scolex (paratype, USNM 1743797). (**B**) Hooks (paratype, LRP 11242). (**C**) Terminal genitalia (holotype, MAGNT D1950). (**D**) Whole worm (holotype, MAGNT D1950). (**E**) Terminal immature proglottid (holotype, MAGNT D1950).

anterior margin of cirrus sac, opening into common genital atrium anterior to cirrus sac. Ovary at posterior margin of proglottid, symmetrical, inverted-A shaped in frontal view, bi-lobed in cross section, lobulated, 197–357 (270 ± 51; 5) long by 133–273 (212 ± 60; 5) wide. Mehlis' gland posterior to ovarian isthmus. Vitelline follicles round to slightly oval, in 2 lateral bands; each band consisting of 1 dorsal and 1 ventral column of follicles, extending from posterior margin of proglottid to anterior margin of testicular field, interrupted dorsally and ventrally by terminal genitalia, uninterrupted by ovary. Uterus saccate, medioventral, extending from ootype to level of terminal genitalia. Excretory ducts in 2 lateral pairs. Gravid proglottids and eggs not observed.

Taxonomic summary

Type and only known host: Eusphyra blochii (Cuvier) (Sphyrnidae: Carcharhiniformes).

Type locality: Dundee Beach (12°45′33″S, 130°21′7″E), Northern Territory, Australia, Fog Bay, Timor Sea, Indian Ocean (unique host specimen no. AU-70). Additional host specimen from the type locality: AU-71.

Additional localities: None.

Site of infection: Spiral intestine.

Specimens deposited: Holotype (MAGNT D1950) and 1 paratype (MAGNT D1951); 3 paratypes (LRP 11242–11244); 2 paratypes (USNM 1743797 and USNM 1743798). Scolex prepared for SEM retained with JNC at the University of Connecticut.

Molecular material: None.

ZooBank registration: urn:lsid:zoobank.org:act:50AF337D-CA75-41DD-871C-E124CDA14AA8.

Etymology: This name refers to the host of this species, which is a member of the hammerhead shark genus *Eusphyra*.

Remarks

Sphyrnacestus eusphyrensis n. sp. conspicuously differs from *S. ananas* and *S. manirei* in that its hooks possess, rather than lack, basal prongs, and its bothridia possess a greater number of subloculi (7–10 vs. 5 and 5, respectively). It differs from *S. pectinatus* in that the basal prong of each medial hook is considerably shorter than, rather than more than half as long as, the axial and abaxial prongs of that hook. Unlike *S. exceptus*, in which the basal prongs are essentially only small tubercles, those of this new species are conspicuous. In addition, the bothridia of this new species bear a greater number of subloculi than do those of *S. exceptus* (7–10 vs. 6). The bothridia of *S. eusphyrensis* n. sp. bear a smaller number of subloculi than those of the relatively poorly known *S. puriensis* (7–10 vs. 12). The new species most closely resembles *S. lewinensis* but is readily distinguished from the latter species in its possession of a greater number of proglottids (17–23 vs. 5–11) and fewer testes (111–120 vs. 173).

***Sphyrnacestus latocapitus* n. sp.**

(Figs. 4I–L, 6)

Description (based on whole mounts of 2 complete immature worms, 2 hologenophores, 1 larval worm, and 1 scolex prepared for SEM): Worms 2.1–2.7 mm (N = 2) long, hyperapolytic, greatest width generally at level of terminal proglottid (Fig. 6C); 12–16 (N = 2) proglottids per worm. Scolex (Fig. 6A) consisting of scolex proper bearing 4 bothridia and cephalic peduncle, 168–186 (179 ± 8; 5) wide at level of subloculi. Bothridia 104–188 (131 ± 26; 5; 10) long by 67–84 (74 ± 6; 5; 10) wide; each with anterior muscular pad, 1 pair of hooks, and post-hook region divided into 1 anterior and 1 posterior loculus (Fig. 6A). Muscular pad 24–29 (27 ± 2; 5; 10) long by 44–66 (58 ± 8; 5; 10) wide, with apical sucker, 4–5 apical papillae, and 5–6 papillae on latero-anterior margins and 2–3 papillae on medio-anterior margins (Fig. 4I). Apical sucker 13–18 (16 ± 1; 5; 10) long by 18–24 (21 ± 2; 5; 10) wide. Anterior loculus considerably longer than posterior loculus, 65–96 (83 ± 10; 5; 9) long, posterior margin without small papillae; boundary between anterior loculus and sublocular region with double septum (Fig. 4I). Posterior loculus 21–31 (25 ± 4; 5; 9) long, subdivided into 9–10 (N = 7) subloculi; subloculi 9–15 (11 ± 2; 5; 14) wide. Hooks tri-pronged, hollow, with basal, axial, and abaxial prongs (Fig. 6B); basal prongs highly reduced in size, located well away from axial prongs, near articulation point of extended bases of hooks; each hook with blunt talon embedded in musculature of scolex, covered with thin layer of tissue (Fig. 4I); bases extremely elongate; bases of lateral hooks longer than bases of medial hooks. Lateral hook measurements: A 25–35 (31 ± 4; 5; 6), B 41–46 (43 ± 2; 5; 6), C 38–52 (45 ± 4; 5; 6), D 46–55 (45 ± 4; 5; 6), E 5–9 (8 ± 1; 5; 6), F 9–17 (13 ± 3; 5; 6); medial hook measurements: A′ 36–43 (39 ± 2; 5; 7), B′ 33–45 (39 ± 4; 5; 7), C′ 28–41 (35 ± 4; 5; 7), D′ 48–59 (54 ± 3; 5; 7), E′ 6–8 (7 ± 1; 4; 5), F′ 14–20 (17 ± 2; 5; 7). Cephalic peduncle 241–728 (N = 3) long.

Apex of scolex proper, muscular pad, and distal bothridial (Fig. 4K) surfaces covered with papilliform filitriches only. Proximal bothridial surfaces covered with papilliform filitriches and small gladiate spinitriches (Fig. 4L). Cephalic peduncle covered with acicular filitriches and extremely large gladiate spinitriches (Fig. 4J). Strobila covered with capilliform filitriches and sparsely arranged smaller gladiate spinitriches decreasing in density posteriorly.

Proglottids acraspedote. Immature proglottids 12–16 (N = 2) in number, initially wider than long, becoming longer than wide with maturity (Fig. 6D). Posterior-most immature proglottid (Fig. 6D) 318–450 (N = 4) long by 174–202 (N = 4) wide. Mature proglottids not observed. Testes 103–111 (N = 4) in total number, 10–14 (N = 4) in post-poral field, elongate oval to round, 9–17 (12 ± 2; 4; 20) long by 16–25 (20 ± 3; 4; 20) wide, 1 layer deep in cross section, extending from anterior margin of ovary, stopping short of anterior margin of proglottid, in 4–5 irregular columns anterior to cirrus sac. Vas deferens minimal, coiling at antero-medial margin of cirrus sac, entering cirrus sac at its antero-medial margin. Cirrus sac dolioform, 23 (N = 1) long by 88 (N = 1) wide, containing coiled cirrus; cirrus spinitriches not observed. Genital pores lateral, irregularly alternating, 48–53% (N = 4) of proglottid length from posterior end. Vagina weakly sinuous, extending along midline of proglottid from ootype region to anterior margin of cirrus sac, then laterally along anterior margin of cirrus sac, opening into common genital atrium anterior to cirrus sac. Ovary at posterior margin of proglottid, symmetrical, inverted-A shaped in frontal view, bi-lobed in cross section, very weakly lobulated, 77–119 (N = 4) long by 100–122 (N = 4) wide. Mehlis' gland posterior to ovarian isthmus. Vitelline follicles too immature for shape determination, in 2 lateral bands; each band consisting of 1 dorsal and 1 ventral column of follicles, extending from posterior margin of proglottid to anterior margin of testicular field, interrupted dorsally and ventrally by terminal genitalia, uninterrupted by ovary. Uterus saccate, medioventral, extending from ootype to level of terminal genitalia. Excretory ducts in 2 lateral pairs. Gravid proglottids and eggs not observed.

Taxonomic summary

Type and only known host: Sphyrna lewini 1 (Sphyrnidae: Carcharhiniformes).

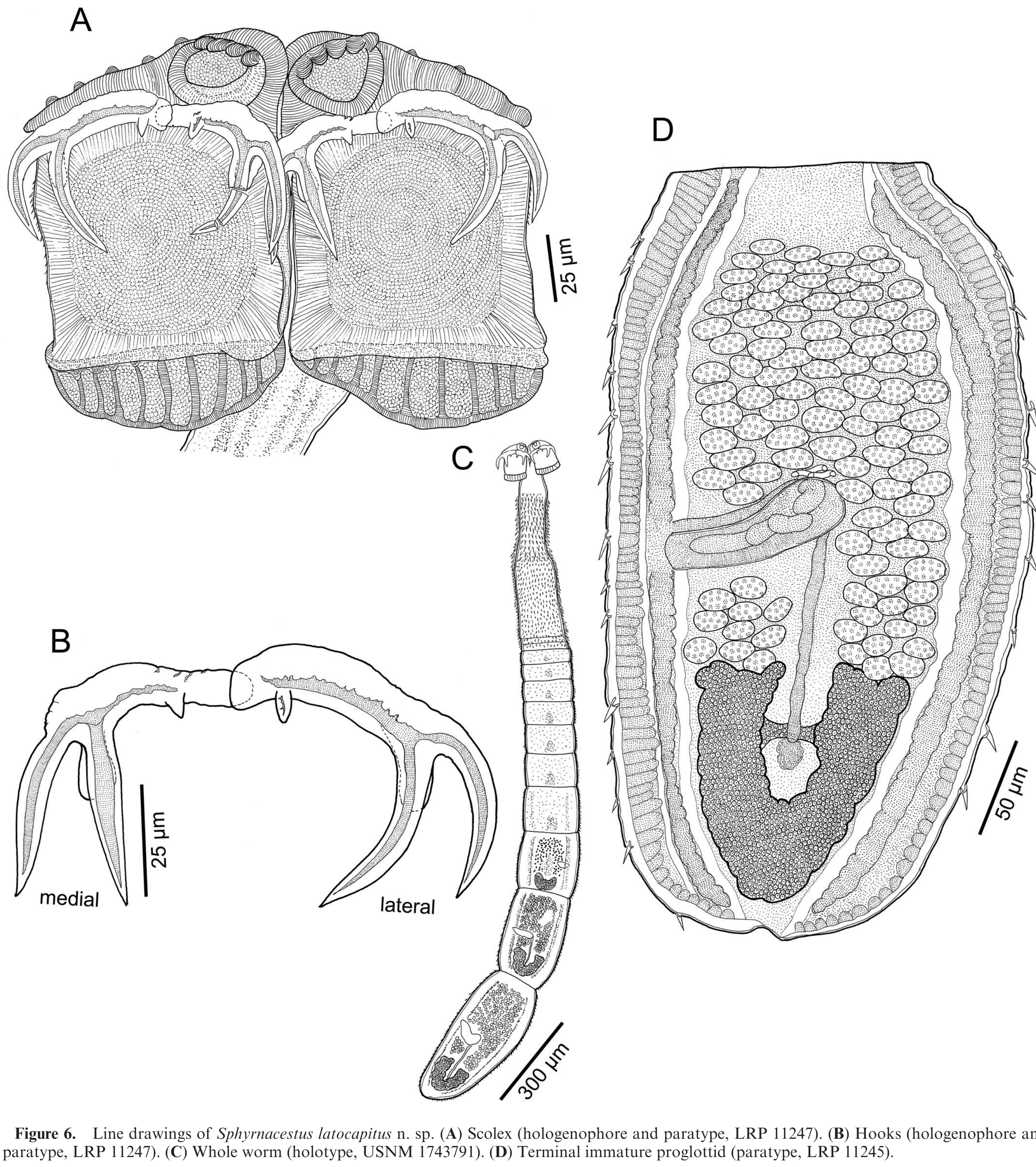

Figure 6. Line drawings of *Sphyrnacestus latocapitus* n. sp. (**A**) Scolex (hologenophore and paratype, LRP 11247). (**B**) Hooks (hologenophore and paratype, LRP 11247). (**C**) Whole worm (holotype, USNM 1743791). (**D**) Terminal immature proglottid (paratype, LRP 11245).

Type locality: Indian Pass (29°40′8″N, 85°13′30″W), Florida, Gulf of Mexico, Atlantic Ocean (unique host specimen no. MS05-433).

Additional localities: None.

Site of infection: Spiral intestine.

Specimens deposited: Holotype (USNM 1743791); 4 paratypes (including 2 hologenophores below) (LRP 11245–11248). Scolex prepared for SEM retained with JNC at the University of Connecticut.

Molecular material: Hologenophores (LRP 11247, JW511; LRP 11248, ON24).

ZooBank registration: urn:lsid:zoobank.org:act:10DCBCB1-989A-4579-B3F4-3B2D6E837F81.

Etymology: This name comes from the Latin for broad (*latus*) and head (*capitis*) in reference to the relatively wide scolex of this species.

Remarks

Sphyrnacestus latocapitus n. sp. conspicuously differs from all 8 of its congeners in that, rather than being short, the bases of both its medial and lateral hooks are extremely elongate. It further differs from its 5 congeners that also possess hooks with basal prongs (i.e., *S. eusphyrensis*, *S. exceptus*, *S. lewinensis*, *S. pectinatus*, and *S. puriensis*) in that the basal prongs are located well away from the axial prongs, near the articulation point of the extended bases of the hooks, rather than immediately adjacent to the axial prongs. It further differs from *S. ananas*, *S. exceptus*, *S. manirei*, and *S. pectinatus* in its possession of a greater number of subloculi (9–10 vs. 5, 6, 5, and 6–7, respectively). It also has a greater number of proglottids than *S. lewinensis* (12–16 vs. 5–11), is a smaller worm than *S. exceptus* (2.0–2.7 mm vs. 14–25 mm), and has fewer testes than *S. puriensis* (103–111 vs. 125–140). It further differs from *S. eusphyrensis* in possessing fewer proglottids (12–16 vs. 17–23) and fewer testes (103–111 vs. 111–120).

Sphyrnacestus paralewinensis n. sp.

(Figs. 7, 8A–D)

Description (based on whole mounts of 6 complete mature worms, 1 complete immature worm, 3 detached mature proglottids, and 2 scoleces prepared for SEM): Worms 6.9–10 mm (8.1 ± 1.1; 7) long, euapolytic, greatest width generally at level of terminal proglottid (Fig. 7D); 20–29 (23 ± 3; 7) proglottids per worm. Scolex (Fig. 7A) consisting of scolex proper bearing 4 bothridia and cephalic peduncle, 185–302 (257 ± 50; 6) wide at level of subloculi. Bothridia 190–239 (218 ± 17; 6; 9) long by 121–179 (141 ± 18; 6; 9) wide; each with anterior muscular pad, 1 pair of hooks, and post-hook region divided into 1 anterior and 1 posterior loculus (Fig. 7A). Muscular pad 75–91 (84 ± 7; 6; 8) long by 100–119 (108 ± 8; 6; 7) wide, with apical sucker and 4–5 apical papillae, lacking papillae on latero-anterior and medio-anterior margins. Apical sucker 26–42 (35 ± 5; 6; 9) long by 33–58 (47 ± 9; 6; 9) wide. Anterior loculus considerably longer than posterior loculus, 170–226 (199 ± 19; 6; 9) long, posterior margin without small papillae; boundary between anterior and posterior sublocular region with double septum. Posterior loculus 21–38 (29 ± 5; 6; 9) long, subdivided into 9–11 (10 ± 1; 5; 7) subloculi; subloculi 11–16 (14 ± 1; 6; 20) wide. Hooks tri-pronged, hollow, with basal, axial, and abaxial prongs (Fig. 7B); basal prongs less than half as long as axial and abaxial prongs; each hook with blunt talon embedded in musculature of scolex and conspicuous base, covered with thin layer of tissue (Fig. 8A); bases short, relatively robust. Lateral hook measurements: A 64–79 (72 ± 5; 7; 9), B 61–90 (78 ± 10; 7; 9), C 33–52 (45 ± 6; 7; 9), D 97–123 (110 ± 10; 7; 9), E 10–16 (13 ± 2; 7; 8), F 15–28 (23 ± 4; 7; 9); medial hook measurements: A′ 60–78 (72 ± 7; 7; 9), B′ 67–80 (75 ± 5; 7; 9), C′ 38–49 (42 ± 3; 7; 9), D′ 87–115 (104 ± 9; 7; 9), E′ 11–18 (15 ± 3; 5; 7), F′ 19–30 (25 ± 4; 7; 9). Cephalic peduncle 1,448–2,158 (1,846 ± 243; 7) long.

Apex of scolex proper, muscular pad, and proximal (Fig. 8D) and distal (Fig. 8C) bothridial surfaces covered with papilliform filitriches only. Cephalic peduncle covered with acicular filitriches and extremely large gladiate spinitriches (Fig. 8B). Strobila covered with capilliform filitriches and sparsely arranged smaller gladiate spinitriches decreasing in density posteriorly.

Proglottids acraspedote. Immature proglottids 19–28 (22 ± 3; 7) in number, initially wider than long, becoming longer than wide with maturity. Posterior-most immature proglottid 631–936 (769 ± 127; 7) long by 397–490 (430 ± 35; 7) wide. Mature proglottids 1 (N = 6) in number. Terminal proglottid essentially mature, 966–1,342 (1,186 ± 145; 6) long by 395–532 (427 ± 52; 6) wide. Detached mature proglottids 2,242–3,126 (N =3) long by 691–846 (N = 3) wide (Fig. 7E). Testes 155–228 (173 ± 24; 8) in total number, 22–31 (26 ± 3; 8) in post-poral field, elongate oval to round, 26–43 (33 ± 4; 6; 29) long by 34–61 (46 ± 7; 6; 29) wide in terminal mature proglottids, 39–71 (55 ± 10; 3; 16) long by 54–83 (68 ± 8; 3; 16) wide in detached mature proglottids, 1 layer deep in cross section, extending from anterior margin of ovary to near anterior margin of proglottid, in 5–8 irregular columns anterior to cirrus sac. Vas deferens minimal, with intermittent patches of darkly staining cells, coiling at antero-medial margin of cirrus sac, entering cirrus sac at its antero-medial margin. Cirrus sac weakly pyriform (Fig. 7C), 146–188 (169 ± 16; 6) long by 56–83 (67 ± 11; 6) wide in terminal mature proglottids, 93–134 (N = 3) long by 234–248 (N = 3) wide in detached mature proglottids, containing coiled cirrus; cirrus armed with small spinitriches. Genital pores lateral, irregularly alternating, 55–62% (58 ± 2; 9) of proglottid length from posterior end. Vagina straight, extending along midline of proglottid from ootype region to anterior margin of cirrus sac, then laterally along anterior margin of cirrus sac, opening into common genital atrium anterior to cirrus sac. Ovary at posterior margin of proglottid, symmetrical, inverted-A shaped in frontal view, bi-lobed in cross section, lobulated, 246–420 (335 ± 60; 6) long by 187–312 (242 ± 42; 6) wide in terminal mature proglottids, 569–977 (N = 3) long by 379–476 (N = 3) wide in detached mature proglottids. Mehlis' gland posterior to ovarian isthmus. Vitelline follicles irregular in shape, in 2 lateral bands; each band consisting of 2 dorsal and 2 ventral columns of follicles, extending from posterior margin of proglottid to anterior margin of testicular field, interrupted dorsally and ventrally by terminal genitalia, uninterrupted by ovary. Uterus saccate, medioventral, extending from ootype to level of terminal genitalia. Excretory ducts in 2 lateral pairs. Gravid proglottids and eggs not observed.

Taxonomic summary

Type and only known host: Sphyrna mokarran (Sphyrnidae: Carcharhiniformes).

Type locality: Off Georgia (31°20′5.4″N, 80°45′45.6″W), Atlantic Ocean (unique host specimen no. CG-8).

Additional localities: Off Florida (25°2′55.8″N, 82°23′3.0″W), Atlantic Ocean (unique host specimen no. KC-9).

Site of infection: Spiral intestine.

Specimens deposited: Holotype (USNM 1743799) and 4 paratypes (USNM 1743800–1743803); 5 paratypes (LRP 11249–11253), 2 paratype SEM vouchers (LRP 11254 and LRP 11255). Scoleces prepared for SEM retained with JNC at the University of Connecticut.

Molecular material: Hologenophore (LRP 11256, ON29).

ZooBank registration: urn:lsid:zoobank.org:act:C482B731-BA0B-4DCA-99F1-0D7DE960E5FC.

Etymology: This species is named for its close relationship (Greek, *para*, for near) to *S. lewinensis*.

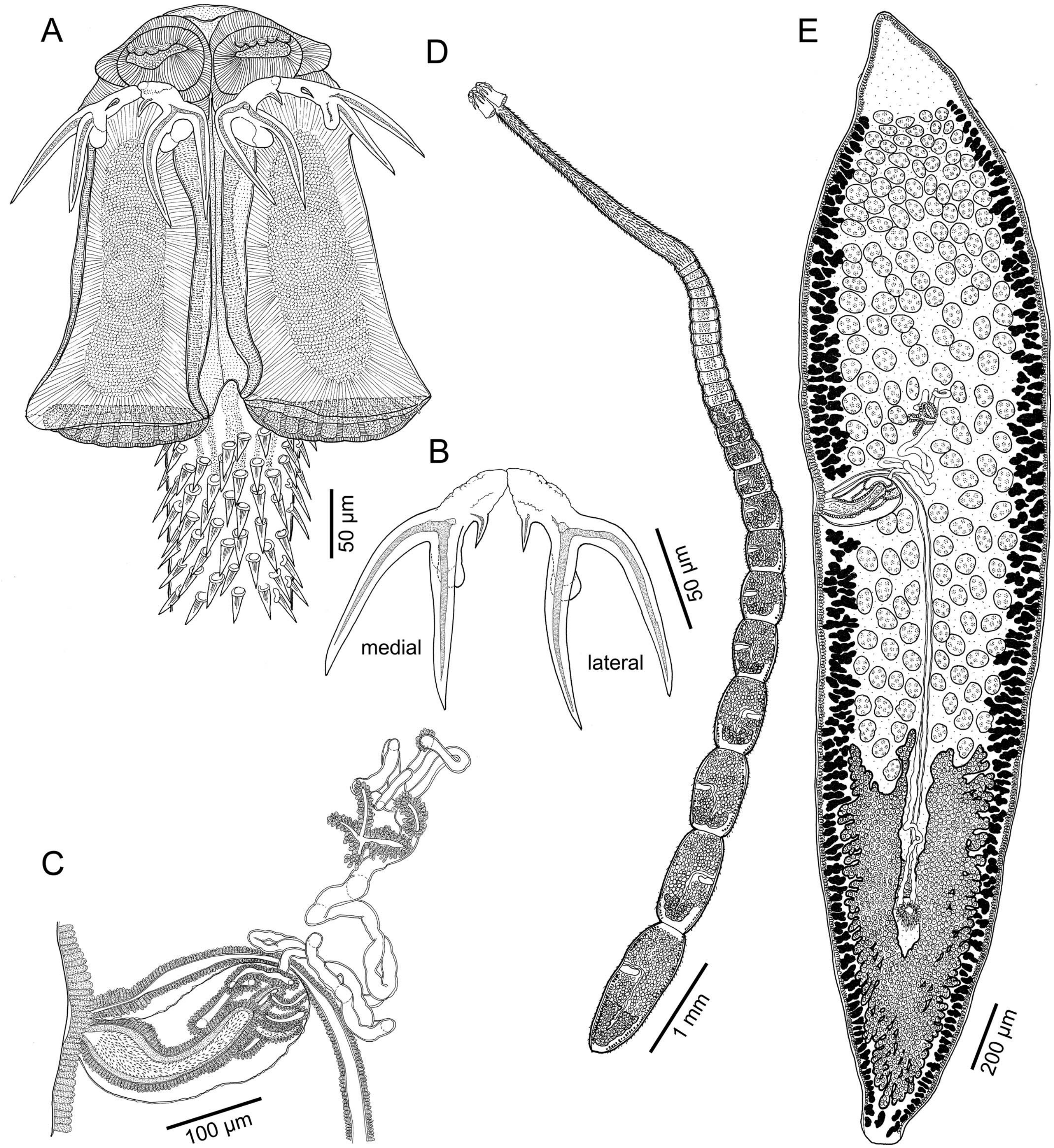

Figure 7. Line drawings of *Sphyrnacestus paralewinensis* n. sp. (**A**) Scolex (holotype, USNM 1743799). (**B**) Hooks (paratype, LRP 11249). (**C**) Terminal genitalia (paratype, USNM 1743802). (**D**) Whole worm (holotype, USNM 1743799). (**E**) Detached mature proglottid (paratype, USNM 1743802).

Remarks

Sphyrnacestus paralewinensis n. sp. exhibits a greater number of subloculi than *S. ananas*, *S. exceptus*, *S. manirei*, and *S. pectinatus* (9–11 vs. 5, 6, 5, and 6–7). It differs from *S. latocapitus* in lacking, rather than possessing, extremely elongate bases of the medial and lateral hooks. It is a longer worm than *S. puriensis* (6.9–10 mm vs. 4–6 mm). This new species further differs from *S. ananas* and *S. manirei* in possessing, rather than lacking, basal prongs on its hooks. The presence of short basal prongs on both

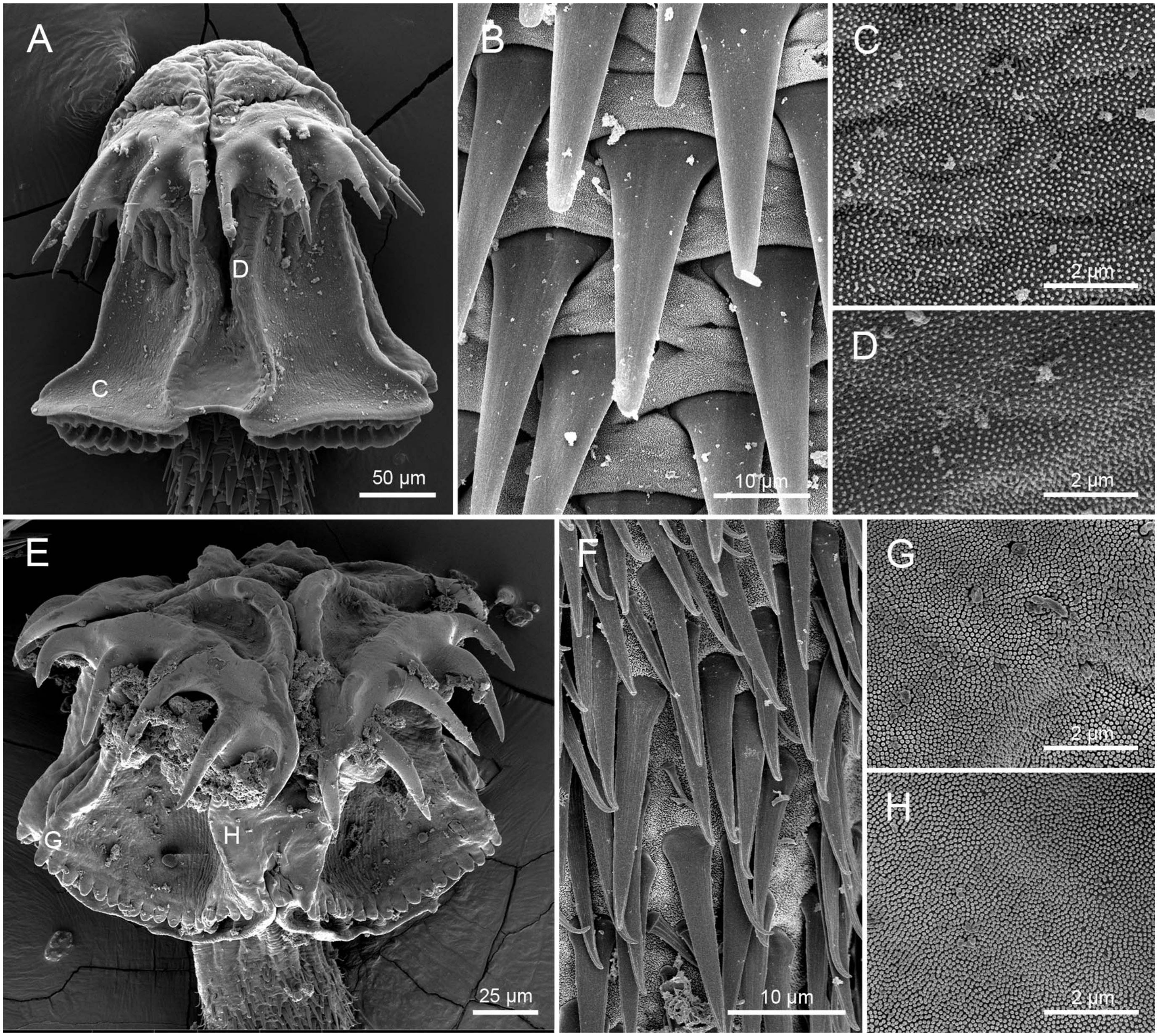

Figure 8. Scanning electron micrographs of *Sphyrnacestus paralewinensis* n. sp. (**A–D**) and *Sphyrnacestus pectinatus* (Linton, 1924) n. comb. (**E–H**). (**A**) Scolex of *S. paralewinensis* n. sp., small letters indicate locations of C, D. (**B**) Extremely large gladiate spinitriches and acicular filitriches on cephalic peduncle of *S. paralewinensis* n. sp. (**C**) Papilliform filitriches on distal surface of bothridium of *S. paralewinensis* n. sp. (**D**) Papilliform filitriches on proximal surface of bothridium of *S. paralewinensis* n. sp. (**E**) Scolex of *S. pectinatus* n. comb., small letters indicate locations of G, H. (**F**) Extremely large gladiate spinitriches and acicular filitriches on cephalic peduncle of *S. pectinatus* n. comb. (**G**) Papilliform filitriches on distal surface of bothridium of *S. pectinatus* n. comb. (**H**) Papilliform filitriches on proximal surface of bothridium of *S. pectinatus* n. comb.

the medial and lateral hooks helps to further distinguish *S. paralewinensis* from *S. exceptus* in which the basal prongs of both the medial and lateral hooks are essentially just small tubercles and from *S. pectinatus* in which the basal prong of the medial hook is more than half as long as the axial and abaxial prongs of that hook. This new species further differs from *S. latocapitus* in bearing more proglottids (19–29 vs. 12–16) and from *S. eusphyrensis* in its possession of a greater number of testes (155–228 vs. 111–120). As its name suggests, *Sphyrnacestus paralewinensis* n. sp. most closely resembles *S. lewinensis* but is a longer worm (6.9–10 mm vs. 1.7–4.4 mm) with a much greater number of proglottids (19–29 vs. 5–11).

Sphyrnacestus pectinatus (Linton, 1924) n. comb.
(Fig. 8E–H)

Anterior margin of muscular pad with 4 apical papillae (Fig. 8E), lacking papillae on latero-anterior margins. Posterior margin of anterior loculus with 18–19 papillae (Fig. 8E). Apex of scolex proper, muscular pad, and proximal (Fig. 8H) and distal (Fig. 8G) bothridial surfaces covered with papilliform filitriches only. Cephalic peduncle covered with papilliform filitriches and extremely large gladiate spinitriches (Fig. 8F). Strobila covered with capilliform filitriches and sparsely arranged smaller gladiate spinitriches decreasing in density posteriorly.

Material deposited: Scolex prepared for SEM retained with JNC at the University of Connecticut.

Molecular material: Hologenophores (LRP 11264, ON33; LRP 11265, JW23; LRP 11266, ON34; LRP 11267, JW503).

Remarks

Neither the original description of *Sphyrnacestus pectinatus* (Linton, 1924) n. comb. by Linton (1924) nor the subsequent redescription by Caira (1985) included SEM images or information on the microthrix pattern on the scolex of this species. Our work here indicates that the pattern of microtriches on the scolex of this species is similar to that of other members of this genus. SEM images also confirm the nature of the structures found on the posterior margin of the anterior loculus of this species (Fig. 8E). These structures were described as "about seventeen short, flat, rounded, and scale-like papillae" by Linton (1924, p. 36). However, SEM reveals there to be 18 to 19 of these papillae, which we consider to be rounded and fleshy rather than flat and scale-like. It also showed that, like all of its congeners, *S. pectinatus* possesses apical papillae on the anterior margin of its muscular pads.

Phoreiobothrium angustivastum n. sp.

(Figs. 9, 10A–D)

Description (based on whole mounts of 3 complete mature worms, and 1 scolex prepared for SEM and its strobilar voucher): Worms 7.6–12.6 mm (N = 3) long, euapolytic, greatest width generally at level of terminal proglottid (Fig. 9D); 30–40 (N = 3) proglottids per worm. Scolex (Fig. 9A) consisting of scolex proper bearing 4 bothridia and cephalic peduncle, 220–228 (N = 2) wide at level of hooks. Bothridia constricted immediately posterior to hooks, 211–233 (222 ± 9; 2; 4) long by 113–144 (N = 2; n = 3) wide; each with anterior muscular pad in form of loculus, 1 pair of hooks, and post-hook region divided into 1 anterior and 1 posterior loculus (Fig. 9A). Muscular pad 32–42 (36 ± 4; 2; 4) long by 116–119 (N = 1; n = 2) wide, lacking apical papillae and papillae on latero-anterior margins. Anterior loculus considerably longer than posterior loculus, 151–175 (163 ± 10; 2; 4) long, posterior margin without small papillae; boundary between anterior loculus and sublocular region with double septum (Fig. 10D). Posterior loculus 27–35 (N = 2; n = 3) long, subdivided into 14–16 (15 ± 1; 2; 4) subloculi; subloculi 9–12 (11 ± 1; 2; 4) wide. Hooks tripronged, hollow, with basal, axial, and abaxial prongs (Fig. 9B); basal prongs more than half as long as axial and abaxial prongs; each hook with blunt talon embedded in musculature of scolex, covered with thin layer of tissue (Fig. 10C); bases short. Lateral hook measurements: A 28–36 (32 ± 4; 3; 4), B 30–36 (33 ± 3; 3; 4), C 37–39 (N=2; n=3), D 44–51 (46 ± 3; 3; 4), E 23–27 (25 ± 1; 3; 4), F 12–20 (17 ± 3.7; 3; 4); medial hook measurements: A′ 28–39 (N = 3), B′ 38–44 (N = 3), C′ 41–52 (N = 3), D′ 51–68 (58 ± 8; 3; 4), E′ 20–29 (24 ± 4.0; 3; 4), F′ 11–22 (17 ± 5; 3; 4). Cephalic peduncle 419–696 (N = 3) long.

Microtriches on proximal and distal bothridial surfaces not visible on SEM specimen. Cephalic peduncle covered with acicular filitriches and large gladiate spinitriches (Fig. 10B). Strobila covered with sparsely arranged smaller gladiate spinitriches decreasing in density posteriorly.

Proglottids acraspedote. Immature proglottids 28–37 (N = 3) in number, initially wider than long, becoming longer than wide with maturity (Fig. 9D). Posterior-most immature proglottid 573–977 (N = 3) long by 265–376 (N = 3) wide. Mature proglottids 2–3 (N = 3) in number. Terminal mature proglottid (Fig. 9E) 954–1,453 (N = 3) long by 323–359 (N = 3) wide; length to width ratio 3–4:1 (3 ± 1; 3). Testes 71–84 (79 ± 4; 3; 6) in total number, 9–11 (10 ± 1; 3; 6) in post-poral field, elongate oval to round, 37–59 (46 ± 9; 3; 9) long by 40–63 (51 ± 8; 3; 9) wide, 1 layer deep in cross section, extending from anterior margin of ovary, stopping short of anterior margin of proglottid, in 4–5 irregular columns anterior to cirrus sac. Vas deferens minimal, coiling at antero-medial margin of cirrus sac, entering cirrus sac at its antero-medial margin. Cirrus sac elliptoid (Fig. 9C), 124–165 (N = 3) long by 79–113 (N = 3) wide, containing coiled cirrus; cirrus armed with small spinitriches. Genital pores lateral, irregularly alternating, 42–47% (N = 3) of proglottid length from posterior end. Vagina weakly sinuous, extending along midline of proglottid from ootype region to anterior margin of cirrus sac, then laterally along anterior margin of cirrus sac, opening into common genital atrium anterior to cirrus sac. Ovary at posterior margin of proglottid, symmetrical, inverted-A shaped in frontal view, bi-lobed in cross section, lobulated, 221–341 (N = 3) long by 209–231 (N = 3) wide. Mehlis' gland posterior to ovarian isthmus. Vitelline follicles round to slightly oval, in 2 lateral bands; each band consisting of 1 dorsal and 1 ventral column of follicles, extending from posterior margin of proglottid to anterior margin of testicular field, interrupted dorsally and ventrally by terminal genitalia, uninterrupted by ovary. Uterus saccate, medioventral, extending from ootype, stopping well short of anterior margin of testicular field. Excretory ducts in 2 lateral pairs. Gravid proglottids and eggs not observed.

Taxonomic summary

Type and only known host: Carcharhinus isodon (Valenciennes in Müller and Henle) (Carcharhinidae: Carcharhiniformes).

Type locality: Round Island (30°17′42.45″N, 88°35′11.55″W), Mississippi, Gulf of Mexico, Atlantic Ocean (unique host specimen no. MS05-86).

Additional localities: None.

Site of infection: Spiral intestine.

Specimens deposited: Holotype (USNM 1743784) and 1 paratype (USNM 1743785); 1 paratype (LRP 11187), 1 paratype SEM voucher (LRP 11188). Scolex prepared for SEM retained with JNC at the University of Connecticut.

Molecular material: Hologenophores (LRP 11190, ON1; LRP 11189, KW8).

ZooBank registration: urn:lsid:zoobank.org:act:18618BFB-8308-40F8-AD60-3B51BCD922C2.

Etymology: The name of this species, Latin for narrow (*angust*) and waist (*vastum*), refers to the constriction of the bothridia immediately posterior to the hooks.

Remarks

Phoreiobothrium angustivastum n. sp. bears fewer subloculi on its bothridia than *P. blissorum*, *P. lasium*, *P. martini*, *P. nadiae*,

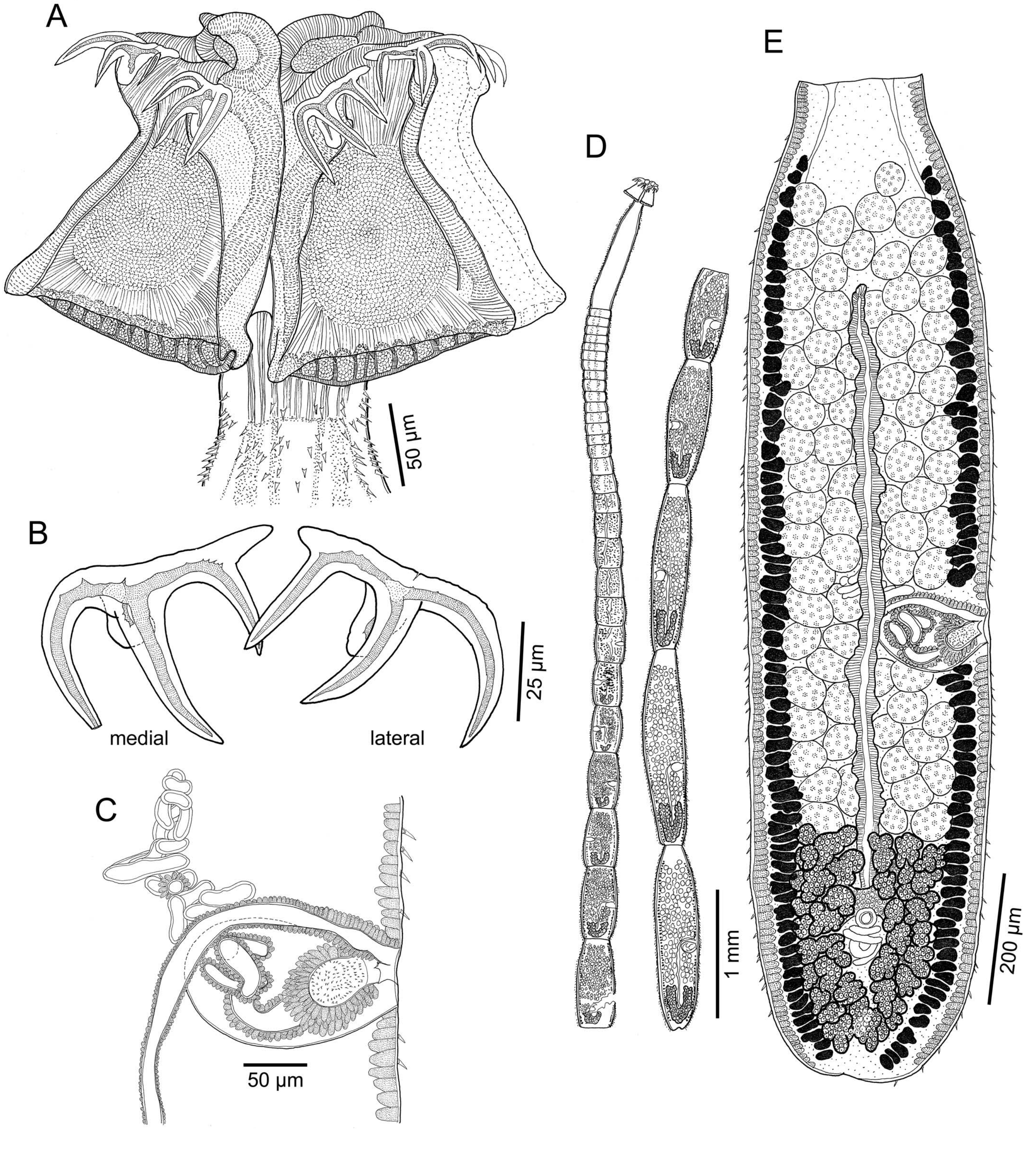

Figure 9. Line drawings of *Phoreiobothrium angustivastum* n. sp. (**A**) Scolex (holotype, USNM 1743784). (**B**) Hooks (paratype, LRP 11187). (**C**) Terminal genitalia (holotype, USNM 1743784). (**D**) Whole worm (holotype, USNM 1743784). (**E**) Terminal mature proglottid (holotype, USNM 1743784).

and *P. robertsoni* (14–16 vs. 23–31, 25–30, 20–22, 18–28, and 25–29, respectively). This new species differs from *P. jahki* in that the posterior locular region is conspicuously shorter than the anterior locular region (only about one-fifth vs. one-third of the post-hook bothridial region). It differs from *P. sarahae* in that its proglottids in which reproductive organs are visible are longer than wide, rather than wider than long, and in that its terminal mature proglottid is much longer than wide (1:3–4.1 vs. 1:1.2–2.2). The

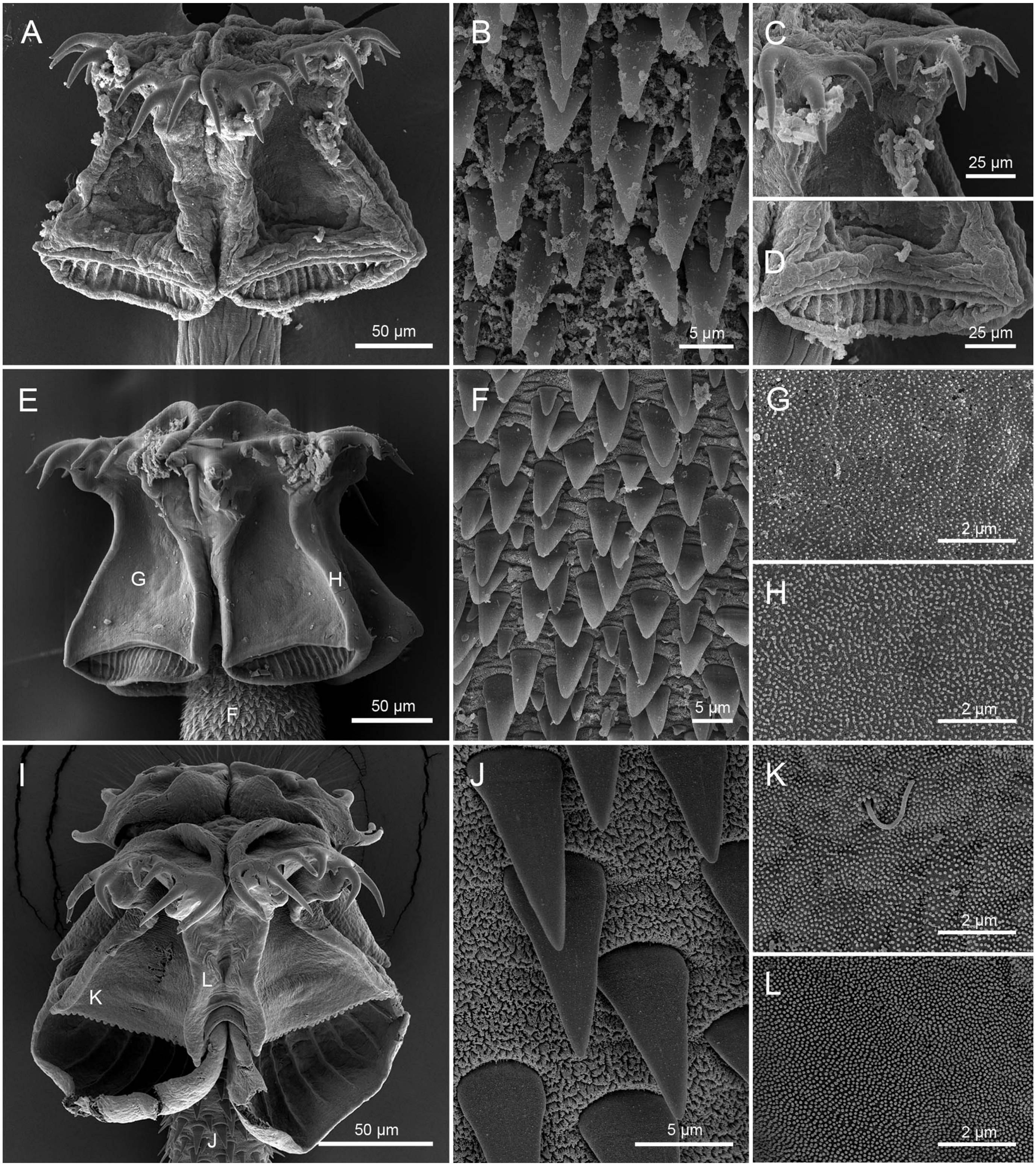

Figure 10. Scanning electron micrographs of *Phoreiobothrium angustivastum* n. sp. (**A–D**), *Phoreiobothrium danae* n. sp. (**E–H**), and *Phoreiobothrium magnaloculum* n. sp. (**I–L**). (**A**) Scolex of *P. angustivastum* n. sp. (**B**) Large gladiate spinitriches and acicular filitriches on cephalic peduncle of *P. angustivastum* n. sp. (**C**) Pre-hook region and hooks of *P. angustivastum* n. sp. (**D**) Sublocular region of *P. angustivastum* n. sp. (**E**) Scolex of *P. danae* n. sp., small letters indicate locations of G, H. (**F**) Large gladiate spinitriches and acicular filitriches on cephalic peduncle of *P. danae* n. sp. (**G**) Papilliform filitriches on distal surface of bothridiium of *P. danae* n. sp. (**H**) Papilliform filitriches on proximal surface of bothridium of *P. danae* n. sp. (**I**) Scolex of *P. magnaloculum* n. sp., small letters indicate locations of J–L. (**J**) Large gladiate spinitriches and acicular filitriches on cephalic peduncle of *P. magnaloculum* n. sp. (**K**) Papilliform filitriches and cilium on distal surface of bothridium of *P. magnaloculum* n. sp. (**L**) Papilliform filitriches on proximal surface of bothridium of *P. magnaloculum* n. sp.

bothridia of *P. angustivastum* n. sp. are longer than those of *P. golchini* (211–233 vs. 122–173). *Phoreiobothrium angustivastum* n. sp. is a larger worm than *P. rozatii*, *P. swaki*, and *P. tiburonis* (7.6–12.6 mm vs. 3–6 mm, 4.2–4.9 mm, and 3.8–5.9 mm, respectively). This new species further differs from *P. robertsoni* and differs from *P. sorrahcola* in that its hooks are much smaller in all respects (e.g., A 28–36 vs. 45–55 and 39–63, respectively; B 30–36 vs. 50–78 and 56–80, respectively; and C 37–39 vs. 53–60 and 46–61, respectively). It further differs from *P. blissorum* and *P. lasium* in possessing fewer proglottids (30–40 vs. 55–79 and 54–107, respectively) and from *P. iraniense* and *P. perilocrocodilus* in its possession of a greater number of proglottids (30–40 vs. 18–29 and 11–22, respectively). This new species also possesses a greater number of testes than *P. anticaporum*, *P. perilocrocodilus*, and *P. swaki* (72–84 vs. 36–54, 36–49, and 55–68, respectively). It further differs from *P. anticaporum* in that its genital pore is located in the posterior half of the proglottid rather than near the anterior margin of the proglottid. *Phoreiobothrium angustivastum* n. sp. is also a smaller worm than *P. martini* (7.6–12.6 mm vs. 16.4–33.1 mm). It further differs from *P. glochini* and *P. tiburonis* in possessing a genital pore that is more posterior in position in the proglottid (42–47% vs. 50–60% and 48–61% from the posterior end, respectively). In addition, *P. jahki*, *P. nadiae*, *P. rosatii*, and *P. sorrahcola* lack, rather than possess, the narrowing of the bothridium immediately posterior to the hooks seen in *P. angustivastum* n. sp.

Phoreiobothrium danae **n. sp.**
(Figs. 10E–H, 11)

Description (based on whole mounts of 9 complete mature worms and 2 scoleces prepared for SEM and their strobilar vouchers): Worms 6.8–11.8 mm (8.8 ± 1.5; 9) long, euapolytic, greatest width generally at level of terminal proglottid (Fig. 11D); 21–35 (28 ± 5; 9) proglottids per worm. Scolex (Fig. 11A) consisting of scolex proper bearing 4 bothridia and cephalic peduncle, 240–273 (260 ± 12; 9) wide at level of hooks. Bothridia weakly constricted immediately posterior to hooks, 274–303 (290 ± 8; 9; 18) long by 157–187 (170 ± 10; 9;17) wide; each with anterior muscular pad in form of loculus, 1 pair of hooks, and post-hook region divided into 1 anterior and 1 posterior loculus (Fig. 11A). Muscular pad 42–73 (57 ± 10; 8; 16) long by 122–156 (133 ± 11; 9; 16) wide, lacking apical papillae and papillae on latero-anterior margins. Anterior loculus considerably longer than posterior loculus, 192–239 (220 ± 13; 9; 18) long, posterior margin without small papillae; boundary between anterior loculus and sublocular region with double septum (Fig. 10E). Posterior loculus 30–45 (36 ± 4; 9; 18) long, subdivided into 16–18 (17 ± 1; 9; 16) subloculi; subloculi 9–13 (11 ± 1; 9; 18) wide. Hooks tri-pronged, hollow, with basal, axial, and abaxial prongs (Fig. 11B); basal prongs more than half as long as axial and abaxial prongs; each hook with blunt talon embedded in musculature of scolex, covered with thin layer of tissue (Fig. 10E); bases short. Lateral hook measurements: A 31–48 (39 ± 5; 9; 11), B 39–59 (49 ± 5; 9; 10), C 45–53 (48 ± 2; 9; 11), D 54–68 (36 ± 4; 9; 11), E 25–35 (31 ± 3; 9; 10), F 19–27 (23 ± 2.5; 9; 11); medial hook measurements: A′ 41–55 (49 ± 4.5; 9; 10), B′ 52–72 (62 ± 6; 9; 11), C′ 48–58 (53 ± 3; 9; 11), D′ 67–80 (73 ± 5; 9; 11), E′ 25–39 (31 ± 5; 9; 11), F′ 21–29 (24 ± 2; 9; 11). Cephalic peduncle 325–564 (442 ± 76; 9) long.

Apex of scolex proper, muscular pad, and proximal (Fig. 10H) and distal (Fig. 10G) bothridial surfaces covered with papilliform filitriches only. Cephalic peduncle covered with acicular filitriches and large gladiate spinitriches (Fig. 10F). Strobila covered with capilliform filitriches and sparsely arranged smaller gladiate spinitriches decreasing in density posteriorly.

Proglottids acraspedote. Immature proglottids 18–32 (25 ± 4.8; 9) in number, initially wider than long, becoming longer than wide with maturity (Fig. 11D). Posterior-most immature proglottid 534–793 (663 ± 74; 9) long by 338–396 (364 ± 21; 9) wide. Mature proglottids 3–4 (3 ± 1; 9) in number. Terminal mature proglottid (Fig. 11E) 1,205–1,791 (1,452 ± 208; 9) long by 457–534 (478 ± 25; 9) wide; length to width ratio 2–4:1 (3 ± 1; 9). Testes 68–88 (79 ± 6; 9; 17) in total number, 7–13 (10 ± 2; 9; 17) in post-poral field, elongate oval to round, 38–67 (53 ± 6; 9; 27) long by 61–112 (79 ± 11; 9; 27) wide, 1 layer deep in cross section, extending from anterior margin of ovary to near anterior margin of proglottid, in 4–5 irregular columns anterior to cirrus sac. Vas deferens minimal, coiling at antero-medial margin of cirrus sac, entering cirrus sac at its antero-medial margin. Cirrus sac elliptoid (Fig. 11C), 144–180 (160 ± 13; 9) long by 77–118 (95 ± 13; 9) wide, containing coiled cirrus; cirrus armed with small spinitriches. Genital pores lateral, irregularly alternating, 45–52% (48 ± 3; 9) of proglottid length from posterior end. Vagina weakly sinuous, extending along midline of proglottid from ootype region to anterior margin of cirrus sac, then laterally along anterior margin of cirrus sac, opening into common genital atrium anterior to cirrus sac. Ovary at posterior margin of proglottid, symmetrical, inverted-A shaped in frontal view, bi-lobed in cross section, lobulated, 338–513 (422 ± 59; 9) long by 293–363 (316 ± 21; 9) wide. Mehlis' gland posterior to ovarian isthmus. Vitelline follicles irregular in shape, much wider than long, in 2 lateral bands; each band consisting of 1 dorsal and 1 ventral column of follicles, extending from posterior margin of proglottid, stopping well short of anterior margin of testicular field, interrupted dorsally and ventrally by terminal genitalia, uninterrupted by ovary. Uterus saccate, medioventral, extending from ootype, stopping well short of anterior margin of testicular field. Excretory ducts in 2 lateral pairs. Gravid proglottids and eggs not observed.

Taxonomic summary

Type and only known host: *Carcharhinus limbatus* (Valenciennes in Müller and Henle) (Carcharhinidae: Carcharhiniformes).

Type locality: Indian Pass (29°40′8.05″N, 85°13′30.17″W), Florida, Gulf of Mexico, Atlantic Ocean (unique host specimen no. MS05-481).

Additional locality: North of west end of Horn Island, Mississippi, Gulf of Mexico, Atlantic Ocean (unique host specimen no. MS05-24).

Site of infection: Spiral intestine.

Specimens deposited: Holotype (USNM 1743781) and 4 paratypes (USNM 1743779, USNM 1743780, USNM 1743782, and USNM 1743783); 4 paratypes (LRP 11191–11194) and 2 paratype SEM vouchers (LRP 11195 and LRP 11196). Scoleces prepared for SEM retained with JNC at the University of Connecticut.

Molecular material: Hologenophore (LRP 11197, KW6).

ZooBank registration: urn:lsid:zoobank.org:act:465B72CB-B6B6-4536-A1C9-616825335A4B.

Etymology: This species honors Dana Bethea of NOAA Fisheries for her assistance with the collection of the type host of this species.

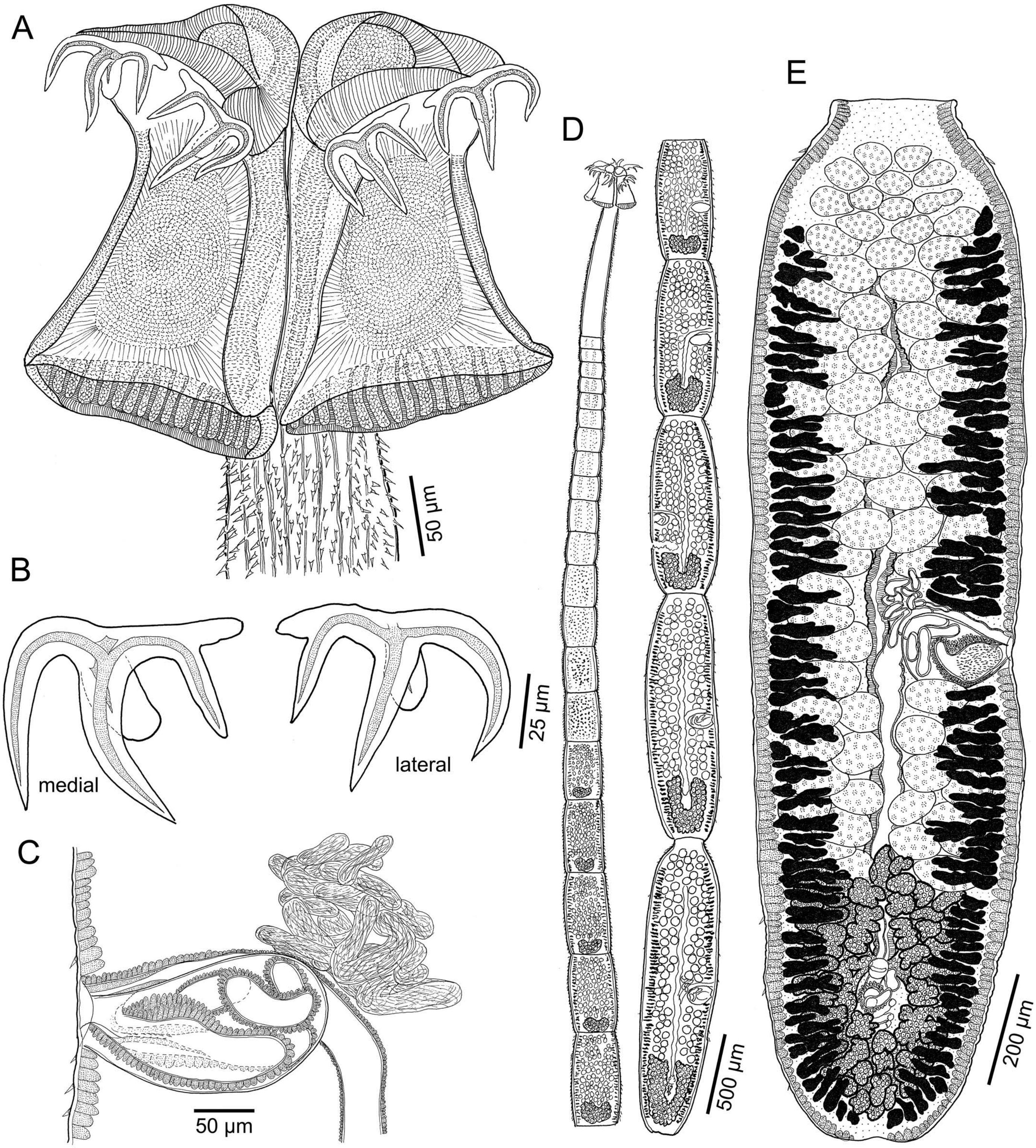

Figure 11. Line drawings of *Phoreiobothrium danae* n. sp. (**A**) Scolex (paratype, LRP 11191). (**B**) Hooks (paratype, USNM 1743782). (**C**) Terminal genitalia (paratype, LRP 11193). (**D**) Whole worm (holotype, USNM 1743781). (**E**) Terminal mature proglottid (holotype, USNM 1743781).

Remarks

Its possession of a greater number of subloculi serves to distinguish *Phoreiobothrium danae* n. sp. from *P. golchini*, *P. jahki*, *P. rozatii*, *P. sorrahcola*, *P. swaki*, and *P. tiburonis* (16–18 vs. 11–15, 10–15, 12–15, 12–14, 11–13, and 8–13, respectively). Its possession of fewer subloculi distinguishes it from *P. blissorum*, *P. lasium*, *P. martini*, and *P. robertsoni* (16–18 vs. 23–31, 25–30, 20–22, and 25–29, respectively). This new species conspicuously differs from *P. anticaporum* in that its genital pore is much more posterior in position (45–52% vs. 85–95% from posterior margin of proglottid). It possesses a greater number of testes than *P. perilocrocodilus* (69–88 vs. 36–49). It differs from *P. nadiae* and *P. angustivastum* and further differs from *P. golchini*, *P. robertsoni*, and *P. sorrahcola* in that its vitelline follicles are irregular in shape and much wider than long rather than being small and round. This new species further differs from *P. nadiae* in lacking, rather than possessing, spinitriches on the proximal bothridial surfaces. *Phoreiobothrium danae* n. sp. can be distinguished from *P. iraniense* by being a larger worm (6.8–11.8 mm vs. 4–5.8 mm) and having genital pores that are more posterior in position (45–52% vs. 54–62% from posterior margin of proglottid). It differs from *P. sarahae* in that proglottids in which reproductive organs are visible are longer than wide, rather than wider than long. It further differs from *P. sarahae* in that each lateral band of vitelline follicle consists of 1 dorsal and 1 ventral column of follicles, rather than 2–3 dorsal and 2–3 ventral columns. *Phoreiobothrium danae* n. sp. is a larger worm than *P. perilocrocodilus*, *P. rozatii*, *P. swaki*, and *P. tiburonis* (6.8–11.8 mm vs. 2.1–6.7 mm, 3–6 mm, 4.2–4.9 mm, and 3.8–5.9 mm, respectively) and a smaller worm than *P. martini* (6.8–11.8 mm vs. 16.4–33.1 mm). This new species has a greater number of testes than *P. anticaporum* (69–88 vs. 36–54) and fewer testes than *P. blissorum* and *P. lasium* (69–88 vs. 103–127 and 95–139, respectively). Unlike *P. jahki*, the posterior locular region of this new species is conspicuously shorter than the anterior locular region (only about one-fifth vs. one-third of post-hook bothridial region).

***Phoreiobothrium magnaloculum* n. sp.**

(Figs. 10I–L, 12)

Description (based on whole mounts of 9 complete immature worms, 1 incomplete mature worm, 6 detached mature proglottids, 1 detached gravid proglottid, and 1 scolex prepared for SEM and its strobilar voucher): Worms 3–6.1 mm (3.9 ± 1; 9) long, essentially hyperapolytic, greatest width generally at level of terminal proglottid (Fig. 12D); 11–27 (17 ± 5; 9) proglottids per worm. Scolex (Fig. 12A) consisting of scolex proper bearing 4 bothridia and cephalic peduncle, 165–231 (195 ± 21; 9) wide at level of subloculi. Bothridia lacking constriction immediately posterior to hooks, 153–233 (174 ± 24; 9; 11) long by 74–144 (112 ± 24; 9; 10) wide; each with anterior muscular pad in form of loculus, 1 pair of hooks, and post-hook region divided into 1 anterior and 1 posterior loculus (Fig. 12A). Muscular pad 20–45 (30 ± 9; 7; 10) long by 61–81 (70 ± 6; 7; 10) wide, lacking apical papillae and papillae on latero-anterior margins. Anterior loculus slightly longer than posterior loculus, 62–118 (93 ± 17; 9; 10) long, posterior margin with numerous small papillae (Figs. 10I, 12A); boundary between anterior loculus and sublocular region with double septum. Posterior loculus 70–112 (84 ± 12; 9; 10) long, subdivided into 8–10 (9 ± 1; 9; 10) subloculi; subloculi 13–23 (18 ± 3; 7; 22) wide. Hooks tri-pronged, hollow, with basal, axial, and abaxial prongs (Fig. 12B); basal prongs half or more than half as long as axial and abaxial prongs; each hook with blunt talon embedded in musculature of scolex, covered with thin layer of tissue (Fig. 10I); bases short. Lateral hook measurements: A 17–28 (23 ± 3; 8; 9), B 23–34 (27 ± 4; 8; 9), C 22–30 (26 ± 3; 8; 9), D 23–36 (31 ± 5; 8; 9), E 10–20 (15 ± 3; 8; 9), F 9–17 (13 ± 2; 8; 9); medial hook measurements: A′ 22–37 (27 ± 4; 9; 10), B′ 22–44 (32 ± 7; 9; 10), C′ 19–37 (29 ± 6; 9; 10), D′ 27–40 (34 ± 4; 9; 10), E′ 7–17 (14 ± 3; 9; 10), F′ 10–17 (15 ± 2; 9; 10). Cephalic peduncle 425–1,015 (635 ± 174; 10) long.

Apex of scolex proper, muscular pad, proximal (Fig. 10L) and distal (Fig. 10K) bothridial surfaces covered with papilliform filitriches only. Cephalic peduncle covered with acicular filitriches and large gladiate spinitriches (Fig. 10J). Strobila covered with capilliform filitriches and sparsely arranged smaller gladiate spinitriches decreasing in density posteriorly.

Proglottids acraspedote. Immature proglottids 11–27 (17 ± 5; 9) in number, initially wider than long, becoming longer than wide with maturity (Fig. 10D). Terminal immature proglottid 472–977 (630 ± 163; 9) long by 120–311 (215 ± 58; 9) wide. Detached mature proglottids (Fig. 10E) 1,589–2,574 (1,954 ± 401; 6) long by 300–669 (480 ± 123; 6) wide. Detached gravid proglottid 6,390 (N = 1) long by 653 (N = 1) wide. Testes 75–112 (91 ± 13; 6) in total number, 8–13 (10 ± 2; 6) in post-poral field, elongate oval to round, 37–69 (54 ± 8; 6; 29) long by 46–97 (69 ± 11; 6; 29) wide, 1 layer deep in cross section, extending from anterior margin of ovary to near anterior margin of proglottid, in 3–4 irregular columns anterior to cirrus sac. Vas deferens minimal, coiling at antero-medial margin of cirrus sac, entering cirrus sac at its antero-medial margin. Cirrus sac elliptoid (Fig. 12C), 95–198 (136 ± 34; 6) long by 73–113 (88 ± 14; 6) wide, containing coiled cirrus; cirrus armed with small spinitriches. Genital pores lateral, irregularly alternating, 53–62% (58 ± 3; 6) of proglottid length from posterior end. Vagina straight, extending along midline of proglottid from ootype region to anterior margin of cirrus sac, then laterally along anterior margin of cirrus sac, opening into common genital atrium anterior to cirrus sac. Ovary at posterior margin of proglottid, symmetrical, inverted-A shaped in frontal view, bi-lobed in cross section, lobulated, 521–879 (685 ± 128; 6) long by 166–407 (291 ± 91; 6) wide. Mehlis' gland posterior to ovarian isthmus. Vitelline follicles essentially oval, sparsely distributed, in 2 lateral bands; each band consisting of 1 dorsal and 1 ventral column of follicles, extending from posterior margin of proglottid, stopping slightly short of anterior margin of testicular field, interrupted dorsally and ventrally by terminal genitalia, uninterrupted by ovary. Uterus saccate, medioventral, extending from ootype, stopping slightly short of anterior margin of testicular field. Excretory ducts in 2 lateral pairs. Eggs too wrinkled for shape to be determined.

Taxonomic summary

Type and only known host: *Loxodon* cf. *macrorhinus* (Carcharhinidae: Carcharhiniformes).

Type locality: Ibo (2°17′3.44″S, 40°35′10.83″E), Cabo Delgado, Mozambique, Mozambique Channel, Indian Ocean (unique host specimen no. MZ-29). Additional host specimens from type locality: MZ-30, MZ-32.

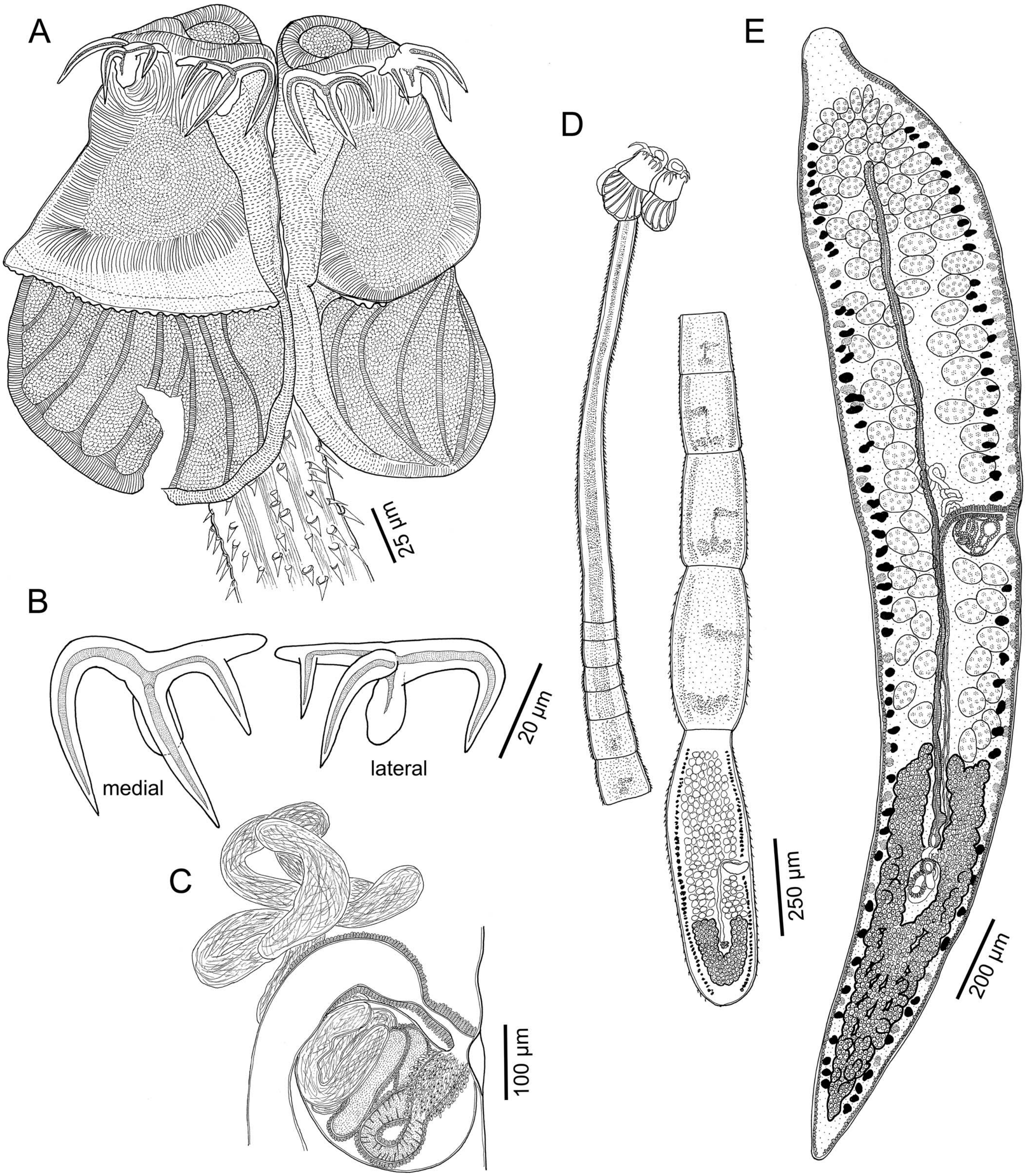

Figure 12. Line drawings of *Phoreiobothrium magnaloculum* n. sp. (**A**) Scolex (paratype, USNM 1743768). (**B**) Hooks (holotype, NMB-P 1067). (**C**) Terminal genitalia (paratype, USNM 1743770). (**D**) Whole worm (paratype, USNM 1743768). (**E**) Detached mature proglottid (paratype, LRP 11200).

Additional localities: None.

Site of infection: Spiral intestine.

Specimens deposited: Holotype (NMB-P 1067) and 4 paratypes (NMB-P 1065, NMB-P 1066, NMB-P 1068, NMB-P 1069); 6 paratypes (LRP 11198–11203) and 1 paratype SEM voucher (LRP 11204); 6 paratypes (USNM 1743768–1743773). Scolex prepared for SEM retained with JNC at the University of Connecticut.

Molecular material: Hologenophore (LRP 11205, JW469).

ZooBank registration: urn:lsid:zoobank.org:act:FA3B4808-F2DE-4686-ADF1-EC3BF0BF1EB4.

Etymology: The name of this species, Latin for large (*magna*) and loculus (*loculus*), highlights the unusually large size of the sublocular region relative to the anterior loculus.

Remarks

Phoreiobothrium magnaloculum n. sp. is readily distinguished from all 17 of its congeners in its possession of a posterior sublocular region that is almost as long as, rather than conspicuously shorter than, the anterior loculus. Although *P. jahki* also possesses an unusually long posterior loculus, that loculus is only about one-third as long as the anterior loculus. In addition, unlike all of its congeners, the vitelline follicles of this new species are sparsely, rather than more densely, arranged.

***Phoreiobothrium posteroporum* n. sp.**

(Figs. 13, 14A–G)

Description (based on whole mounts of 6 complete immature worms, 2 incomplete immature worms, 2 proglottid cross sections, and 2 scoleces prepared for SEM and their strobilar vouchers): Worms 5.4–8.9 mm (7.4 ± 1.3; 7) long, essentially hyperapolytic, greatest width generally at level of terminal proglottid (Fig. 13D); 27–43 (33 ± 5; 7) proglottids per worm. Scolex (Fig. 13A) consisting of scolex proper bearing 4 bothridia and cephalic peduncle, 223–409 (313 ± 66; 7) wide at level of subloculi. Bothridia constricted immediately posterior to hooks, 203–309 (240 ± 35; 7; 9) long by 98–201 (154 ± 32; 7; 10) wide; each with anterior muscular pad in form of loculus, 1 pair of hooks, and post-hook region divided into 1 anterior and 1 posterior loculus (Fig. 13A). Muscular pad 45–56 (52 ± 4; 7; 10) long by 72–118 (90 ± 18; 6; 9) wide, lacking apical papillae and papillae on latero-anterior margins. Anterior loculus considerably longer than posterior loculus, 186–281 (226 ± 34; 6; 7) long, posterior margin without small papillae; boundary between anterior loculus and sublocular region with double septum. Posterior loculus 14–36 (25 ± 9; 6; 7) long, subdivided into 14–16 (15 ± 1; 6; 10) subloculi; subloculi 10–16 (13 ± 2; 6; 20) wide. Hooks tri-pronged, hollow (Fig. 13B), with basal, axial, and abaxial prongs; basal prongs more than half as long as axial and abaxial prongs; each hook with blunt talon embedded in musculature of scolex, covered with thin layer of tissue (Fig. 14A); bases short. Lateral hook measurements: A 36–64 (50 ± 9; 7; 9), B 38–54 (46 ± 5; 7; 9), C 45–70 (55 ± 8; 7; 9), D 60–84 (77 ± 7; 7; 9), E 34–45 (40 ± 4; 7; 9), F 17–37 (26 ± 8; 7; 9); medial hook measurements: A′ 34–58 (47 ± 7; 8; 12), B′ 30–63 (52 ± 8; 8; 12), C′ 43–66 (53 ± 8; 8; 12), D′ 53–88 (74 ± 11; 8; 12), E′ 33–61 (44 ± 9; 8; 12), F′ 15–41 (29 ± 9; 8; 12). Cephalic peduncle 349–672 (528 ± 127; 8) long.

Apex of scolex proper and muscular pad surfaces covered with papilliform filitriches only. Distal bothridial surfaces (Fig. 14C) with sparsely arranged capilliform and acicular filitriches. Microtriches on lateral proximal bothridial surfaces differ along bothridial length; anterior proximal surfaces (Fig. 14E) bearing densely arranged small gladiate spinitriches with capilliform filitriches and papilliform filitriches near bothridial margin and with only papilliform filitriches away from margin; more posterior proximal surfaces (Fig. 14F) with sparsely arranged small gladiate spinitriches and papilliform filitriches; posterior-most proximal surfaces (Fig. 14G) with papilliform filitriches only. Proximal surfaces between bothridia (Fig. 14D) with capilliform and papilliform filitriches near bothridial margins and papilliform filitriches only away from bothridial margins. Cephalic peduncle covered with acicular filitriches and large gladiate spinitriches (Fig. 14B). Strobila covered with capilliform filitriches and sparsely arranged smaller gladiate spinitriches decreasing in density posteriorly.

Proglottids acraspedote. Immature proglottids 27–43 (33 ± 5; 7) in number, initially wider than long, becoming longer than wide with maturity (Fig. 13D). Posterior-most immature proglottids 439–776 (579 ± 109; 7) long by 190–382 (284 ± 67; 7) wide (Fig. 13E). Fully mature proglottids not observed. Testes 76–88 (N = 4) in total number, 4–7 (N = 4) in post-poral field, elongate oval to round, 19–30 (24 ± 3; 4; 20) long by 34–61 (45 ± 8; 4; 20) wide, 1 layer deep in cross section, extending from anterior margin of ovary, stopping short of anterior margin of proglottid, in 4 irregular columns anterior to cirrus sac. Vas deferens minimal, coiling at antero-medial margin of cirrus sac, entering cirrus sac at its antero-medial margin. Cirrus sac dolioform (Fig. 13C), 62–127 (94 ± 26; 5) long by 26–37 (31 ± 5; 5) wide, containing coiled cirrus; cirrus armed with small spinitriches. Genital pores lateral, irregularly alternating, 26–38% (32 ± 4; 7) of proglottid length from posterior end. Vagina straight, extending along midline of proglottid from ootype region to anterior margin of cirrus sac, then laterally along anterior margin of cirrus sac, opening into common genital atrium anterior to cirrus sac. Ovary at posterior margin of proglottid, symmetrical, inverted-A shaped in frontal view, bi-lobed in cross section, lobulated, 91–145 (N = 4) long by 113–211 (N = 4) wide. Mehlis' gland posterior to ovarian isthmus. Vitelline follicles round to slightly oval, in 2 lateral bands; each band consisting of 1 dorsal and 1 ventral column of follicles, extending from posterior margin of proglottid, stopping short of anterior margin of testicular field, interrupted dorsally and ventrally by terminal genitalia, uninterrupted by ovary. Uterus saccate, medioventral, extending from ootype, stopping well short of anterior margin of testicular field. Excretory ducts in 2 lateral pairs. Gravid proglottids and eggs not observed.

Taxonomic summary

Type and only known host: Lamiopsis tephrodes (Fowler) (Carcharhinidae: Carcharhiniformes).

Type locality: Mukah (2°53′52.16″N, 112°05′44.12″E), Borneo, Malaysia, South China Sea, Pacific Ocean (unique host specimen no. BO-74). Additional host specimens from the type locality: BO-259, BO-488.

Additional localities: None.

Site of infection: Spiral intestine.

Specimens deposited: Holotype (MZUM[P] 2025.2 [H]) and 2 paratypes (MZUM[P] 2025.3 [P] and MZUM[P] 2025.4 [P]); 2

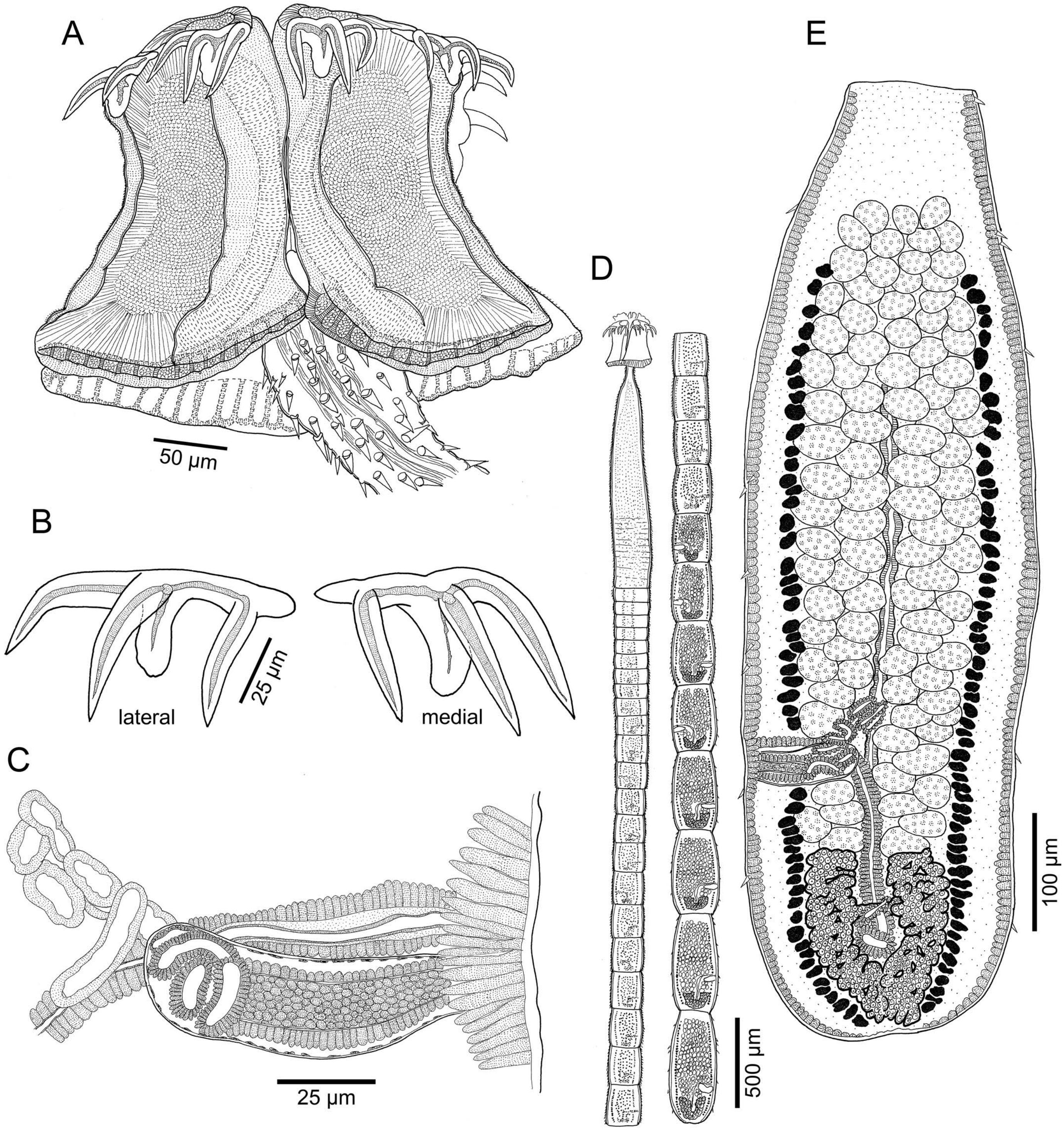

Figure 13. Line drawings of *Phoreiobothrium posteroporum* n. sp. (**A**) Scolex (paratype, LRP 11206). (**B**) Hooks (paratype, USNM 1743777). (**C**) Terminal genitalia (holotype, MZUM[P] 2025.2 [H]). (**D**) Whole worm (holotype, MZUM[P] 2025.2 [H]). (**E**) Terminal mature proglottid (paratype, USNM 1743776).

paratypes (LRP 11206 and LRP 11207), 2 paratype SEM vouchers (LRP 11208 and LRP 11209), 2 proglottid cross sections (LRP 11210 and LRP 11211); 3 paratypes (USNM 1743776–1743778). Scoleces prepared for SEM retained with JNC at the University of Connecticut.

Molecular material: Hologenophore (LRP 11212, ON15).

ZooBank registration: urn:lsid:zoobank.org:act:3AEB575F-2607-4095-8922-513F88900DF5.

Etymology: The name of this species is named for the posterior (L. *postero*) position of its genital pore (*L. porum*).

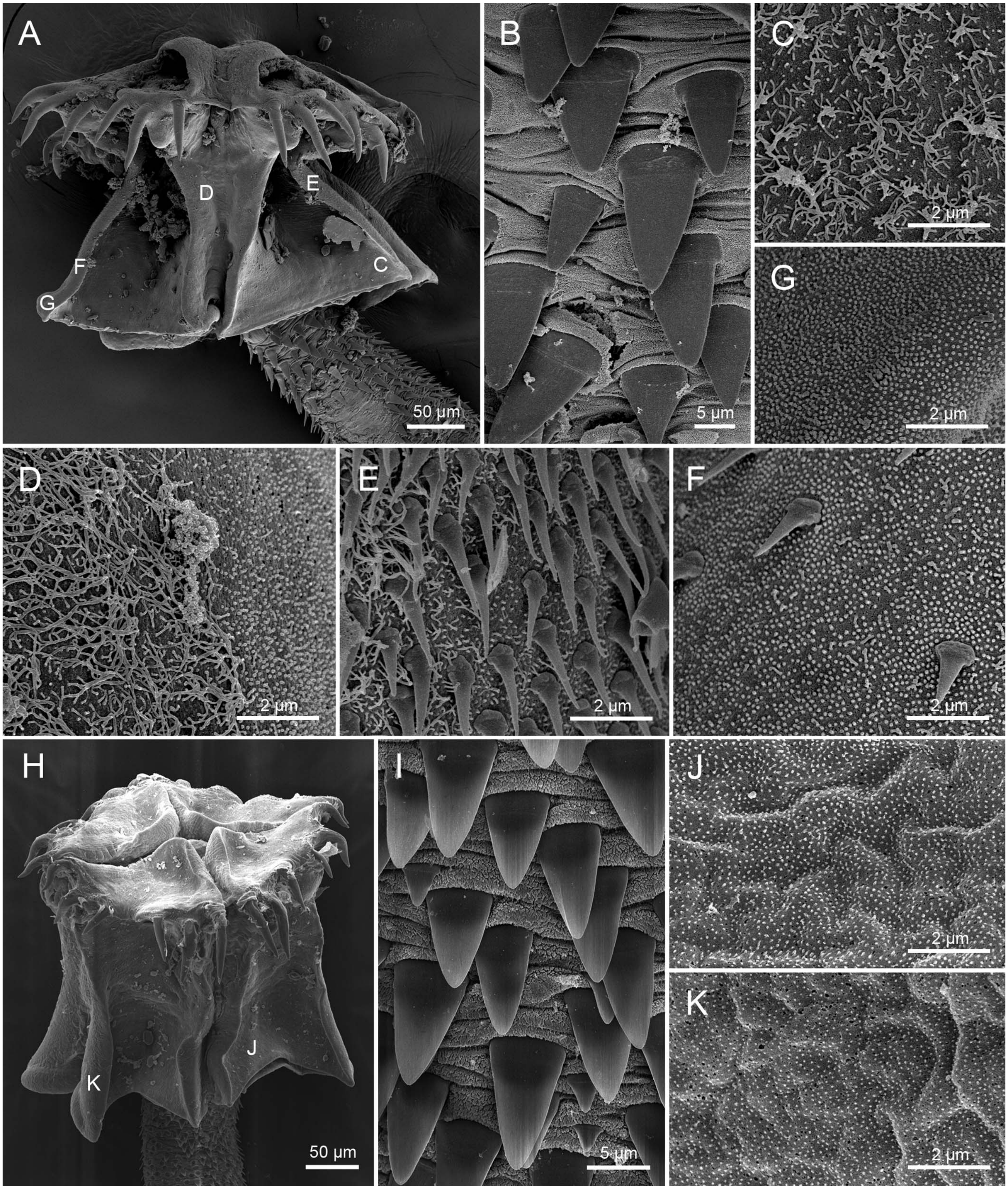

Figure 14. Scanning electron micrographs of *Phoreiobothrium posteroporum* n. sp. (**A–G**) and *Phoreiobothrium tesserascolex* n. sp. (**H–K**). (**A**) Scolex of *P. posteroporum* n. sp., small letters indicate locations of C–G. (**B**) Large gladiate spinitriches and acicular filitriches on cephalic peduncle of *P. posteroporum* n. sp. (**C**) Sparsely arranged capilliform and acicular filitriches on distal surfaces of bothridia of *P. posteroporum* n. sp. (**D**) Capilliform and papilliform filitriches on proximal surfaces near margin between bothridia; papilliform filitriches only away from bothridial margins of *P. posteroporum* n. sp. (**E**) Densely arranged small gladiate spinitriches on proximal surface of anterior region of bothridium, with capilliform

Remarks

Phoreiobothrium posteroporum n. sp. differs from all 18 of its congeners in its possession of a genital pore that is more posterior in position (26–38% vs. 42–47%, 85–95%, 47–55%, 45–52%, 50–60%, 54–62%, 39–57%, 39–49%, 53–62%, 51–68%, 43–48%, 55–61%, 42–50%, 43–64%, 46–57%, 45–58%, 46–52%, and 48–61%, respectively) than that of *P. angustivastum*, *P. anticaporum*, *P. blissorum*, *P. danae*, *P. golchini*, *P. iraniense*, *P. jahki*, *P. lasium*, *P. magnaloculum*, *P. martini*, *P. nadiae*, *P. perilocrocodilus*, *P. robertsoni*, *P. rozatii*, *P. sarahae*, *P. sorrahcola*, *P. swaki*, and *P. tiburonis*. It further differs from each of these species as follows. It possesses a greater number of subloculi than *P. angustivastum*, *P. magnaloculum*, and *P. tiburonis* (14–16 vs. 9–12, 8–10, and 8–13) and a smaller number of subloculi than *P. blissorum*, *P. lasium*, *P. martini*, *P. nadiae*, and *P. robertsoni* (14–16 vs. 23–31, 25–30, 20–22, 18–28, and 25–29, respectively). This new species has a greater number of proglottids than *P. perilocrocodilus* (27–43 vs. 11–22). It differs further from *P. jahki* in that its sublocular region is conspicuously shorter than its anterior locular region (only about one-fifth vs. one-third of the post-hook bothridial region). Unlike *P. danae*, the vitelline follicles of *P. posteroporum* n. sp. are round rather than irregular in shape and do not extend towards the medial line of the proglottid; unlike those of *P. iraniense* and *P. sarahae*, the vitelline follicles in each lateral band of this new species are arranged in 1 dorsal and 1 ventral column, rather than in 2–3 dorsal and 2–3 ventral columns. The axial prongs of both the medial and lateral hooks are longer in this new species than in *P. sorrahcola* (B 38–54 vs. 56–80; B′ 30–63 vs. 66–98); the axial prong of the medial hook is shorter in the new species than in *P. anticaporum* (B′ 30–63 vs. 65–83). This new species also differs from *P. golchini* and *P. rozatii* in possessing, rather than lacking, small gladiate spinitriches on its proximal bothridial surfaces. *Phoreiobothrium posteroporum* n. sp. further differs from *P. swaki* in possessing longer bases on both the lateral (C 45–70 vs. 26–34) and medial (C′ 43–63 vs. 31–39) hooks.

***Phoreiobothrium tesserascolex* n. sp.**

(Figs. 14H–K, 15)

Description (based on whole mounts of 9 mature worms and 2 scoleces prepared for SEM and their strobilar vouchers): Worms 11.0–19.5 mm (14.9 ± 2.8; 9) long, euapolytic, greatest width generally at level of scolex (Fig. 15D); 31–49 (41 ± 6; 9) proglottids per worm. Scolex (Fig. 15A) consisting of scolex proper bearing 4 bothridia and cephalic peduncle, 294–376 (331 ± 25; 9) wide at level of hooks. Bothridia lacking constriction immediately posterior to hooks, 304–382 (341 ± 24; 9; 18) long by 182–246 (212 ± 18; 9;15) wide; each with anterior muscular pad in form of loculus, 1 pair of hooks, and post-hook region divided into 1 anterior and 1 posterior loculus (Fig. 15A). Muscular pad 40–66 (50 ± 9; 8; 13) long by 138–187 (161 ± 15; 7; 9) wide, lacking apical papillae and papillae on latero-anterior margins. Anterior loculus considerably longer than posterior loculus, 254–335 (290 ± 24; 9; 18) long, without small papillae; boundary between anterior loculus and sublocular region with double septum. Posterior loculus 22–40 (31 ± 6; 9; 18) long, subdivided into 15–19 (17 ± 1; 8; 12) subloculi; subloculi 11–17 (14 ± 2; 9; 18) wide. Hooks tri-pronged, hollow, with basal, axial, and abaxial prongs (Fig. 15B); basal prongs more than half as long as axial and abaxial prongs; each hook with blunt talon embedded in musculature of scolex, covered with thin layer of tissue (Fig. 14H); bases short. Lateral hook measurements: A 42–70 (57 ± 10; 7), B 41–69 (59 ± 10; 9), C 62–76 (67 ± 4; 8), D 87–108 (98 ± 6; 9), E 32–40 (36 ± 3; 9), F 26–36 (30 ± 3; 9); medial hook measurements: A′ 61–81 (70 ± 6; 9), B′ 69–88 (78 ± 7; 9), C′ 61–81 (70 ± 6; 9), D′ 71–127 (102 ± 20; 8), E′ 30–55 (42 ± 8; 9), F′ 32–38 (35 ± 2; 9). Cephalic peduncle 541–1,251 (820 ± 252; 9) long.

Apex of scolex proper, muscular pad, proximal (Fig. 14K) and distal (Fig. 14J) bothridial surfaces covered with papilliform filitriches only. Cephalic peduncle covered with acicular filitriches and large gladiate spinitriches (Fig. 14I). Strobila covered with capilliform filitriches and sparsely arranged smaller gladiate spinitriches decreasing in density posteriorly.

Proglottids acraspedote. Immature proglottids 27–44 (37 ± 5; 9) in number, initially wider than long, becoming longer than wide with maturity (Fig. 15D). Posterior-most immature proglottid 628–998 (813 ± 155; 9) long by 205–361 (268 ± 47; 9) wide. Mature proglottids 3–6 (4 ± 1; 9) in number. Terminal mature proglottid (Fig. 15E) 1,582–2,122 (1,882 ± 182; 9) long by 265–352 (317 ± 25; 9) wide; length to width ratio 3–6:1 (4 ± 1; 9). Testes 66–90 (79 ± 7; 9; 13) in total number, 8–13 (10 ± 1; 9; 13) in post-poral field, elongate oval to round, 41–76 (60 ± 8; 9; 27) long by 56–78 (63 ± 5; 9; 27) wide, 1 layer deep in cross section, extending from anterior margin of ovary to near anterior margin of proglottid, in 4–5 irregular columns anterior to cirrus sac. Vas deferens minimal, coiling at antero-medial margin of cirrus sac, entering cirrus sac at its antero-medial margin. Cirrus sac elliptoid (Fig. 15C), 137–167 (151 ± 11; 9) long by 77–124 (112 ± 15; 9) wide, containing coiled cirrus; cirrus armed with small spinitriches. Genital pores lateral, irregularly alternating, 44–54% (48 ± 3; 9) of proglottid length from posterior end. Vagina weakly sinuous, extending along midline of proglottid from ootype region to anterior margin of cirrus sac, then laterally along anterior margin of cirrus sac, opening into common genital atrium anterior to cirrus sac. Ovary at posterior margin of proglottid, symmetrical, inverted-A shaped in frontal view, bi-lobed in cross section, lobulated, 343–606 (479 ± 81; 9) long by 175–239 (211 ± 23; 9) wide. Mehlis' gland posterior to ovarian isthmus. Vitelline follicles round to slightly oval, in 2 lateral bands; each band consisting of 1 dorsal and 1 ventral column of follicles, extending from posterior margin of proglottid to anterior margin of testicular field, interrupted dorsally and ventrally by terminal genitalia, uninterrupted by ovary. Uterus saccate, medioventral, extending from ootype, stopping short of anterior margin of testicular field. Excretory ducts in 2 lateral pairs. Gravid proglottids and eggs not observed.

←
filitriches near margin and papilliform filitriches away from margin of *P. posteroporum* n. sp. (**F**) Sparsely arranged gladiate spinitriches and papilliform filitriches on proximal surface of mid-posterior region of bothridium of *P. posteroporum* n. sp. (**G**) Papilliform filitriches on proximal surface of posterior most region of bothridium of *P. posteroporum* n. sp. (**H**) Scolex of *P. tesserascolex* n. sp., small letters indicate locations of J, K. (**I**) Large gladiate spinitriches and acicular filitriches on cephalic peduncle of *P. tesserascolex* n. sp. (**J**) Papilliform filitriches on distal surfaces of *P. tesserascolex* n. sp. (**K**) Papilliform filitriches on proximal surfaces of *P. tesserascolex* n. sp.

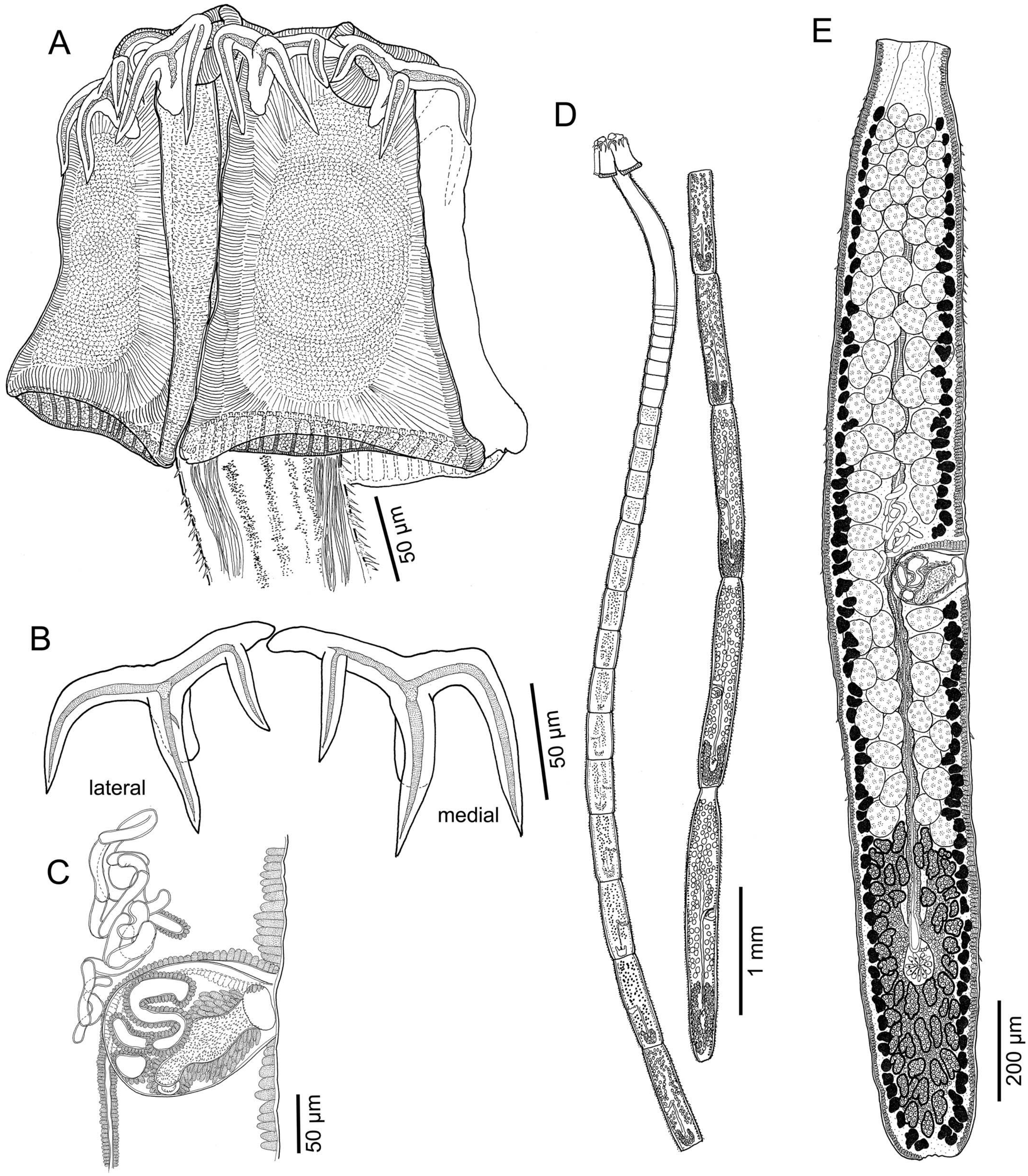

Figure 15. Line drawings of *Phoreiobothrium tesserascolex* n. sp. (**A**) Scolex (holotype, USNM 1743786). (**B**) Hooks (paratype, LRP 11213). (**C**) Terminal genitalia (holotype, USNM 1743786). (**D**) Whole worm (holotype, USNM 1743786). (**E**) Terminal mature proglottid (holotype, USNM 1743786).

Taxonomic summary

Type and only known host: *Carcharhinus brevipinna* (Valenciennes in Müller and Henle) (Carcharhinidae: Carcharhiniformes).

Type locality: Off Louisiana (29°58′58.20″N, 88°36′16.80″W), Gulf of Mexico, Atlantic Ocean (unique host specimen no. MS05-357).

Additional localities: Off Mississippi (29°37′22.8″N, 88°30′11″W), Gulf of Mexico, Atlantic Ocean (unique host specimen no. MS05-5).

Site of infection: Spiral intestine.

Specimens deposited: Holotype (USNM 1743786) and 4 paratypes (USNM 1743787–1743790); 4 paratypes (LRP 11213–11216) and 2 paratype SEM vouchers (LRP 11217 and LRP 11218). Scoleces prepared for SEM retained with JNC at the University of Connecticut.

Molecular material: Hologenophore (LRP 11219, KW2).

ZooBank registration: urn:lsid:zoobank.org:act:48EAA1F4-EEB7-468C-B10B-E60C1114E851.

Etymology: The name of this species is derived from the Latin *tessera* (paving stone) in reference to the form of its scolex.

Remarks

Phoreiobothrium tesserascolex n. sp. is longer in total length than *P. anticaporum*, *P. golchini*, *P. iraniense*, *P. jahki*, *P. magnaloculum*, *P. nadiae*, *P. perilocrocodilus*, *P. posteroporum*, *P. rozatii*, *P. sarahae*, *P. sorrahcola*, *P. swaki*, and *P. tiburonis* (11–19.5 mm vs. 3.8–7.1 mm, 3.2–8 mm, 4–5.8 mm, 4.4–7.8 mm, 3–6.1 mm, 4.7–7.9 mm, 2.1–6.7 mm, 5.3–8.9 mm, 3–6 mm, and 3.8–5.9 mm, respectively). The new species can be distinguished from *P. blissorum*, *P. lasium*, *P. martini*, and *P. robertsoni* in its possession of fewer subloculi (15–19 vs. 23–31, 25–30, 20–22, and 25–29, respectively). It conspicuously differs from *P. angustivastum* in possessing much larger medial and lateral hooks, in fact, there is no overlap in the ranges of any of the measurements between these 2 species. This new species differs from *P. danae* in that its vitelline follicles are round to slightly oval, rather than being irregular in shape and extending towards the medial line of the proglottid. *Phoreiobothrium tesserascolex* n. sp. differs further from each of its congeners as follows. It has fewer proglottids than *P. blissorum* and *P. lasium* (31–49 vs. 55–79 and 54–107, respectively). The genital pore of the new species is located much more posteriorly than that seen in *P. anticaporum* and more anteriorly than seen in *P. posteroporum* (44–54% vs. 85–95% and 26–38%, respectively). *Phoreiobothrium tesserascolex* n. sp. possesses more testes than *P. nadiae* (66–90 vs. 54–64), many fewer testes in the post-poral field than *P. martini* (8–13 vs. 26–31) and a greater number in that field than seen in *P. swaki* (8–13 vs. 4–7). Unlike *P. jahki* and *P. magnaloculum*, both of which possess a posterior locular region of the bothridium that approaches the length of the anterior locular region, the posterior locular region of *P. tesserascolex* is inconspicuous. Whereas the bothridia of *P. angustivastum*, *P. danae*, and *P. robertsoni* are constricted immediately posterior to the hooks, this constriction is lacking in the new species. This new species further differs from *P. tiburonis* in lacking, rather than possessing, small gladiate spinitriches on its proximal bothridial surfaces. It further differs from *P. sorrahcola* in possessing a longer anterior locular region (254–335 vs. 151–244). The terminal mature proglottid of *Phoreiobothrium tesserascolex* n. sp. is considerably longer than that of *P. rozatii* (1,582–2,122 vs. 416–940). This new species differs further from *P. golchini* in its possession of much larger bothridia (304–382 long by 182–246 wide vs. 122–173 long by 80–115 wide). Finally, *P. tesserascolex* n. sp. further differs from *P. iraniense* and *P. sarahae* in that its lateral bands of vitelline follicles consist of 1 dorsal and 1 ventral column, rather than 2–3 dorsal and 2–3 ventral columns.

***Phoreiobothrium waeschenbachae* n. sp.**
(Fig. 16)

Description (based on whole mounts of 5 complete immature worms): Worms 3.4–7.9 mm (5.2 ± 1.9; 5) long, essentially hyperapolytic, greatest width generally at level of terminal proglottid (Fig. 16D); 11–28 (21 ± 7; 5) proglottids per worm. Scolex (Fig. 16A) consisting of scolex proper bearing 4 bothridia and cephalic peduncle, 195–279 (233 ± 36; 5) wide at level of subloculi. Bothridia lacking constriction immediately posterior to hooks, 138–209 (159 ± 28; 5) long by 95–129 (115 ± 15; 4) wide; each with anterior muscular pad in form of loculus, 1 pair of hooks, and post-hook region divided into 1 anterior and 1 posterior loculus (Fig. 16A). Muscular pad 21–38 (31 ± 6; 4; 5) long by 71–79 (N = 1; n = 2) wide, lacking apical papillae and papillae on latero-anterior margins. Anterior loculus considerably longer than posterior loculus, 119–183 (137 ± 27; 5) long, posterior margin without small papillae; boundary between anterior loculus and sublocular region with double septum. Posterior loculus 22–38 (30 ± 8; 5) long, subdivided into 18–19 subloculi (N = 1; n = 2); subloculi 8–10 (N = 1; n = 4) wide. Hooks tri-pronged, hollow, with basal, axial, and abaxial prongs (Fig. 16B); basal prongs more than half as long as axial and abaxial prongs; each hook with blunt talon embedded in musculature of scolex, covered with thin layer of tissue; bases short. Lateral hook measurements: A 28–40 (N = 3; n = 4), B 26–45 (N = 3; n = 4), C 27–37 (N = 3; n = 4), D 39–52 (N = 3; n = 4), E 15–20 (N = 3; n = 4), F 12–18 (N = 3; n = 4); medial hook measurements: A′ 30–51 (N = 4; n = 6), B′ 20–53 (N = 4; n = 6), C′ 31–42 (N = 4; n = 6), D′ 40–60 (N = 4; n = 6), E′ 13–26 (N = 4; n = 6), F′ 9–22 (N = 4; n = 6). Cephalic peduncle 332–811 (533 ± 186; 5) long. Microtriches not observed on scolex proper. Cephalic peduncle with gladiate spinitriches (Fig. 16A). Strobila covered with sparsely arranged smaller gladiate spinitriches decreasing in density posteriorly (Fig. 16E).

Proglottids acraspedote. Immature proglottids 11–28 (N = 4) in number, initially wider than long, becoming longer than wide with maturity (Fig. 16D). Posterior-most immature proglottid 427–967 (813 ± 225; 5) long by 212–323 (274 ± 40; 5) wide (Fig. 16E). Mature proglottids not observed. Testes 50–62 (N = 4) in total number, 5 (N = 4) in post-poral field, elongate oval to round, 27–49 (41 ± 7; 4; 18) long by 35–67 (51± 9; 4; 18) wide, 1 layer deep in cross section, extending from anterior margin of ovary to near anterior margin of proglottid, in 5–6 irregular columns anterior to cirrus sac. Vas deferens minimal, coiling at antero-medial margin of cirrus sac, entering cirrus sac at its antero-medial margin. Cirrus sac elliptoid (Fig. 16C), 93–132 (N = 4) long by 48–107 (N = 4) wide, containing coiled cirrus; cirrus armed with small spinitriches. Genital pores lateral, irregularly alternating, 52–59% (55 ± 3; 5) of proglottid length from posterior end. Vagina straight, extending along midline of proglottid from ootype region to anterior margin of cirrus sac, then laterally along anterior margin of cirrus sac, opening into common genital atrium anterior to cirrus sac. Ovary at posterior margin of proglottid, symmetrical, inverted-A shaped in frontal view, bi-lobed

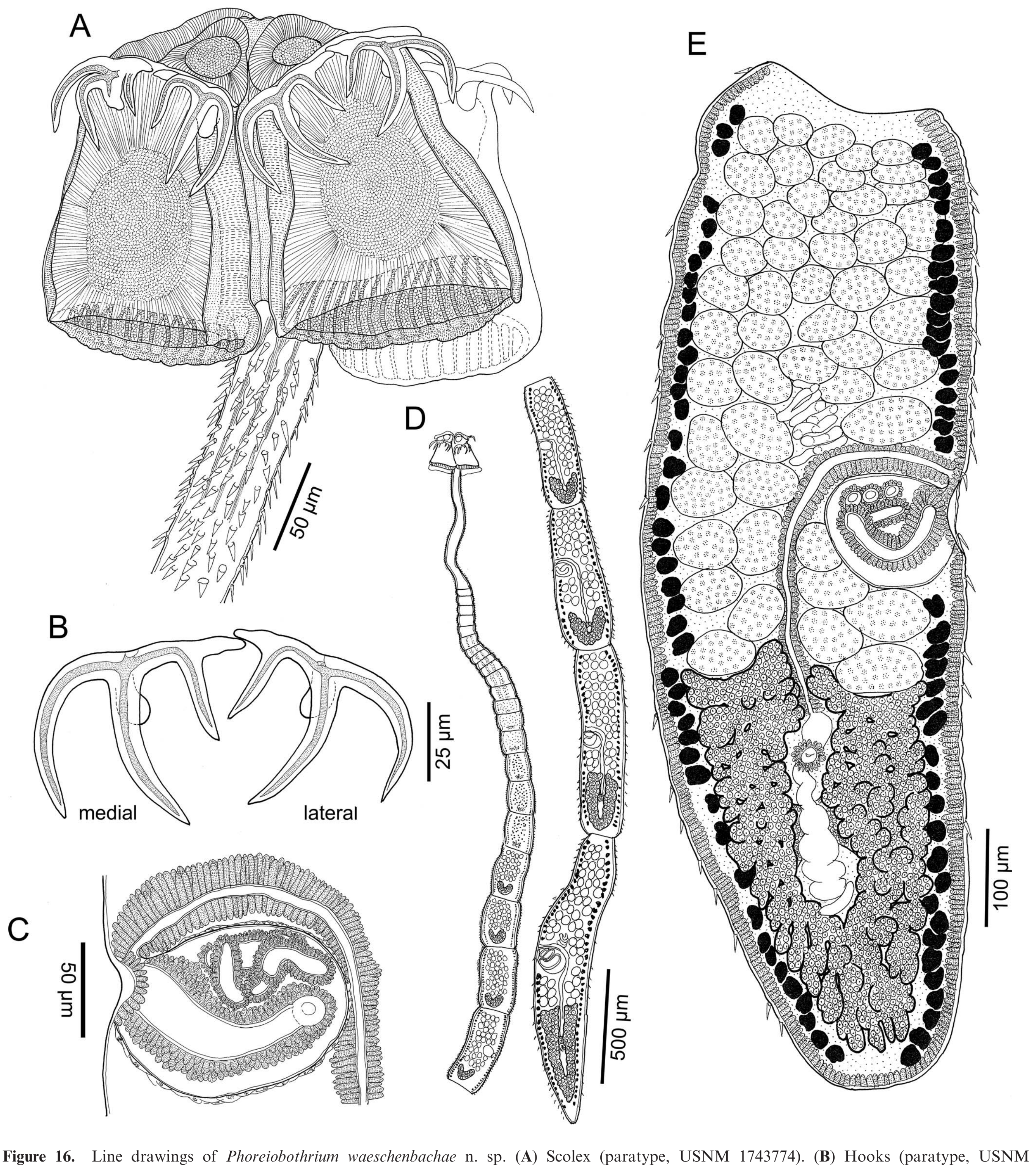

Figure 16. Line drawings of *Phoreiobothrium waeschenbachae* n. sp. (**A**) Scolex (paratype, USNM 1743774). (**B**) Hooks (paratype, USNM 1743774). (**C**) Terminal genitalia (holotype, MZUM[P] 2025.1 [H]). (**D**) Whole worm (holotype, MZUM[P] 2025.1 [H]). (**E**) Terminal mature proglottid (paratype, LRP 11220).

in cross section, lobulated, 272–463 (N = 4) long by 182–219 (N = 4) wide. Mehlis' gland posterior to ovarian isthmus. Vitelline follicles round to slightly oval, in 2 lateral bands; each band consisting of 1 dorsal and 1 ventral column of follicles, extending from posterior margin of proglottid to anterior margin of testicular field, interrupted dorsally and ventrally by terminal genitalia, uninterrupted by ovary. Uterus saccate, medioventral, extending from ootype, stopping well short of anterior margin of testicular field. Excretory ducts in 2 lateral pairs. Gravid proglottids and eggs not observed.

Taxonomic summary

Type and only known host: Scoliodon macrorhynchos (Bleeker) (Carcharhinidae: Carcharhiniformes).

Type locality: Mukah (2°53′52.16″N, 112°05′44.12″E), Borneo, Malaysia, South China Sea, Pacific Ocean (unique host specimen no. BO-266). Additional host specimens from type locality: BO-244, BO-262.

Additional localities: Cat Ba Island (20°43′31.1″N, 107°02′54.9″E), Haiphong Province, Vietnam, Gulf of Tonkin, Pacific Ocean (unique host specimen no. VN-11).

Site of infection: Spiral intestine.

Specimens deposited: Holotype (MZUM[P] 2025.1 [H]); 2 paratypes (LRP 11220 and LRP 11221); 2 paratypes (USNM 1743774 and USNM 1743775).

Molecular material: Hologenophore (LRP 11222, JW310; LRP 11223, ON19 [image voucher]).

ZooBank registration: urn:lsid:zoobank.org:act:9CD7419E-D9FC-427B-9B12-1467E3F343F9.

Etymology: This species honors Andrea Waeschenbach of the Natural History Museum of London for generating sequence data for a subset of the specimens included in our molecular phylogenetic analysis.

Remarks

Phoreiobothrium waeschenbachae n. sp. can be easily distinguished from the majority of its congeners based on the number of bothridial subloculi. It bears a greater number of subloculi than *P. angustivastum*, *P. golchini*, *P. iraniense*, *P. jahki*, *P. magnaloculum*, *P. posteroporum*, *P. rozatii*, *P. sarahae*, *P. sorrahcola*, *P. swaki*, and *P. tiburonis* (18–19 vs. 14–16, 11–15, 13–16, 10–15, 8–10, 14–16, 12–15, 12–16, 12–14, 11–13, and 8–13, respectively) and fewer subloculi than *P. blissorum*, *P. lasium*, *P. martini*, and *P. robertsoni* (18–19 vs. 23–31, 25–30, 20–22, and 25–29, respectively). It differs from *P. danae* in possessing fewer testes (50–62 vs. 69–88) and in that its vitelline follicles are round to slightly oval, rather than irregular in shape and much wider than long. Relative to *P. nadiae*, this new species has smaller lateral hooks (A 28–40 vs. 47–53, C 27–37 vs. 41–51, D 39–52 vs. 63–97, E 15–20 vs. 22–33 and F 9–22 vs. 24–33). With respect to *P. perilocrocodilus*, it has a greater number of testes (50–62 vs. 36–49) and its bothridia lack a constriction immediately posterior to the hooks. This new species has a genital pore that is much more posterior in position than that of *P. anticaporum* (52–59% vs. 85–95% of proglottid length from the posterior end). *Phoreiobothrium waeschenbachae* n. sp. differs further from its other congeners as follows. It has fewer testes than *P. angustivastum*, *P. blissorum*, *P. jahki*, *P. lasium*, *P. magnaloculum*, *P. martini*, *P. posteroporum*, *P. robertsoni*, *P. rozatii*, *P. sarahae*, *P. sorrahcola*, and *P. tesserascolex* (50–62 vs. 72–84, 103–127, 72–163, 95–139, 75–112, 88–96, 76–88, 74–132, 66–103, 83–115, 68–103, 66–90, respectively). It has fewer post-poral testes than *P. anticaporum*, *P. golchini*, *P. iraniense*, *P. nadiae*, and *P. tiburonis* (5 vs. 18–25, 6–15, 7–11, 7–11, and 9–17, respectively). It further differs from *P. swaki* in possessing a longer ovary (272–463 vs. 115–221) and from *P. tesserascolex* in being a smaller worm (3.4–7.9 mm vs. 11–19.5 mm).

Undescribed species of *Phoreiobothrium* and *Triloculatum*

Beyond the 6 new species of *Phoreiobothrium* we have formally described here, we encountered evidence of 16 additional, likely new, species of *Phoreiobothrium* and 1 new species of *Triloculatum*, for which insufficient material was available for the morphological work required for formal description. Nonetheless, this material provides evidence to expand the diversity, geographic distributions, and known hosts for members of the family. Material preserved in ethanol of 9 of these new species of *Phoreiobothrium* allowed for their inclusion in our phylogenetic analysis; they were assigned the provisional numerical designations *Phoreiobothrium* n. sp. 1 through *Phoreiobothrium* n. sp. 9. Localities, hosts, GenBank numbers for the sequence data, and LRP accession numbers for the hologenophores of these 9 species are given in Table II. Our formalin-fixed material yielded specimens of 7 additional potentially new species of *Phoreiobothrium*; these were assigned the provisional numerical designations *Phoreiobothrium* n. sp. 10 through *Phoreiobothrium* n. sp. 16. Also among the formalin-fixed material was 1 new species of *Triloculatum* and a specimen of *Phoreiobothrium* n. sp. 5. Scanning electron microscope images of the scolex of a specimen of each of these 9 species are provided in Figure 17. These species are as follows: *Phoreiobothrium* n. sp. 10 (Fig. 17A) from *Carcharhinus altimus* (Springer) in the western Atlantic Ocean (unique host specimen no. KC-18), *Phoreiobothrium* n. sp. 11 (Fig. 17B, SEM voucher LRP 11236) from *Carcharhinus amblyrhynchoides* (Whitley) in Australia (unique host specimen no. AU-100), *Phoreiobothrium* n. sp. 5 from *Carcharhinus amboinensis* 1 (Fig. 17C) in Australia (unique host specimen no. AU-22), *Phoreiobothrium* n. sp. 12 (Fig. 17D) from *Carcharhinus* cf. *leucas* 1 in the Gulf of California (unique host specimen no. BJ-191), *Phoreiobothrium* n. sp. 14 (Fig. 17E) from *Carcharhinus pleurotaenia* in Australia (unique host specimen no. AU-8), *Phoreiobothrium* n. sp. 13 (Fig. 17F) from *Sphyrna zygaena* (L.) in the Gulf of California (unique host specimen no. BJ-666), *Phoreiobothrium* n. sp. 16 (Fig. 17G, SEM voucher LRP 11237) from *Rhizoprionodon terraenovae* in the western Atlantic Ocean (unique host specimen no. PE-18), *Phoreiobothrium* n. sp. 15 (Fig. 17H) from *Triaenodon obesus* in Australia (unique host specimen no. TJL-1), and *Triloculatum* n. sp. 1 from *Carcharhinus* cf. *leucas* 1 (Fig. 17I) from the Gulf of California (unique host specimen no. BJ-191).

DISCUSSION

Our focus on scolex features in the taxonomic comparisons made here is fueled by the fact that proglottid anatomy across species of *Phoreiobothrium*, *Sphyrnacestus*, and *Triloculatum* is highly conserved. Species in all 3 genera possess a large number of testes that are distributed throughout the proglottid. The ovary is inverted A-shaped, or occasionally H-shaped, in frontal view and bi-lobed in cross section. The vitelline follicles are arranged in 2 lateral bands that extend much of the length of proglottid. Although *Sphyrnacestus* bears a uterus that extends only to the midlevel of the proglottid rather than to near the anterior margin of the proglottid as in *Phoreiobothrium* and *Triloculatum*, the uterus is saccate and medioventral in all 3 genera. With the exception of *P. anticaporum* and *P. posteroporum*, the genital pore, and thus the terminal genitalia, are located near or slightly posterior to the midlevel of the proglottid. As their names suggest, in the

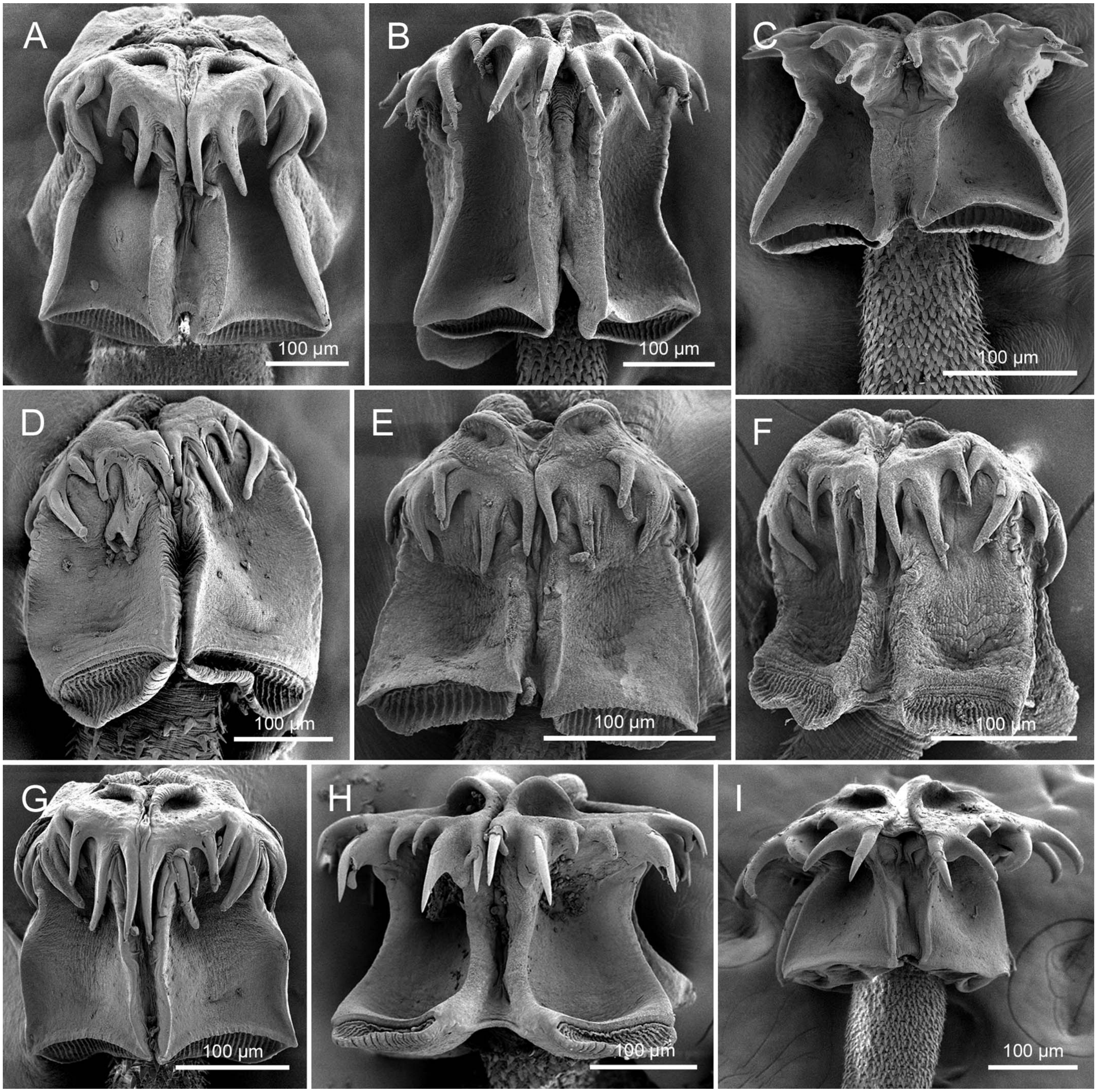

Figure 17. Undescribed species of *Phoreiobothrium* Linton, 1889 and *Triloculatum* Caira and Jensen, 2009. (**A**) *Phoreiobothrium* n. sp. 10 from *Carcharhinus altimus* (Springer). (**B**) *Phoreiobothrium* n. sp. 11 from *Carcharhinus amblyrhynchoides* (Whitley). (**C**) *Phoreiobothrium* n. sp. 5 from *Carcharhinus amboinensis* 1. (**D**) *Phoreiobothrium* sp. 12 from *Carcharhinus* cf. *leucas* 1. (**E**) *Phoreiobothrium* n. sp. 14 from *Carcharhinus pleurotaenia*. (**F**) *Phoreiobothrium* n. sp. 13 from *Sphyrna zygaena* (L.). (**G**) *Phoreiobothrium* n. sp. 16 from *Rhizoprionodon terraenovae* (Richardson). (**H**) *Phoreiobothrium* n. sp. 15 from *Triaenodon obesus* (Rüppell). (**I**) *Triloculatum* n. sp. 1 from *Carcharhinus* cf. *leucas* 1.

former 2 species the genital pore is located near the anterior margin of the proglottid or more posteriorly in the proglottid, respectively.

The results of the phylogenetic analysis yielded a tree with 3 subclades of species of phoreiobothriids that are consistent with membership of the genera *Triloculatum*, *Sphyrnacestus*, and *Phoreiobothrium*. However, in addition to the fact that our analysis was based solely on sequence data for a portion of the *28S* rDNA gene, the following limitations should be noted when interpreting our results. Only 1 of the 6 described species of *Triloculatum* was included in the dataset. Although the replicates of this species grouped outside of the 2 other subclades, suggesting that this genus may be sister to this pair of genera, this result should be confirmed with broader taxon sampling of this genus. The group containing the specimens of *Phoreiobothrium* was relatively highly supported and appears to include a well-supported subclade comprising the species parasitizing requiem sharks in the Pacific and Indian Oceans (i.e., *P. magnaloculum*, *P. posteroporum*, *P. waeschenbachae*, and *Phoreiobothrium* n. sp. 1 through 5). Of the 16 species of *Phoreiobothrium* in the analysis, 1 was previously described (i.e., *P. perilocrocodilus*), 6 are described here, and 9 remain to be formally described. In addition, 15 previously described species were not included in the dataset. Taxon sampling in *Sphyrnacestus* was somewhat more extensive; 6 of the 9 described species, including 2 of the 4 described here, were included. However, this subclade was not well supported. Nonetheless, given the striking morphological similarities within, and differences among, these subclades, we believe recognition of *Sphyrnacestus* as a separate genus is justified.

Unlike the hooks of *Phoreiobothrium* and *Triloculatum*, which are relatively uniform across species in consisting of medial and lateral hooks that each bear 3 prongs, with the basal prong being the shortest, hook morphology across species of *Sphyrnacestus* is quite variable. The medial and lateral hooks of *S. ananas*, *S. manirei*, and *S. exceptus* entirely lack, or in the latter case possess extremely tiny, basal prongs. The latter 2 species are grouped as sister taxa in the tree resulting from our phylogenetic analysis. In *S. eusphyrensis*, *S. lewinensis*, *S. paralewinensis*, and possibly also *S. puriensis*, the medial and lateral hooks bear small basal prongs; the 2 of these species included in our phylogenetic analysis grouped as sister taxa, *S. lewinensis* and *S. paralewinensis*. In *S. pectinatus*, the lateral hook bears a relatively short basal prong, but the medial hook bears a basal prong that is essentially the same length as the axial and abaxial prongs. Whereas the bases of the medial and lateral hooks in the above 8 species of *Sphyrnacestus* are approximately equal in length, in *S. latocapitus* the base of the lateral hook is much longer than that of the medial hook, and both hooks bear short basal prongs that are located well away from the axial prongs, near the point of articulation of the 2 hooks. It is thus interesting that this species groups as the sister to all other species of *Sphyrnacestus*. In terms of the 3 species of *Sphyrnacestus* not included in our current tree, based on these features, once material for molecular work becomes available, we predict that *S. ananas* will group with *S. manirei* and *S. exceptus*, and *S. eusphyrensis* and *S. puriensis* will group with *S. lewinensis* and *S. paralewinensis*.

Before delving into the revised host associations of the phoreiobothriids, some discussion of the use of specific names for a subset of our host specimens is in order. In our earlier efforts (Naylor et al., 2012b) to develop a strategy for providing unique specific designations for what appear to be molecularly distinct elasmobranch taxa (i.e., based on NADH2 sequence data) that await formal description, in that paper we assigned numerical designations to such putative new species. Several of those are relevant here (see Tables I and II). *Carcharhinus amboinensis* 1 was the designation given to 1 of the 2 subclades of *C. amboinensis* Müller and Henle, 1839, that occurs in northern Australia. The identity of both of our specimens from northern Australia was confirmed as *C. amboinensis* 1 using NADH2 sequence data. *Sphyrna lewini* 1 was the designation given to the subclade of *S. lewini* (Griffith and Smith) that occurs in the Atlantic Ocean by Naylor et al. (2012b); all 4 of the host specimens we examined were collected from this region, and the identity of 1 of these was confirmed with NADH2 sequence data. Our most problematic host identification is the bull shark (BJ-191) we examined from the Gulf of California. This is because none of the 3 subclades of bull sharks recognized by Naylor et al. (2012b) include specimens from the Gulf of California. The subclade from the western Atlantic Ocean was designated *Carcharhinus leucas* (Valenciennes in Müller and Henle), the subclade from Borneo was designated *Carcharhinus* cf. *leucas* 1, and the subclade from South Africa was designated *Carcharhinus* cf. *leucas* 2. Unfortunately, we were unable to generate sequence data for our specimen from the Gulf of California to assist with determining its identity. As a consequence, we have used the designation *Carcharhinus* cf. *leucas* 1 for this host since that subclade includes the specimens from the Pacific Ocean and the Gulf of California is essentially an inlet of the Pacific Ocean. Finally, perhaps the most interesting host species is the 1 we have provisionally referred to as *Loxodon* cf. *macrorhinus*. At present, the genus *Loxodon* is monotypic, its only recognized species being *Loxodon macrorhinus* Müller and Henle. This species is reported to occur from Indonesia to eastern Africa (Ebert et al., 2021). However, our NADH2 sequence data suggest that the taxon that occurs off Mozambique is a distinct species (J. Caira and K. Jensen, pers. obs.).

Finally, recent work on the distribution of the winghead shark, *E. blochii*, by Fernando et al. (2019) is relevant to the identity of species of *Sphyrnacestus* reported from that shark species. *Sphyrnacestus puriensis* was originally described from a host identified as *Eusphyra blochii* (as *Zygaena blochii* Cuvier) collected off Orissa, India, by Srivastav and Capoor (1982). Until recently, *E. blochii* was considered to be the only valid member of its genus, being broadly distributed throughout the northern Indian Ocean and the waters of Southeast Asia (e.g., Ebert et al., 2021). However, based on collections from Sri Lanka, Fernando et al. (2019) resurrected the name *Eusphyra laticeps* (Cantor) for specimens of *Eusphyra* found in the western regions of the original distribution of *E. blochii* and retained the name *E. blochii* for specimens found in the more eastern regions of its distribution, including Australia. As a consequence, the type host of *S. puriensis* should be considered to be *E. laticeps*. *Sphyrnacestus eusphyrensis* n. sp., which was collected from hosts off Australia, is now the only member of its genus known to parasitize *E. blochii*.

We found 3 interesting instances in which species of *Phoreiobothrium* that are morphologically distinct and parasitize different host species, and, in some cases, different host genera, showed little to no variation in the D1–D3 region of the *28S* rDNA gene. The first is *P. angustivastum* (Figs. 9, 10A–D), *P. danae* (Figs. 10E–H, 11), *P. tesserascolex* (Figs. 14H–K, 15), and *Phoreiobothrium* n. sp. 6 in *C. isodon*, *C. limbatus*, *C. brevipinna*, and *R. terraenovae*, respectively. The second is *Phoreiobothrium* n. sp. 1 and *Phoreiobothrium* n. sp. 2 in *C. brevipinna* and *C. tilstoni*, respectively. The third is *P. waeschenbachae* and *Phoreiobothrium* n. sp. 3. in *S. macrorhynchus* and *R. oligolinx*, respectively. It will be interesting to explore these relationships using additional markers in the future.

The new material has brought to light several additional instances of multiple species of *Phoreiobothrium* parasitizing the same host species. Beyond hosting the previously described *P. martini*, *Carcharhinus brevipinna* is now known to also host the new species *P. tesserascolex* and the undescribed species *Phoreiobothrium* n. sp. 1. The latter undescribed species does not appear to be conspecific with *P. martini*, given that it possesses bothridia with 12 rather than 20–22 subloculi and proglottids with 56 rather than 88–96 testes. *Carcharhinus isodon* was found to host the new species *P. angustivastum* and the undescribed species *Phoreiobothrium* n. sp. 7. *Carcharhinus limbatus* hosts the new species *P. danae* and the undescribed species *Phoreiobothrium* n. sp. 9. In addition to the previously described *P. perilocrocodilus*, *Negaprion acutidens* hosts the undescribed species *Phoreiobothrium* n. sp. 4. In addition to the previously described *P. sarahae*, *Rhizoprionodon oligolinx* hosts the undescribed species *Phoreiobothrium* n. sp. 3. The latter species differs from *P. sarahae* in its possession of 51 rather than 83–115 testes and basal prongs of the medial hooks that are considerably longer than, rather than approximately the same length as, the talon of those hooks. Finally, *Rhizoprionodon terraenovae* hosts the undescribed species *Phoreiobothrium* n. sp. 6 and *Phoreiobothrium* n. sp. 16; these species conspicuously differ from 1 another in number of subloculi (10–11 vs. 23–24). Moreover, given these results, all species of *Triloculatum* are now known to co-occur with 1 (i.e., *T. jodyi*, *T. oregontwoae*, *T. triloculatum*, and *Triloculatum* n. sp. 1), 2 (i.e., *T. andersonorum* and *T. geeceearelensis*), or 3 (i.e., *T. bullardi*) species of *Phoreiobothrium*.

At least initially, *Phoreiobothrium tiburonis* from the bonnethead shark, *Sphyrna tiburo*, was the exception to the rule that species of *Sphyrnacestus* parasitize hammerhead sharks and species of *Phoreiobothrium* parasitize requiem sharks. Even though no material of this species preserved for molecular work was available, the morphology of *P. tiburonis* is fully consistent with species of *Phoreiobothrium* (see Cheung et al., 1982; Caira et al., 2005). The discovery of *Phoreiobothrium* n. sp. 13 in *Sphyrna zygaena*, which is also parasitized by *Sphyrancestus exceptus* and *Sphyrnacestus pectinatus*, provides additional evidence that hammerhead sharks can host species of *Sphyrnacestus* and species of *Phoreiobothrium*. This not only supports the current generic assignment of *P. tiburonis*, but it also leads us to predict that the bonnethead shark will ultimately likely be found to be parasitized by a species of *Sphyrnacestus*.

This work has expanded our understanding of the host associations of all 3 genera of cestodes. The hosts of *Triloculatum* now include a seventh species of *Carcharhinus*, *C.* cf. *leucas* 1. Having revised the host of *S. puriensis* to *E. laticeps*, we have expanded the host associations of *Sphyrnacestus* to include the other species of *Eusphyra*, *E. blochii*. The 3 other new species of *Sphyrnacestus* described here parasitize hammerhead species already known to host other members of the genus. *Sphyrna lewini* 1 hosts *S. ananas*, *S. paralewinensis*, and *S. lewinensis*. *Sphyrna mokarran* hosts *S. manirei* and *S. paralewinensis*, and *Sphyrna zygaena* hosts *S. exceptus* and *S. pectinatus*, and now also *Phoreiobothrium* n. sp. 13.

By far the greatest number and diversity of new host records are associated with species of *Phoreiobothrium*. Species of *Carcharhinus* known to host this genus have been expanded to include the following 10 species: *C. acronotus*, *C. altimus*, *C. amblyrhynchoides*, *C. amboinensis* 1, *C. brevipinna*, *C.* cf. *leucas* 1, *C. isodon*, *C. limbatus*, *C. pleurotaenia* and *C. tilstoni*. In terms of other carcharhinid genera, a second species of *Rhizoprionodon* (i.e., *R. terraenovae*) as well as a species each of *Lamiopsis* (i.e., *L. tephrodes*), *Loxodon* (i.e., *L.* cf. *macrorhinus*), *Scoliodon* (i.e., *S. macrorhynchos*), and the monotypic *Triaenodon* (i.e., *T. obesus*) have also been added to the list of hosts of *Phoreiobothrium*.

This work has expanded the known distribution of *S. exceptus* beyond the western Atlantic Ocean to include the Gulf of California. It has also extended the distribution of *S. pectinatus* beyond the western Atlantic Ocean to include the Gulf of California and the waters off Japan, Taiwan, and Senegal. This is perhaps not unexpected given that its host, the smooth hammerhead (*S. zygaena*), occurs in all of these regions.

This brings the total number of known species in the Phoreiobothriidae to 53. Thirty-six of these are described; 17 await description once additional material becomes available. At present, *Triloculatum* houses 6 described and 1 undescribed species, *Sphyrnacestus* houses 9 described species, and *Phoreiobothrium* houses 21 described and 16 undescribed species. However, we believe this is just the tip of the iceberg. Based on our results, all species in all carcharhinid genera that have not yet been examined for phoreiobothriids, including *Carcharhinus*, *Glyphis* Agassiz, *Lamiopsis*, *Loxodon*, *Rhizoprionodon*, *Scoliodon*, and the monotypic *Isogomphodon* Gill are candidate hosts for additional species of *Phoreiobothrium* and possibly also *Triloculatum*. However, given the considerable morphological variation seen across species of *Sphyrnacestus* relative to that seen in members of *Phoreiobothrium* and *Triloculatum*, examination of additional species of hammerhead sharks is likely to be the most productive avenue for discovering more extensive morphological variation in scolex features. To our knowledge, of the 8 species of Sphyrnidae, *Sphyrna corona* Springer, *Sphyrna gilberti* Quattro, Driggers, Grady, Ulrich, and Roberts, *Sphyrna media* Springer, and *Sphyrna tudes* (Valenciennes) have never been examined for cestodes.

The potential sister group relationship between *Sphyrnacestus* and *Phoreiobothrium* observed here is reflected in the potential sister group relationship between the Sphyrnidae and Carcharhinidae (see Naylor et al., 2012a). But what about the members of other families of Carcharhiniform sharks? To date, there are no published records of either genus, or *Triloculatum*, from members of any of the 7 other families in this order (i.e., the Galeocerdidae Poey, Hemigaleidae Compagno, Leptochariidae Gray, Proscylliidae Compagno, Pseudotriakidae Gill, Scyliorhinidae Gill, and Triakidae Gray). Furthermore, during our survey work over the past 4 decades, we have examined species in all of these families and have never encountered phoreiobothriids. We predict that none of these 7 families will be found to host members of the Phoreiobothriidae. This is because, among all elasmobranchs only the Carcharhinidae and Sphyrnidae share the unique possession of a spiral intestine with an internal mucosal surface that is of the scroll-type configuration, rather than the conicospiral-type configuration (Compagno, 1988). Although we do not understand the mechanism that may explain this correlation, it appears that phoreiobothriids are restricted to species of sharks that possess a scroll-type spiral intestine.

ACKNOWLEDGMENTS

We are grateful to Hannah Owens and Siobhan Durkin for preparing some of the whole mounts used in this study. We thank the following individuals for their assistance with fieldwork: Tom Lisney, Richard Mounsey, Raymond Passey, and Lyle Squire Jr. (Australia); Fahmi (Indonesian Borneo); Gordon Yearsley and Annie Lim (Malaysian Borneo); Fernando Marques and Sam Bila (Mozambique); Hsuan-Wien Chen (Taiwan); Ash Bullard, Claire Healy, Eric Hoffmayer, Lisa Hollensead, Charles Manire, Valerie McKenzie, Jody Peterson, Gaines Tyler, and Megan Winton (United States); and Tran Thi Binh (Vietnam). We greatly appreciate the comments of an anonymous reviewer on an earlier version of this manuscript. This work was supported with funds from National Science Foundation awards DEB 0818696 and 0818823. Any opinions, findings, conclusions, or recommendations expressed are those of the authors and do not reflect the views of the National Science Foundation.

LITERATURE CITED

BAER, J.-G., AND L. EUZET. 1955. *Prosobothrium armigerum* Cohn 1902 (Cestoda). Historique, synonymie, description et position systématique. Recueil des Travaux des Laboratoires de Botanique, Géologie et Zoologie de la Faculté des Sciences de l'Université de Montpellier, Série Zoologique 1: 44–55.

BERNOT, J. P., J. N. CAIRA, AND M. PICKERING. 2015. The dismantling of *Calliobothrium* (Cestoda: Tetraphyllidea) with erection of *Symcallio* n. gen. and description of two new species. Journal of Parasitology 101: 167–181. doi:10.1645/14-571.1.

CAIRA, J. N. 1985. An emendation of the generic diagnosis of *Phoreiobothrium* Linton, 1889 (Tetraphyllidea: Onchobothriidae) with a detailed description of bothridia and hooks. Canadian Journal of Zoology 63: 1199–1206. doi:10.1139/z85-179.

CAIRA, J. N., AND K. JENSEN. 2009. Erection of a new onchobothriid genus (Cestoda: Tetraphyllidea) and the description of five new species from whaler sharks (Carcharhinidae). Journal of Parasitology 95: 924–940. doi:10.1645/GE-1963.1.

CAIRA, J. N., K. JENSEN, AND E. BARBEAU (eds.) 2024. Global Cestode Database. Available at: www.tapewormdb.uconn.edu. Accessed 15 July 2024.

CAIRA, J. N., K. JENSEN, AND V. A. IVANOV. 2017a. Onchoproteocephalidea II Caira, Jensen, Waeschenbach, Olson & Littlewood, 2014. *In* Planetary Biodiversity Inventory (2008–2017): Tapeworms from Vertebrate Bowels of the Earth, J. N. Caira, and K. Jensen (eds.). University of Kansas, Natural History Museum, Special Publication No. 25, Lawrence, Kansas, p. 279–304.

CAIRA, J. N., K. JENSEN, AND T. R. RUHNKE. 2017b. "Tetraphyllidea" van Beneden, 1849 relics. *In* Planetary Biodiversity Inventory (2008–2017): Tapeworms from Vertebrate Bowels of the Earth, J. N. Caira, and K. Jensen (eds.). University of Kansas, Natural History Museum, Special Publication No. 25, Lawrence, Kansas, p. 371–400.

CAIRA, J. N., K. JENSEN, A. WAESCHENBACH, P. D. OLSON, AND D. T. J. LITTLEWOOD. 2014. Orders out of chaos—Molecular phylogenetics reveals the complexity of shark and stingray tapeworm relationships. International Journal for Parasitology 44: 55–73. doi:10.1016/j.ijpara.2013.10.004.

CAIRA, J. N., C. RICHMOND, AND J. SWANSON. 2005. A revision of *Phoreiobothrium* (Tetraphyllidea: Onchobothriidae) with descriptions of five new species. Journal of Parasitology 91: 1153–1174. doi:10.1645/ge-3459.1.

CHERVY, L. 2009. Unified terminology for cestode microtriches: A proposal from the International Workshops on Cestode Systematics in 2002–2008. Folia Parasitologica 56: 199–230. doi:10.14411/fp.2009.025.

CHEUNG, P. L., R. F. NIGRELLI, AND G. D. RUGGIERI. 1982. *Phoreiobothrium tiburonis*, new species, (Cestoda: Onchobothriidae) from bonnethead shark, *Sphyrna tiburo* (L.). Journal of Aquariculture 2: 81–85.

CLOPTON, R. E. 2004. Standard nomenclature and metrics of plane shapes for use in gregarine taxonomy. Comparative Parasitology 71: 130–140. doi:10.1654/4151.

COMPAGNO, L. J. V. 1988. Sharks of the Order Carcharhiniformes. Princeton University Press, Princeton, New Jersey, 486 p.

EBERT, D. A., M. DANDO, AND S. FOWLER. 2021. Sharks of the World: A Complete Guide. Princeton University Press, Princeton, New Jersey, 608 p.

EUZET, L. 1959. Recherches sur les cestodes tétraphyllides des sélaciens des cotes de France. Docteur dés Sciences Naturelles. Université de Montpellier, Montpellier, France, 263 p.

EUZET, L. 1994. Order Tetraphyllidea Carus, 1863. *In* Keys to the Cestode Parasites of Vertebrates, L. F. Khalil, A. Jones, and R. A. Bray (eds.). CAB International, Wallingford, U.K., p. 149–194.

FERNANDO, D., R. M. K. BOWN, A. TANNA, R. GOBIRAJ, H. RALICKI, E. L. JOCKUSCH, D. A. EBERT, K. JENSEN, AND J. N. CAIRA. 2019. New insights into the identities of the elasmobranch fauna of Sri Lanka. Zootaxa 4585: 201–238. doi:10.11646/zootaxa.4585.2.1.

FOWLER, S., A. BRÄUTIGAM, N. OKES, AND G. SANT. 2021. Conservation, Fisheries, Trade and Management Status of CITES-Listed Sharks, 607th edition. Bundesamt für Naturschutz, Bonn, Germany, 76 p.

HAHN, C., L. BACHMANN, AND B. CHEVREUX. 2013. Reconstructing mitochondrial genomes directly from genomic next-generation sequencing reads—A baiting and iterative mapping approach. Nucleic Acids Research 41: e129. doi:10.1093/nar/gkt371.

HILLIS, D. M., AND J. J. BULL. 1993. An empirical test of bootstrapping as a method for assessing confidence in phylogenetic analysis. Systematic Biology 42: 182–192. doi:10.1093/sysbio/42.2.182.

KALYAANAMOORTHY, S., B. Q. MINH, T. K. F. WONG, A. VON HAESELER, AND L. S. JERMIIN. 2017. ModelFinder: Fast model selection for accurate phylogenetic estimates. Nature Methods 14: 587–589. doi:10.1038/nmeth.4285.

KATOH, K., J. ROZEWICKI, AND K. D. YAMADA. 2019. MAFFT online service: Multiple sequence alignment, interactive sequence choice and visualization. Briefings in Bioinformatics 20: 1160–1166. doi:10.1093/bib/bbx108

KATOH, K., AND D. M. STANDLEY. 2013. MAFFT multiple sequence alignment software version 7: Improvements in performance and usability. Molecular Biology and Evolution 30: 772–780. doi:10.1093/molbev/mst010.

LINTON, E. 1924. Notes on cestode parasites of sharks and skates. Proceedings of the United States National Museum 64: 1–114. doi:10.5479/si.00963801.64-2511.1.

LITTLEWOOD, D. T. J., M. CURINI-GALLETTI, AND E. A. HERNIOU. 2000. The interrelationships of Proseriata (Platyhelminthes: Seriata) tested with molecules and morphology. Molecular Phylogenetics and Evolution 16: 449–466. doi:10.1006/mpev.2000.0802.

LOCKYER, A. E., P. D. OLSON, AND D. T. J. LITTLEWOOD. 2003. Utility of complete large and small subunit rRNA genes in resolving the phylogeny of the Neodermata (Platyhelminthes): Implications and a review of the cercomer theory. Biological Journal of the Linnean Society 78: 155–171. doi:10.1046/j.1095-8312.2003.00141.x.

NAYLOR, G. J. P., J. N. CAIRA, K. JENSEN, K. A. M. ROSANA, N. STRAUBE, AND C. LAKNER. 2012a. Elasmobranch

Phylogeny: A mitochondrial estimate based on 595 species. *In* Biology of Sharks and Their Relatives, J. C. Carrier, J. A. Musick, and M. R. Heithaus (eds.). CRC Press, Boca Raton, Florida, 31–56 pp.

Naylor, G. J. P., J. N. Caira, K. Jensen, K. A. M. Rosana, W. T. White, and P. R. Last. 2012b. A DNA sequence-based approach to the identification of shark and ray species and its implications for global elasmobranch diversity and parasitology. Bulletin of the American Museum of Natural History 367: 1–262. doi:10.1206/754.1.

Nguyen, L. T., H. A. Schmidt, A. Von Haeseler, and B. Q. Minh. 2015. IQ-TREE: A fast and effective stochastic algorithm for estimating maximum-likelihood phylogenies. Molecular Biology and Evolution 32: 268–274. doi:10.1093/molbev/msu300.

Olson, P. D., and J. N. Caira. 1999. Evolution of the major lineages of tapeworms (Platyhelminthes: Cestoidea) inferred from 18S ribosomal DNA and elongation factor-1 alpha. Journal of Parasitology 85: 1134–1159. doi:10.2307/3285679.

Pleijel, F., U. Jondelius, E. Norlinder, A. Nygren, B. Oxelman, C. Schander, P. Sundberg, and M. Thollesson. 2008. Phylogenies without roots? A plea for the use of vouchers in molecular phylogenetic studies. Molecular Phylogenetics and Evolution 48: 369–371. doi:10.1016/j.ympev.2008.03.024.

Srivastav, A. K., and V. N. Capoor. 1982. On a new cestode, *Phoreiobothrium puriensis* n. sp. Journal of the Zoological Society of India 34: 82–85.

Tkach, V. V., D. T. J. Littlewood, P. D. Olson, J. M. Kinsella, and Z. Swiderski. 2003. Molecular phylogenetic analysis of the Microphalloidea Ward, 1901 (Trematoda: Digenea). Systematic Parasitology 56: 1–15. doi:10.1023/A:1025546001611.

Van Der Auwera, G., S. Chapelle, and R. De Wachter. 1994. Structure of the large ribosomal subunit RNA of *Phytophthora megasperma*, and phylogeny of the oomycetes. FEBS Letters 338: 133–136. doi:10.1016/0014-5793(94)80350-1.